

UNIVERSITY OF CAPE COAST

ASSESSING THE INFLUENCE OF TILLAGE ON MAIZE  
PERFORMANCE USING UNMANNED AERIAL VEHICLE IMAGERY



MURANGAZA FUMBA HANS

2024



©2024

Murangaza Fumba Hans

University of Cape Coast

UNIVERSITY OF CAPE COAST

ASSESSING THE INFLUENCE OF TILLAGE ON MAIZE  
PERFORMANCE USING UNMANNED AERIAL VEHICLE IMAGERY

BY

MURANGAZA FUMBA HANS

Thesis submitted to the Department of Agricultural Engineering of the School  
of Agriculture, University of Cape Coast, in partial fulfilment of the  
requirements for the award of Master of Philosophy degree in Agricultural  
Mechanisation and Machinery Technology

DECEMBER, 2024

## DECLARATION

### Candidate's Declaration

I hereby declare that this thesis is the result of my own original research and that no part of it has been presented for another degree in this university or elsewhere.

Candidate's Signature:..... Date:.....

Name: Murangaza Fumba Hans

### Supervisor's Declaration

I hereby declare that the preparation and presentation of the thesis were supervised in accordance with the guidelines on supervision of thesis laid down by the University of Cape Coast.

Principal Supervisor's Signature:..... Date:.....

Name: Dr Francis Kumi

## ABSTRACT

Maize is a staple food in Sub-Saharan Africa, and tillage is widely used to boost its yield, though it affects soil and the environment both positively and negatively. To support farmers and policymakers, a data-driven approach using UAV technology was introduced.

This study was conducted for two seasons in a randomized complete block design with four treatments (Harrowing only, Ploughing only, Ploughing and Harrowing, and No-tillage). The results showed that No-tillage had the lowest growth parameters, while Ploughing and Harrowing recorded the highest in terms of LAI (1.50–1.75), stem diameter (20–22.5 mm), plant height (165–175 cm), and yield (7.20–10.93 t/ha biomass, 4.619–5.67 t/ha grain yield). Despite its lower yields, No-tillage showed the highest yield improvement (+1.11 t/ha). UAVs imagery with Yolov8-small achieved high germination rate detection (mAP50: 0.89–0.95) and accurate plant height estimation (RMSE < 7 cm,  $R^2$ : 0.98–0.99). For LAI estimation, UAV technology coupled with Huber regression model achieved  $R^2$  scores of 0.80–0.94 and RMSE as low as 0.14, and coupled with Gradient Boosting Machines reached  $R^2$  of 0.87 and RMSE of 0.281 t/ha at the vegetative stage for Yield prediction. Ploughing and Harrowing is recommended for short-term tillage, while No-tillage is better for the long term. UAV imagery with machine learning reliably monitors maize and predicts yield. Future research should explore the long-term effects of No-tillage, UAV-based stem girth estimation, and the cost-benefit of UAV adoption in small-scale farming.

Keywords: Tillage, UAV technology, maize, yield prediction, maize

## ACKNOWLEDGMENTS

This thesis marks the culmination of a fulfilling journey, and I am deeply grateful to all those who have contributed to its success in various ways.

Above all, I give thanks to God Almighty for His grace and protection throughout this journey.

First and foremost, I am profoundly indebted to my supervisor, Dr. Francis Kumi, for his unwavering support, insightful guidance, and expert mentorship throughout this research.

I extend my heartfelt gratitude to the Regional Universities Forum for Capacity Building in Agriculture (RUFORUM) for the financial support provided through the Graduate Teaching Assistantship programme.

Additionally, I am thankful to the University of Cape Coast Teaching and Research Farms for providing the resources and technical support to facilitate my field experiments.

I am particularly appreciative of the invaluable support I received from Dr. Richard Adade and Ms. Harriet Quarshie, both of the Center for Coastal Management at the University of Cape Coast for the assistance offered with the use of the Unmanned Aerial Vehicle technology equipment for my research.

I acknowledge with gratitude the encouragement I received from Université Catholique de Bukavu, particularly the Faculty of Agriculture and its Dean, Prof. Janvier Bashagaluke, who inspired me to pursue excellence in my academic endeavours.

I also wish to thank my classmates, Mr Seth Osei, Mr Joseph Conduah, and Mr Right-Rolands Atareburo Adompika and other friends like Mr Samuel Badu, Mr Solomon Amamu, Ms Evangeline Tashie, Ms Axelle Kikie, Mr Marcel Yao, Mr Thomas Boateng, Mr Kester Ilechie, Dr Philip Kamanda, Dr Emmanuel Ogyiri Adu, and Mr. Eraste Amuli for their unwavering support throughout the programme.

To my family, I owe immeasurable gratitude for their financial and emotional support, particularly to the families of Murangaza, Kahamire, Mweze, Mushagalusa, as well as Hans & Paulien Post.

Lastly, I would like to acknowledge everyone whose names may not have been mentioned here but contributed to my journey in one way or another. Your efforts, however small they may seem, have made a significant difference. To all, I extend my heartfelt thanks for being part of this academic milestone.

## **DEDICATION**

To my family, for the unconditional support provided

**TABLE OF CONTENTS**

DECLARATION	ii
ABSTRACT	iii
ACKNOWLEDGMENTS	iv
DEDICATION	v
TABLE OF CONTENTS	vi
LIST OF TABLES	x
LIST OF FIGURES	xi
LIST OF ABBREVIATIONS	xiv
CHAPTER ONE: INTRODUCTION	
Background to the Study	1
Problem statement	3
Aim and Specific Objectives	5
Aim	5
Specific objectives	5
Research questions	5
Hypothesis	6
Significance of the study	6
Organisation of the thesis	6
CHAPTER TWO: LITERATURE REVIEW	
Maize phenology and botany	7
The Ecological Requirements of Maize	10



Importance of Tillage	15
Tillage effects on soil properties	16
Tillage effects on the environment	19
Tillage effects on crop yield	20
Remote sensing and Unmanned Aerial Vehicle Technology	21
Remote sensing applications in agriculture	23
Application of UAV technology in crop phenotyping of maize	24
UAV estimation of plant height	25
Application of the UAV technology in crop yield prediction	27
Use of Deep learning approach in Agriculture and maize production	28
CHAPTER THREE: MATERIALS AND METHODS	
Study area	34
Location of the study area	34
Climate Conditions	34
General Description of Soils and Relief	35
Materials	37
Planting materials	37
Tractor and Implements	37
Equipment for Field data collection	37
Unmanned Aerial Vehicle technology	38
Methods	39
Experimental design	39
Cultural practices	40
Manual Field data collection	41
UAV data collection	43

UAV flight accuracy	44
Estimation of plant height	45
Assessment of Vis	46
Germination rate assessing using UAV-acquired pictures	48
Estimation of LAI	52
Prediction of Yield	53
Study methodology limitations	55
Statistical Analyses	55
CHAPTER FOUR: RESULTS AND DISCUSSION	
Effects of tillage on maize growth parameters	56
Effects of tillage on germination rate	56
Effects of Tillage on Plant Height and Stem Diameter	57
Effects of tillage on number of leaves and leaf Area Index (LAI)	61
Effects of Tillage on Days to 50% Flowering	64
Effect of Tillage on Root System Architecture of maize	65
Effects of Tillage on maize yield components	66
Relationship between growth parameters and yield components	70
UAV Estimation of growth parameters.	71
Estimation of Germination rate	71
Comparison of measured and UAV estimated plant growth parameters	77
Measured and UAV estimated plant height	77
Estimation of the Leaf Area Index (LAI)	80
UAV estimation of the number of tasseled plants	82
Yield Prediction	84
CHAPTER FIVE: CONCLUSION AND RECOMMENDATIONS	
Conclusion	95

Recommendations	96
REFERENCES	97
APPENDICES	138

**LIST OF TABLES**

Table	Page
Table 1: Soil physico-chemical properties at the experiment site	36
Table 2: UAV survey accuracy across growth stages	44
Table 3: Assessed RGB Vegetation indices	47
Table 4: Characteristics of the images capturing process and environment	48
Table 5: Training parameters of the selected models	50
Table 6: Hyperparameters used for the Random Forest, Decision Tree and Gradient Boosting for yield prediction (classification and regression)	54
Table 7: Effects of tillage on maize Root System Architecture	65
Table 8: Effects of tillage on the yield components for Season One	67
Table 9: Effects of tillage on the yield components for Season Two	67
Table 10: Models evaluation summary across the 3 weeks of the early-stage growth of maize seedlings	74
Table 11: Linear and Machine Learning models performance in estimating the Leaf Area Index (LAI)	81
Table 12: Machine Learning yield prediction performance for yield prediction	84
Table 13: Machine Learning yield prediction performance (classification)	87

**LIST OF FIGURES**

Figure	Page
Figure 1: Location of the study site (a) experimental area, (b) the University of Cape Coast research farms, (c) the Central region in Ghana.	34
Figure 2: Experiment layout	40
Figure 3: Project flowchart with UAV and manual data collection and processing	44
Figure 4: UAV estimation of plant height at different growth stages (source: Akyeaw et al., 2023)	46
Figure 5: Bounding box sizes per dataset (a - two weeks maize, b – three weeks maize , c - Four weeks maize	49
Figure 6: Effects of Tillage on Maize germination rate for the two seasons	56
Figure 7: Effects of different tillage systems on maize plant height for Season One	58
Figure 8: Effects of different tillage systems on maize stem diameter growth rate for Season One	58
Figure 9: Effects of tillage systems on maize plant height growth rate for Season Two	59
Figure 10: Effects of tillage on maize stem diameter growth rate for Season Two	59
Figure 11: Effects of tillage on Number of leaves growth rate for Season One	61
Figure 12: Effects of tillage on Number of leaves growth rate for Season Two	62

Figure 13: Effects of tillage on Leaf Area Index (LAI) growth rate for Season One	62
Figure 14: Effects of tillage on Leaf Area Index (LAI) growth rate for Season Two	63
Figure 15: Effects of tillage on the Number of days to 50 percent flowering for both seasons one and two	64
Figure 16: Correlation matrix between growth parameters and yield components of maize	70
Figure 17: Precision-Recall curves during the validation of the models on three weeks of the early growth stage of maize seedlings (Two weeks aged - left, Three weeks aged - middle, Four weeks aged - right)	73
Figure 18: Precision - Confidence curves during the validation of the models on the three weeks of the early growth stage of maize seedlings (Two weeks aged - left, Three weeks aged - middle, Four weeks aged - right)	73
Figure 19: Recall - Confidence curves during the validation of the models on the three weeks of the early growth stage of maize seedlings (Two weeks aged - left, Three weeks aged - middle, Four weeks aged - right)	74
Figure 20: Highlights of model confusion in dense maize seedlings population	75
Figure 21: Illustration of inaccuracies caused by the weeds	76
Figure 22: Linear relation between manually measured and UAV technology estimated plant heights across plant growth stages of different tillage treatments in Season one.	78

Figure 23: Linear relation between manually measured and UAV technology estimated plant heights across plant growth stages of different tillage treatments in Season Two.	79
Figure 24: Maize tassel detection using YOLOv8	83
Figure 25: Sources of inaccuracy in Tassel detection during the Season Two	84
Figure 26: Feature importance scores of yield prediction using Decision Tree (E: Establishment, V: Vegetative, T: Tasselling, M: Maturity growth stages)	90
Figure 27: Feature importance scores of yield prediction using Random Forest (E: Establishment, V: Vegetative, T: Tasselling, M: Maturity growth stages)	90
Figure 28: Feature importance scores of yield prediction using Gradient Boosting Machines (E: Establishment, V: Vegetative, T: Tasselling, M: Maturity growth stages)	91
Figure 29: Feature importance scores of yield class prediction using Decision Tree (E: Establishment, V: Vegetative, T: Tasselling, M: Maturity growth stages)	91
Figure 30: Feature importance scores of yield class prediction using Random Forest (E: Establishment, V: Vegetative, T: Tasselling, M: Maturity growth stages)	92
Figure 31: Feature importance scores of yield class prediction using Gradient Boosting Machines (E: Establishment, V: Vegetative, T: Tasselling, M: Maturity growth stages)	92

## LIST OF ABBREVIATIONS

FAO	Food and Agriculture Organisation
UAV	Unmanned Aerial Vehicle
VI	Vegetation Index
DSM	Digital Surface Model
mAP	Mean Average Precision
DL	Deep Learning
YOLO	You Only Look Once
CNN	Convolutional Neural Network
LAI	Leaf Area Index



## CHAPTER ONE

### INTRODUCTION

#### Background to the Study

Maize (*Zea mays*) is an important crop in many parts of the world, including Africa where it is grown by smallholder farmers due to its high nutritional value, multi-usage purpose, and resilience to harsh environmental conditions (Liu et al., 2021). Maize is also used as a forage crop for livestock (Shiferaw et al., 2011). In recent decades, the global production of maize has witnessed substantial growth due to increasing demand, technological progress, improved yields, and expansion of cultivation areas (Erenstein et al., 2022). This is largely due to the utilisation of key agricultural practices associated with land preparation and maintenance such as tillage. Tillage is a key crop cultivation practice and has shown to have influenced soil properties and crop performance (Alam et al., 2014; Angon et al., 2023a). Tillage refers to the use of mechanical methods to modify the surface layer of soil with the aim of bringing favourable alterations in its physical, chemical, and biological characteristics for the purpose of creating optimal conditions for seed germination, promote the growth of plant seedlings, and enhance overall plant growth and development (Angon et al., 2023a). These mechanical methods have gradually replaced traditional manual tillage practices among farmers in the Sub-Sahara Africa region and offer higher efficiency and productivity (Mohammed et al., 2023). Such operations involve the use of machines and equipment ranging from power tillers to tractors with attached tillage implements (Müller et al., 2011) for cultivating the soil. Recent studies have shown that not only structural properties of the soil can be modified but the

whole systems in it including nutrient availability, firmness and porosity while influencing further how resilient the soil is to weather adversity such as water and wind erosion (Nafi et al., 2021; Sokolowski et al., 2020; D. Zhang et al., 2022).

Tillage practices such as ploughing, harrowing, and no-tillage each present a balance of benefits and challenges that influence soil health, crop productivity, and sustainability. While ploughing improves aeration, incorporates organic matter, and effectively buries weed seeds, it also disrupts soil structure, increases erosion risks, and accelerates moisture loss (Roger-Estrade et al., 2010). Harrowing, whether used alone or in combination with ploughing, refines the seedbed and helps distribute crop residues, yet excessive tillage can lead to soil compaction and higher labour and fuel costs (Finch et al., 2002). Thus, some studies recommended the No-tillage, as it preserves soil integrity, reduces erosion, and enhances moisture retention, but the accumulation of surface residues can still promote weed growth and requires special equipment for planting (Gellatly & Dennis, 2011). Striking a balance between these methods requires considering soil type, crop needs, and long-term sustainability, ensuring that soil remains productive while minimizing environmental degradation.

Monitoring the effects of tillage on maize growth performance is crucial to ensure its productivity. The monitoring of crop growth could be done through manual data collection or remote sensing data collection methods or both.

Remote sensing with Unmanned Aerial Vehicles (UAVs) has emerged as a powerful tool in data collection in various fields. Utilising UAVs in

agriculture offers numerous advantages over traditional monitoring and manual data collection methods. These aerial platforms provide a bird's-eye view of agricultural fields, capturing high-resolution images and collecting valuable spatial data with unprecedented efficiency (Tsouros et al., 2019).

By employing advanced sensors and imaging systems, UAVs can acquire information related to crop health, growth patterns, nutrient deficiencies, pest infestations, and irrigation needs, among other vital parameters and insights (Zhao et al., 2019). Further, its use has enhanced decision-making using sophisticated image analysis techniques to provide actionable insights for farmers. By pinpointing problem areas or differences in crop performance, farmers can make well-informed choices about irrigation, fertilization, and pest management, enabling them to use resources efficiently while reducing environmental impacts (Zhang et al., 2022).

### **Problem statement**

While Tillage practices have shown several advantages to crop growth by providing adequate soil conditions to crop roots, they also have been linked to soil disturbance that increases its vulnerabilities to soil erosion, carbon emission into the atmosphere, and soil compaction (Busari et al., 2015). The selection of the tillage implement is complex and challenging as each tillage implement causes unique soil disruption, and its effects on crops depend on specific factors like weather, crop type, and site characteristics (Sun et al., 2024; Wasaya et al., 2019a).

Accurately estimating and monitoring crop/maize growth parameters are critical for optimizing agricultural practices and maximizing crop yield. Traditional methods of assessing crop growth and performance are often

labour-intensive, time-consuming, and prone to human error (Meer & Jong, 2001; Wiegand et al., 1991). As a result, in recent times, there have been efforts to utilize UAVs to capture images and have them analysed to monitor the detection and growth of crops. However, there have been some challenges. For instance, the detection of seedlings at the early-stage growth stage is quite challenging due to the Ground Sampling Distance which sometimes makes the resolution of UAV images constrained to small size images while having multiple small objects in them (Hao et al., 2022; Velumani et al., 2021). Some have proposed using deep learning techniques for object detection as a promising option but this has rarely been explored especially under small-scale level typically of farmholdings in sub-Saharan Africa with low computing power (Albahar, 2023; Dhillon & Moncur, 2023). As Deep Learning (DL) is known to have a high computational resource demand, several DL models have opted to trade off some accuracy for portability, making those lite models to be fast and edge devices friendly. Existing free access datasets such as Microsoft Common Objects in Context (COCO)(Lin et al., 2014) or ImageNet (Deng et al., 2009) on which popular Object detection models are trained are not complete for all agriculture use cases (Lu & Young, 2020), making it challenging to find pre-trained models for transfer learning, thus decreasing training performance and overall accuracy.

Moreso, yield prediction is an important component of agricultural planning. Traditional yield sampling methods involve manually selecting random samples. This technique depends on historical yield data and visual assessments, which are then extrapolated to estimate overall yield. However, this approach fails to consider field heterogeneity, leading to inaccurate

sample collection and biased predictions. Yield prediction highly relies on the availability, quantity and quality of collected data, and thus remains unreliable under manually collected data (Elbasi et al., 2023). With the advent of Unmanned Aerial Vehicles (UAVs) and advanced remote sensing technologies, there is a significant opportunity to revolutionize agricultural monitoring and management. Despite these technological advancements, there remains a gap in comprehensive research that leverages UAVs to predict end-of-season maize yield and estimate growth parameters using a low-cost RGB camera under a small-scale farm holding.

### **Aim and Specific Objectives**

#### **Aim**

The study aimed at assessing the performance of maize growth and yield under different tillage systems using UAV technology.

#### **Specific objectives**

The specific objectives of this research are as follows:

1. To manually measure the effect of different tillage types (no-tillage, ploughing and harrowing, ploughing only and harrowing only) on the growth and yield of maize.
2. To detect and count maize seedlings using UAV imagery and deep learning models (YOLOv8, Faster R-CNN MobileNetv3).
3. To estimate maize growth parameters such as germination rate, plant height, leaf area index, days to 50 percent flowering using UAV remote sensing technique.
4. To predict the end-of-season yield of maize using UAV-derived data.

#### **Research questions**

This research answers the following questions:

1. What is the effect of tillage on the growth and yield of maize?
2. How efficient is the UAV imagery in estimating maize growth parameters?
3. How accurate is the UAV technology in estimating the end-of-the-season yield of maize?

### **Hypothesis**

- Tillage practices influence the maize growth and yield parameters
- The UAV technology is effective in monitoring the maize growth parameters and predict the end-of-season yield

### **Significance of the study**

This study will highlight the effects of conservative and conventional tillage on the maize and thus help farmers and policy makers to take more guided actions towards agriculture practices.

Additionally, the finding of this study could contribute to knowledge regarding the use of UAV technology to estimate growth and predict the yield of maize crop. Subsequently it stands to arouse interest in the use of the UAV technology in low-income and small-scale farming characteristic of agriculture in the Sub-Saharan Africa.

### **Organisation of the thesis**

This thesis is organized into five chapters. The first chapter is the Introduction which includes the background of the study, the problem statement, and the objectives. Chapter two reviews the main topics relevant to the maize, tillage practices, and UAV technology. The third chapter outlines the materials and methods employed in the study. Chapter four presents the results and provides a detailed discussion of the findings. The final chapter concludes the study by summarizing the key findings and providing recommendations for future research.

## CHAPTER TWO

### LITERATURE REVIEW

#### Maize phenology and botany

Maize originated in Central America and was subsequently introduced to different continents mainly Europe, Africa and Asia the endeavours of traders and explorers, with its ancestor (*Zea Mexicana*) from which it was domesticated (Sauer, 2008). *Zea*, a genus within the grass family (Graminae or Poaceae), includes maize, a monoecious plant. Similar to other grasses, maize leaves are structured with a sheath that encircles the stem and an elongated blade extending outward to capture sunlight efficiently.

The leaf blade of maize is long, narrow, and tapers towards the tip with a wavy structure. It is supported throughout its length by a prominent midrib (Hochholdinger, 2009). The stem of a maize plant is a tall central stalk that supports all parts of the plant. Its only branches are those bearing the reproductive structures. The stem enables maize to grow to impressive heights, reaching up to 12 feet (4 meters) depending on the variety. Unlike many other grasses, the interior of the maize stem is solid in both the nodal and internodal regions (Al-Zube et al., 2018; Cutler & Cutler, 1948).

Maize develops a complex root system comprising distinct embryonic and postembryonic root types formed at different developmental stages. Initially, the early seedling root system is dominated by embryonically preformed roots. As the plant matures, an extensive shoot-borne root system defines the adult root structure. Additionally, maize has a fibrous root system that penetrates deeply into the soil, providing stability to the plant while efficiently absorbing water and nutrients (Hochholdinger et al., 2018).

Maize plants possess three distinct types of roots: - Seminal roots, which originate from the radicle and persist for an extended period, forming the initial root system; - Adventitious roots, which emerge from the lower stem nodes below ground level and constitute the primary active root system of the plant; and - Brace or prop roots, which develop from the lower two stem nodes, providing additional support and stability to the plant (Sparks, 2023).

The root system of maize, classified as a grass, is fibrous rather than a tap root. The maize root system comprises roots formed during embryogenesis and postembryonic development. The embryonic root system includes a primary root, which originates at the basal pole of the embryo, and a varying number of seminal roots. The postembryonic root system consists of shoot-borne roots, which develop at successive shoot nodes, and lateral roots, which emerge from the pericycle of all root types (Hochholdinger, 2004).

The maize root system has a unique architecture which ensures the effective absorption of water and nutrients while providing stability. The development of the maize root system is governed by an internal genetic mechanism, influenced by interactions with the rhizosphere, and shaped by its ability to adapt to changing environmental conditions (Hochholdinger, 2009).

Maize plants are monoecious, meaning they possess both male and female reproductive organs on a single plant. The male reproductive organs, or stamens, are located in the tassels at the top of the plant and release pollen when mature (Kellogg, 2015; Weatherwax, 1916). The female reproductive organs, or pistils, are located in the ears of the maize plant. The process of sex determination in maize involves various factors including genes, and



hormones like jasmonic acid, brassinosteroid, and gibberellin (Guerrero-Méndez & Abraham-Juárez, 2023).

During germination, the primary root tip of maize pushes through the surrounding tissues that compose the coleorhiza at the proximal end of the emerging primary root. The growth, distribution, and coordination of the root system within the soil are influenced by factors such as weather conditions, soil properties, fertilizers, and pest activity (Chen et al., 2022; Şimon et al., 2023).

The male flowers of maize, located in the tassel, produce pollen essential for pollination. The tassel originates from the plant's growing point, with the innermost leaf at this point being the final leaf formed after tasselling. Pollination occurs when pollen from the tassel reaches the silks of the female flowers, initiating kernel development (Li et al., 2023). Maize is predominantly cross-pollinated, with self-pollination accounting for less than 5%. Following pollination, the female flowers develop into kernels (Weatherwax, 1916). The reproductive phase begins with the silking stage, where female flowers or cobs form 2–3 days after tasselling. By day seven post-silking, the cobs, husks, and shanks are fully developed.

After fertilization, the soft dough or milky stage begins, marked by the initial grain development. At this stage, the grains are soft, and the silks and husks remain partially green. Physiological maturity is reached approximately 30 days after silking when the plant achieves maximum dry weight. At this stage, a black layer forms at the tip of each kernel, signalling the cessation of starch accumulation (Adu et al., 2014). Grain maturity, occurring 4–6 weeks after fertilization, leads to the hard dough stage where the leaves and stems wither,

silks dry and become brittle, and the cobs begin to droop, signalling the readiness for harvest (Adu et al., 2014).

## **The Ecological Requirements of Maize**

### **Soil requirements of maize**

Maize prefers loose soils that offer proper aeration and drainage while maintaining sufficient amounts of water close to the roots making too heavy or too sandy and poorly drained soils are not suitable (Fang & Su, 2019). Maize cultivation thrives best in loamy, clay loam, or silty loam soils, which are considered highly suitable. Sandy loam and silty clay soils are moderately suitable, while clay soils are marginally suitable for maize growth. Optimal soil texture for healthy maize production typically falls within 10% to 30% clay content (Du Plessis, 2003).

The plant thrives at pH levels above 5.51, with an optimal range between 5.8 and 6.81. A pH close to 5 can lead to a reduction in yield of up to 35%. It can grow in soils with pH from 4 to 8 (Edmeades et al., 2017; Negese et al., 2022). Corn is slightly sensitive to increased salinity levels<sup>1</sup>. It has low to moderate tolerance of soil salinity (Amer, 2010). The ideal soil for maize is characterized by significant depth, a favourable structure, efficient internal drainage, optimal moisture levels, and a sufficient balance of plant nutrients (Fang & Su, 2019). Proper seedbed preparation is crucial for maize cultivation, as it significantly impacts germination, crop emergence, establishment, and overall growth, ultimately leading to higher yields. Farmers are encouraged to adopt a balanced approach to soil preparation, minimizing excessive tillage to avoid damaging soil structure and preventing soil compaction (Bahadur & Shrestha, 2014).

**Rainfall**

Maize requires approximately 5 to 7 tons of water per hectare during the dry season as over the entire growing season, water requirements range from 6 to 9 tons per hectare. During months with high temperatures and little or no rainfall, well-established maize plants may need up to 60 mm of water per week (Bhat et al., 2017; Du Plessis, 2003).

Maize grows best in regions with an annual rainfall of 600–1000 mm<sup>3</sup>, though it can tolerate a minimum seasonal rainfall of 200 mm. However, cultivating maize as a purely rainfed crop can be risky in areas with an average annual rainfall of 400 mm. Even in regions receiving 600 mm of rainfall, supplemental irrigation is often required to achieve high yields (Bagula et al., 2022).

Maize growth ideally requires an annual rainfall of 250 mm to 5000 mm (Tripathi et al., 2011). For every millilitres of water used, approximately 10 to 16 kg of maize grain is produced. To achieve a grain yield of 3152 kg ha<sup>-1</sup>, between 350 mm to 450 mm of rainfall is needed per year. Under optimal moisture conditions, each maize plant will use about 250 litres of water by the time it reaches maturity (Du Plessis, 2003).

**Temperature**

Maize is sensitive to the growing conditions such as temperature which ultimately influence its performance (Wu et al., 2024). During the day, the optimal temperature for maize ranges from 25 to 33°C, with 25–30°C being ideal for proper growth and development. At night, the suitable temperature is between 17 and 23°C, and maize can thrive as long as the night temperature does not drop below 15.6°C (Edmeades et al., 2017; Waqas et al., 2021). Soil inner temperature ranging from 26° to 30°C is optimum for both germination

and seedling growth. Maize crop reaches higher germination at 25–28°C (Waqas et al., 2021). Maize can grow within a temperature range of 9° to 46°C, with an optimal temperature of around 34°C. When average daily temperatures drop below 20°C, the crop's growth duration extends by 10–20 days for every 0.5°C decrease, depending on the variety.

However, maize tends to grow poorly in cold regions with temperatures below 5°C and in areas where temperatures exceed 40°C (Wu et al., 2024). These extreme temperatures can ultimately cause the plant's death. Maize grows within latitudes ranging from 58°N to 40°S and can thrive at altitudes from sea level up to approximately 3000 meters (Jaidka et al., 2020; Ragasa et al., 2013).

### **Nutrient requirements**

Maize requires a variety of soil nutrients for optimal growth, with nitrogen, phosphorus, and potassium being the most important. At maturity, a maize plant takes up 8.7 g of nitrogen(N), 5.1 g of phosphorus(P), and 4.0 g of potassium(K). For every ton of maize grain harvested, approximately 15 to 18 kg of nitrogen, 2.5 to 3 kg of phosphorus, and 3 to 4 kg of potassium are depleted from the soil (Du Plessis, 2003). Electrical conductivity (EC) levels below 1.7 dS m<sup>-1</sup> do not affect yield, but values between 2.5 dS m<sup>-1</sup> and 10 dS m<sup>-1</sup> can lead to yield losses ranging from 10% to 100% (Amer, 2010). A cation exchange capacity (CEC) greater than 24 cmol (+) kg<sup>-1</sup> is highly suitable for maize cultivation, while a CEC between 16 and 24 cmol (+) kg<sup>-1</sup> is moderately suitable. A CEC of less than 16 cmol (+) kg<sup>-1</sup> is considered marginally suitable for growing maize (Amer, 2010). Base saturation levels greater than 50% are considered highly suitable for maize cultivation. Levels

between 20% and 35% are moderately suitable, while base saturation below 20% is deemed marginally suitable (Alessana et al., 2015). Organic carbon content greater than 2% is highly suitable for maize cultivation. Levels between 1.2% and 2% are moderately suitable, 0.8% to 1.2% are marginally suitable, and values below 0.8% are considered unsuitable (Goswami et al., 2022; Lugato & Jones, 2015). Available phosphorus levels greater than 22 mg per kg are highly suitable for maize cultivation, while levels between 7 and 13 mg per kg are moderately suitable, and 3 to 7 mg per kg are barely suitable. For total nitrogen, levels greater than 0.15% are highly suitable, between 0.08% and 0.10% are moderately suitable, and 0.04% to 0.08% are slightly suitable (Ochieng et al., 2021).

### **Soil tillage**

Soil tillage refers to the physical, chemical, or biological alteration of the soil to improve conditions for germination, seedling establishment, and crop growth (Ref). It is defined as any process that physically loosens the soil through various cultivation methods, whether done manually or mechanically (Angon et al., 2023; Mehra et al., 2018). The choice of a tillage practice is influenced by various factors, including soil characteristics like organic matter, texture, relief, erodibility, structure, mineralogy and rooting depth. Climatic conditions such as rainfall, water balance, growing season length, and temperature also play a role. Crop-related factors like growing duration, rooting characteristics, and water requirements are important considerations, as well as socio-economic factors such as farm size, power source availability, family structure, and labour availability (Mehra et al., 2018; Steponavičienė et al., 2024).

Tillage is a high energy and capital demand activity as its practices requires high labour specifically in low resource agriculture practiced by small landholders. Recurrent soil disturbance can degrade soil structure, leading to compaction, low organic matter levels, and increased vulnerability to erosion and desertification (Taye et al., 2013).

Traditional soil management methods such as conventional tillage, often lead to the loss of soil, water, and nutrients, which can degrade the soil structure and decrease crop yields and efficiency. As a result, there's a growing emphasis on conservation tillage systems (Cárceles et al., 2022).

Conventional tillage involves soil cultivation to create a fine tilth, breaking up the soil through ploughing and harrowing before forming ridges. Vegetation may be cleared and partially decomposed or burnt to facilitate digging, incorporating residues into the soil (Youdeowei et al., 1986).

Conservation tillage preserves the roughness of the field surface and leaves most crop residues on the surface, which helps reduce water runoff and soil erosion (Carretta et al., 2021). It involves using tools like cutlasses, hoes, pickaxes, herbicides, or mulch tillage, which leaves crop residue on the soil surface to promote quick germination and satisfactory yields. Conservation tillage and no-tillage methods are favoured for soil conservation, as conventional tillage can be detrimental (Iqbal et al., 2005). Conservation agriculture has led to increased maize yields and greater profitability by lowering production costs (Saldivia-Tejeda et al., 2024).

When compared to traditional conventional tillage, conservation tillage has several advantages, including cost savings, protection against erosion, conservation of soil and water, and enhanced fertility (Arshad et al., 2023;

Duchene et al., 2023). It enhances the storage of water in the soil and increases soil macro-porosity. Research has shown that different tillage practices can have varying effects on soil bulk density and hydraulic conductivity (Khan et al., 2017; OKORIE et al., 2022; Steponavičienė et al., 2024).

Effective tillage systems are those that create optimal conditions for seed germination, plant growth, and root development. The right tillage practices can prevent soil degradation while maintaining crop yields and ecosystem stability. The best management practices involve the least amount of tillage necessary for crop growth, which not only saves energy but also maintains soil productivity (Wasaya et al., 2019).

### **Importance of Tillage**

Effective tillage systems establish optimal conditions in the seedbed, such as appropriate moisture, temperature, and penetration resistance, which are essential for plant emergence, development, and unobstructed root growth (Blanco & Lal, 2023). Manipulating the soil can significantly alter its fertility status, resulting in either beneficial or detrimental effects on crop performance. The primary goal of tillage is to create a soil environment conducive to plant growth by modifying its physical properties to help plants achieve their full potential (Carter & McKyes, 2005). Techniques like ploughing are used to ensure good seedbed and root development, weed control, residue management, erosion reduction, and to level the soil surface for planting, irrigation, and incorporation of fertilizers or pesticides. However, subsoil compaction can reduce water and nutrient availability, thus lowering crop yields (Khurshid et al., 2006).

Tillage has shown to have a significant impact on maize growth and yield parameters, as well as soil properties, contributing up to 20% to crop production factors (Khurshid et al., 2006). Primary tillage treatments for maize include conventional tillage, that is ploughing and harrowing.

### **Tillage effects on soil properties**

#### **Tillage Effects on Soil Water Content and Water Use Efficiency**

Tillage effects vary across agro-ecological zones. In semi-arid regions, moisture conservation is crucial (El Mekkaoui et al., 2023). Abdullah (2014) discovered that tillage and residue management helped increase soil water content. Another study demonstrated that no-till soils retained the highest moisture, followed by minimum tillage, raised bed, and conventional tillage (Skaalsveen & Clarke, 2021). Tillage treatments also affect water intake and infiltration rates. Several researchers have highlighted the importance of tillage for soil moisture management (Hu, 2022). Tillage improves soil water content by improving its surface roughness and managing weeds during fallow periods, which can boost crop production in subsequent seasons by supplementing precipitation during the growing period (Alsamin et al., 2022). Studies have shown that deep tillage significantly enhances water storage and crop production.

Tillage practices have significant impacts on water use efficiency (WUE). Research has found that tillage practices have impacts on soil environmental factors and thus on the crop yield too. For instance, a study found that subsoiling tillage combined with straw incorporation improved the soil moisture content, reduced soil temperature, boosted water consumption patterns, and enhanced the effective use of soil water (Peng et al., 2023). This



led to the accumulation of a higher biomass yield and overall yield, a greater number of ears, a higher and enhanced water use efficiency.

Another study conducted on wheat showed that Long-term conservation tillage can increase yield and WUE of crops by regulating substances related to stress, no-tillage with straw mulching improved the soil's physical and chemical properties, maintained higher soil water content, and increased dry matter accumulation along the growth stage ( Du et al., 2023). It led to higher grain yields and WUE compared to other tillage practices. This has been confirmed by another research by Ali et al. (2017), which reported that crop yield was enhanced by more than 30%, and water use efficiency (WUE) ranged from 0.7 to 5.7 kg/m<sup>3</sup> for wheat, corn, and flax, and from 30 to 40 kg/m<sup>3</sup> for vegetables. The WUE is very sensitive to the topography, as the soil susceptible to erosion and rapid water loss. This study is held on the assumption that the tillage influences the soil properties that later have an effect on the growth parameters of maize through the roots.

### **Tillage and Topography Interaction**

The interaction between tillage practices and topography can also influence water use efficiency. For example, on sloping lands, certain tillage practices can help reduce runoff and increase water infiltration, thereby improving water use efficiency. Coupled with the spatial variability in topography across a field it can lead to differences in water availability and use, which can be managed through site-specific tillage practices (Tobiašová et al., 2023).

### **Tillage effects on soil porosity**

Soil porosity properties are crucial for soil physical reactions, overall root penetration, and water flow and vary among tillage methods (Sasal et al.,

2006). It was found that returning the straw could enhance total soil porosity, while conservative tillage like minimal and no-tillage reduce soil void spaces but increase its capillary properties, enhancing soil water capacity and poor aeration (Chen et al., 2020; Głab & Kulig, 2008). It was also observed no significant impact of tillage and straw methods on the soil total porosity and its porosity size distribution (J. Wang et al., 2024). Tangyuan et al. (2009) showed that soil total porosity at the 0–10 cm depth is most affected by conventional tillage which tend to increase soil capillary porosity.

### **Tillage Effects on Soil Bulk Density**

Soil bulk density is a key soil physical property that significantly influence hydraulic conductivity, a crucial factor in soil compaction and agricultural management (Assouline, 2011). Bulk density represents the mass of soil solids per unit volume, where high bulk density indicates soil compaction, reducing pore space for water movement and root growth. It is generally influenced by organic matter content. Effective porosity refers to the proportion of soil volume available for water movement, with high porosity enhancing water infiltration, aeration, and nutrient transport (Tiab & Donaldson, 2004). Soil structure significantly affects porosity and Hydraulic conductivity and measures how easily water moves through the soil (Jabro, 1992).

Studies comparing no-tillage with conventional tillage have shown mixed results. Some studies found greater bulk density in no-till soils at 5 to 10 cm depth (Osunbitan et al., 2005), while others found no differences. (Tripathi et al., 2005) reported increased bulk density with conventional tillage in silty loam soil. It has been noted the highest soil bulk density ( $1.52 \text{ g cm}^{-3}$ ) and penetration resistance (1250 kPa) in no-till, and the lowest ( $1.41 \text{ g cm}^{-3}$  and

560 kPa) in conventional tillage, with higher soil moisture content (19.6%) in conventional tillage and lower (16.8%) in no-till (Rashidi & Keshavarzpour, 2008).

### **Tillage effects on the environment**

Tillage practices have significant effects on the environment, particularly concerning soil health and carbon emissions. A meta-analysis by Allam et al. (2021) highlighted the importance of environmental and agronomical factors in understanding how conservation tillage can impact crop yield by adopting environmentally friendly fertilization sources. Conservation tillage, which includes methods like no-tillage, strip tillage, minimal tillage, and reduced tillage, is shown to decrease soil CO<sub>2</sub> emissions without reducing crop yields. This increases net ecosystem productivity (NEP) and has a positive effect on ecosystem carbon balance (Xue et al., 2024).

Sustainable tillage practices help protect the soil from water and wind erosion and runoff, minimize the leaching of chemicals into water bodies, and enhance soil moisture retention by optimizing soil porosity (Šarauskis et al., 2018).

Light tillage practices and no-tillage methods aim to reduce the negative effects on soil quality and help preserve soil organic carbon (Haddaway et al., 2017). In contrast, intensive soil cultivation breaks down soil organic matter (SOM), producing CO<sub>2</sub> and lowering soil carbon sequestration. Building SOM through conservation tillage, especially with crop residue return, can substantially reduce CO<sub>2</sub> emissions (Xue et al., 2024). In the UK, conservation tillage led to an 8% higher soil carbon content compared to conventional tillage, equivalent to 285g SOM m<sup>-2</sup>. The No-tillage was introduced to this

study as a solution to the problem raised by the conventional tillage and help to understand at what extent

### **Tillage effects on crop yield**

The impact of tillage systems on crop yield varies among crop species and soil types. Murillo et al. (2004) compared traditional conventional tillage, where the soil was ploughed to a 30 cm depth after burning the previous crop's straw, with conservation tillage, where crop residues were left as mulch, and minimum vertical tillage (chiselling to 25 cm depth) and disc harrowing (5 cm depth) were conducted. Their results showed higher crop yields with conservation tillage.

Extensive published data indicates that crop yields are generally higher with conventional tillage compared to conservation tillage. However, numerous studies present conflicting findings. In both scenarios, the economic aspects of tillage practices, such as energy and labour costs and the capital investment in equipment, are often not taken into account. A study by Rashidi & Keshavarzpour (2007) revealed that the tillage method had a significant impact on the number of plants per hectare and the number of rows per cob, with the former being the primary yield component influencing maize grain yield across different tillage practices. The highest plant population per hectare was recorded under the mouldboard plough plus two passes of disc harrow by two passes of disc harrow, while the lowest was observed under the no-tillage system. The findings indicated that tillage methods significantly affected maize grain yield in the descending order of - mouldboard plough plus two passes of disc harrow followed by - mouldboard plough combined with one pass of rotary tiller followed by - Two passes of disk harrow

followed by – A single pass of tine cultivator combined with a single pass of disk harrow followed by - One pass of rotary tiller then One pass of tine cultivator and at the last position, the no-tillage, primarily due to differences in plant population per hectare. Consequently, mouldboard ploughing combined with disc harrowing proved to be a more effective and profitable tillage approach for enhancing maize grain yield, as it reduced soil compaction, improved seed-to-soil contact, increased soil moisture retention, and suppressed weed growth. Evaluating the effect of tillage on different crop parameters and the yield is key factor in addressing its negative impact on the soil and may help the farmer decide of the equipment or the tillage system to use.

### **Remote sensing and Unmanned Aerial Vehicle Technology**

Remote sensing is a technology used to detect and measure radiation across various wavelengths that is reflected or emitted by distant objects or materials, enabling their identification and classification. It offers a powerful method for observing and monitoring the physical characteristics of an area from a substantial distance (Kumar et al., 2019).

The concept of remote sensing can be traced back to the 16th century with Galileo Galilei, who used a telescope to observe celestial bodies. The modern form of remote sensing began with the advent of photography in the 19th century, where cameras attached to balloons were used for topographic purposes (Efremenko & Kokhanovsky, 2021). In remote sensing, special cameras or sensors collect images or data, typically from satellites, aircraft or unmanned aircraft. These digital sensors measure the electromagnetic radiation reflected or emitted from both sources in the atmosphere and on the

earth surface. Various materials reflect and absorb different wavelengths of electromagnetic radiation, which helps identify the type of material based on its spectral signature.

For instance, vegetation strongly absorbs wavelengths of visible (red) light and reflects wavelengths of near-infrared light, which is invisible to human eyes<sup>1</sup>. Water absorbs longer visible wavelengths (green and red) and near-infrared radiation more than shorter visible wavelengths (blue), making water appear blue or blue-green (Horning, 2019).

Despite its wide range of applications, remote sensing faces challenges such as the need for high-resolution data, cloud cover interference, and the requirement for advanced data processing techniques. However, ongoing research and technological advancements continue to push the boundaries of what remote sensing can achieve (Abdelmajeed & Juszczak, 2024).

Unmanned Aerial Vehicles (UAVs), also known as drones, are miniature aircrafts that operate without a pilot on board. They can function autonomously or be remote-controlled. UAVs have gained significant attention in the last decade due to their wide range of applications and advancements in control, miniaturization, and computerization (Ahmed et al., 2022; Mohsan et al., 2023).

UAVs are equipped with payloads such as cameras, radar, and sensors for different applications. These payloads are supported by data systems like GPS trackers and wireless connectivity, allowing the components to work together from afar. This makes UAVs highly versatile, capable of performing tasks like photography. The operation of a UAV involves several components, including a physical model, a Ground Control Station (GCS), advanced sensors, and a

mean of communication between them. The flight dynamics of UAVs are an essential aspect of their operation (Colomina & Molina, 2014). These dynamics involve the forces and moments that affect the motion of the UAV, including lift, drag, thrust, and weight.

One of the primary challenges in UAV technology is flight endurance, which is constrained by the power provided by batteries. This issue can be addressed through the development of various battery types, the use of hybrid systems, or the incorporation of internal combustion engines. Additionally, docking stations present a promising solution, as they can recharge or swap batteries, store UAVs, and even handle communication tasks (Pekias et al., 2022).

### **Remote sensing applications in agriculture**

Agricultural stakeholders, including farmers, agricultural cooperatives, and local, national, or international authorities, must balance multiple objectives: maintaining economically viable operations, ensuring sufficient agricultural production to feed a growing population, and mitigating negative environmental impacts by minimizing resource depletion and contributing to climate change mitigation. Remote sensing, as a non-destructive method for spatially and temporally monitoring vegetation, emerges as an essential tool to support these efforts (Weiss et al., 2020). Remote sensing can aid in identifying new crop varieties better suited to challenging conditions (e.g., phenotyping), monitoring agricultural land use, forecasting within-season crop production, optimizing short-term production, and providing ecosystem services related to soil and water resources, as well as supporting animal and plant biodiversity (Weiss et al., 2020).

### **Application of UAV technology in crop phenotyping of maize**

Remote sensing has emerged as a transformative tool in crop phenotyping and breeding, offering non-destructive, spatially extensive, and temporally continuous monitoring of agricultural landscapes. This technology plays a critical role in modern agriculture by providing valuable data that supports the selection of superior cultivars, enhances crop management practices, and accelerates breeding programmes (Pinto et al., 2023).

Traditionally, crop phenotyping involved manual measurements of plant traits, which were labour-intensive, time-consuming, and often subject to human error. Remote sensing, however, enables the automated collection of phenotypic data across large areas, improving the efficiency and accuracy of these measurements (Herr et al., 2023; Kharraz & Szabó, 2023). This method encompasses a range of technologies, including satellite imagery, aerial photography from drones (UAVs), and ground-based sensors, each providing different scales of observation and levels of detail.

High-throughput field phenotyping, facilitated by remote sensing, allows researchers to assess numerous genotypes under realistic field conditions. Unlike controlled environment studies, which may not fully replicate the complexities of field environments, remote sensing captures data on crop performance in actual agricultural settings. This is crucial for understanding how different cultivars respond to real-world conditions, including varying soil types, weather patterns, and management practices (Pinto et al., 2023).

Key to remote sensing in crop phenotyping is the use of various spectral bands to capture detailed information about plant health and development. Multispectral and hyperspectral imaging are particularly valuable, as they can



detect specific wavelengths of light reflected by plants, revealing information about their physiological status (Omia et al., 2023; Wong et al., 2023).

Han et al. (2019) utilized a high-throughput phenotyping (HTP) platform mounted on an unmanned aerial vehicle (UAV) to gather RGB and multispectral images for a maize breeding program. Through this approach, they successfully measured various phenotypic traits, including plant height, normalized difference vegetation index (NDVI), biomass accumulation, plant height growth rate, lodging, and leaf colour. This approach collected more data on a single pass than the manual data collection.

The integration of remote sensing data with machine learning algorithms has further revolutionized crop phenotyping. Machine learning models can analyze vast amounts of data to identify patterns and predict outcomes, facilitating the identification of superior genotypes. For instance, deep learning techniques have been employed to classify plant species, detect diseases, and estimate crop yields with high accuracy. These models require extensive training datasets, which remote sensing can provide, ensuring robust and reliable predictions (Sheikh et al., 2024).

### **UAV estimation of plant height**

The use of Unmanned Aerial Vehicles (UAVs) for estimating plant height has emerged as a highly effective method in precision agriculture, offering several advantages over traditional ground-based measurements. UAV-based estimation provides rapid, high-throughput, and non-destructive means to monitor crop growth and development (Anthony et al., 2014; X. Han et al., 2018).

The first stage of the process is the data acquisition where UAVs are equipped with various sensors, including RGB cameras, multispectral cameras, and LiDAR (Light Detection and Ranging) sensors. These sensors capture high-resolution images and point cloud data of the crop fields from above across the whole field. This stage is then followed by the Image Processing that involves Structure from Motion (SfM) techniques to reconstruct the 3D structure from 2D images. Structure from Motion (SfM) involves the creation of 3D models from 2D images captured from multiple viewpoints (Schönberger & Frahm, 2016). SfM is particularly beneficial in agricultural applications due to its ability to generate detailed and accurate 3D representations of crop canopies. SfM software identifies common features (e.g., distinct points, patterns) in the overlapping images. Algorithms like SIFT (Scale-Invariant Feature Transform) (Lindeberg, 2012) or SURF (Speeded-Up Robust Features) (Bay et al., 2008) detect and match these features across the image set. By analysing the matched features, SfM estimates the relative positions and orientations of the UAV's camera for each image. This process is known as camera pose estimation and is fundamental to reconstructing the 3D structure.

The height estimation is then derived from the Digital Surface Model (DSM) by subtracting its value to the Digital Terrain Model as both represents the elevation of the crop canopy and bare ground. It is derived from the 3D point cloud data or photogrammetry-based models. This study implements the UAV imagery in plant height estimation. The topic has gain focus but its evaluation under different tillage treatment has not gain so much attention, specifically knowing that farm operations may affect growth parameters and influence the

performance of remote sensing methods, such as the sowing space that affect the LAI further impacting the accuracy of the CSM.

### **Application of the UAV technology in crop yield prediction**

The simplest method to connect remote sensing with yield involves establishing empirical relationships between field yield data and remotely sensed indicators. One common approach uses the peak NDVI (Normalized Difference Vegetation Index) from coarse spatial resolution time series (approximately 5.5 km) (Becker-Reshef et al., 2010). This can be refined for example by incorporating cumulative temperature sums to anticipate the peak (Franch et al., 2015). Some studies have explored other indices, including phenological metrics from vegetation index time series to enhance yield estimates (Bolton & Friedl, 2013; Sakamoto et al., 2014). Yield quality, which is more genotype-dependent and harder to assess, has been less frequently studied (Moriondo et al., 2007; Wang et al., 2014). These methods are typically applied to homogeneous landscapes, such as those in the US and China. In more heterogeneous agricultural landscapes, like those found elsewhere, the diversity of crop types and management practices complicates yield estimation (Duveiller & Defourny, 2010).

Theoretically, any empirical yield-satellite relationship could be replaced by dynamically integrating remote sensing products into a mechanistic crop growth model. This could facilitate near real-time forecasting and potentially simulate future crop growth based on seasonal weather forecasts (Weiss et al., 2020).

Models for predicting crop yield using remote sensing data include statistical models, machine learning models, process-based models, and hybrid

approaches. Statistical models, like regression and time-series analysis, correlate yield with remote sensing-derived variables such as vegetation indices. Machine learning models, including Random Forests, Support Vector Machines, and Neural Networks, manage large datasets and capture complex, non-linear relationships (Joshi et al., 2023).

Hybrid models combine statistical, machine learning, and process-based elements to utilize their combined strengths (Blessie et al., 2024). Data assimilation techniques integrate remote sensing observations with process-based models, while coupled models merge different modelling approaches for improved predictions. Remote sensing data sources include satellite imagery (Landsat, Sentinel-2, MODIS), aerial imagery from UAVs, and ground-based sensors (Gao, 2021; Soccolini & Vizzari, 2023).

Applications of these models include using NDVI for yield prediction in regression models, applying machine learning in precision agriculture, and utilizing process-based models like DSSAT and APSIM for simulating crop growth (Blessie et al., 2024). These models are crucial for providing accurate, timely insights into crop performance, and supporting sustainable and efficient agricultural practices through advanced remote sensing and computational methods. In the era of data-driven decision-making scheme, implementing the UAV imagery at a small-scale farming, more specifically the yield prediction enhances the response time of farmers and policy makers.

### **Use of Deep learning approach in Agriculture and maize production**

Deep learning has made a major improvement the field of computer vision, particularly in object classification and detection. Object classification involves identifying the category of objects within an image, while object

detection extends this by going beyond classification by localizing target objects in the image (LeCun et al., 2015).

Initially, object classification and detection relied on traditional machine learning techniques with handcrafted features. Algorithms such as the Histogram of Oriented Gradients (HOG) and Scale-Invariant Feature Transform (SIFT) were used extensively. However, these methods had limitations in handling variations in object appearance and environmental conditions (Routray et al., 2017).

The breakthrough in deep learning for object classification came with the introduction of Convolutional Neural Networks (CNNs), particularly with the success of AlexNet in the ImageNet competition in 2012. CNNs automatically learn hierarchical features from data, making them significantly more powerful than traditional methods (Liu et al., 2023).

CNNs is made of a bunch of layers, among them, the convolutional layers, pooling layers, and fully connected layers. These networks have shown remarkable success in object classification tasks. Key architectures such as VGGNet, ResNet, and Inception have pushed the boundaries of performance on benchmarks like ImageNet (Liu et al., 2023).

For object detection, Region-based CNNs (R-CNN) were a significant advancement. R-CNNs generate region proposals and classify them using CNNs. Fast R-CNN and Faster R-CNN are its major improvements by making use of the region proposal network (RPN) within the CNN, enhancing both speed and accuracy (S. Ren et al., 2016). Different algorithms have been introduced since aiming at bringing efficiency and accuracy in object detection.

YOLO (You Only Look Once) introduced a real-time object detection framework by framing detection as a regression problem, directly predicting class probabilities and bounding boxes of target objects from the full images in one evaluation. YOLO's architecture enables fast and efficient object detection, making it suitable for real-time applications (Jocher et al., 2023; Treven & Cordova-Esparaza, 2023).

Similar to YOLO, The Single Shot MultiBox Detector (SSD) performs object detection in a single pass through the neural network. It divides the output space of bounding boxes into a set of default boxes with different aspect ratios and scales at each feature map location. SSD's efficiency and accuracy have made it widely used in various applications (Liu et al., 2016).

Those deep learning models have shown great performance as their improvement has been sustained by advanced techniques such as Transfer learning, generative adversarial networks or data augmentation.

Transfer learning is the mechanism of leveraging pre-trained models on large labelled datasets like ImageNet and fine-tuning them on specific tasks. This method has been proven to be useful in improving performance and reducing training time for object classification and detection (Houlsby et al., 2019).

Data augmentation algorithms such colour jittering, flipping and random cropping, have been essential in enhancing the strength and generalization of DL models. These techniques help in artificially increasing the diversity of training data (Shorten & Khoshgoftaar, 2019).

Generative Adversarial Networks (GANs) have been used to generate synthetic data for training object detection models. This is especially useful in scenarios where labelled data is scarce. GANs can create realistic images that

augment the training dataset, improving model performance (Goodfellow et al., 2020).

Deep learning models require large amounts of labelled data for training. Obtaining and annotating such data can be expensive and time-consuming (Whang et al., 2023). Implementing deep learning training processes is computationally high resource demand, necessitating adequate hardware, like GPUs or TPUs, which may not be accessible to all practitioners. Deep learning models, especially deep CNNs, are often considered black boxes due to their complex architectures. Improving the interpretability and explainability of these models remains a significant challenge (Talaie Khoei et al., 2023).

The applications of deep learning methods in crop sciences can be divided into three categories: classification, detection, and segmentation. For the purpose of this work, only the first two have been described.

### **Plant Classification**

Classification is the most fundamental image understanding task and was the first area where deep learning models made significant breakthroughs and achieved large-scale applications. Numerous studies have successfully used various convolutional neural network (CNN) models to classify plant images. Frequently used models include ResNet (19 times), VGG (7 times), DenseNet (7 times), Inception (6 times), EfficientNet (5 times), transformer-based models (4 times), MobileNet (3 times), and Xception (1 time) (Chen et al., 2023).

In the classification process, features are gathered from plant images using convolutional layers and then combined in the Dense layer (Fully connected layers), which produces a value. The softmax function then normalizes the

network's output, providing probability scores for the predicted classes, with the final classification result determined by the highest probability. However, because of parameter redundancy in the FC layer, high-performing models like ResNet and GoogLeNet use global average pooling (GAP) instead, which reduces the number of parameters and improves prediction performance (Xu et al., 2021).

Some studies use classifiers other than the softmax function, such as random forest or support vector machine (SVM). SVM is the most commonly used and often provides the best results (Mathur & Foody, 2008).

### **Plant Detection**

Unlike image classification, target detection addresses both classification and positioning problems. Common models for plant image detection include YOLO (24 times), Faster R-CNN (6 times), CenterNet (4 times), SSD (2 times), RetinaNet (1 time), and a transformer-based model (1 time). Detection models are divided into region-based and region-free categories (Chen et al., 2023).

Faster R-CNN, a notable region-based method, comprises four sections: feature extraction components, region proposal network, Region of Interest pooling, and classification. Feature extractors create image feature maps, often replaced with classic alternatives to find the best match. The region proposal network generates region proposals, with anchor boxes selected through experience, K-means clustering, or as hyperparameters (S. Ren et al., 2016). The RoI pooling layer collects feature maps and proposals, sending them to the classification layer to determine the target category, while bounding box regression obtains precise detection frame positions. Region-based models like



Faster R-CNN achieve high detection accuracy but are complex and slow. Region-free methods (S. Ren et al., 2016), like YOLO, treat object detection as a regression problem, directly regressing class probability and position coordinates. YOLO divides each image into grids, assigning each grid to detect targets if the target's centre falls within it, predicting bounding boxes, confidence scores, and conditional probabilities (Treven & Cordova-Esparaza, 2023).

While these algorithms approximate target positions using bounding boxes, they cannot precisely extract contour and shape information. Mask R-CNN (He et al., 2017), however, predicts accurate contour information along with position, providing a more detailed analysis.

## CHAPTER THREE

### MATERIALS AND METHODS

#### Study area

##### Location of the study area

This study was conducted at the Teaching and Research farm of the University of Cape Coast in the Central Region of Ghana as shown in Figure 1 below. The site is geo-located at Lat.  $5^{\circ}07'52.2''$  N and Long.  $1^{\circ}17'31.8''$  W. The site lies within the Coastal Savanna Agro-ecological zone of Ghana.

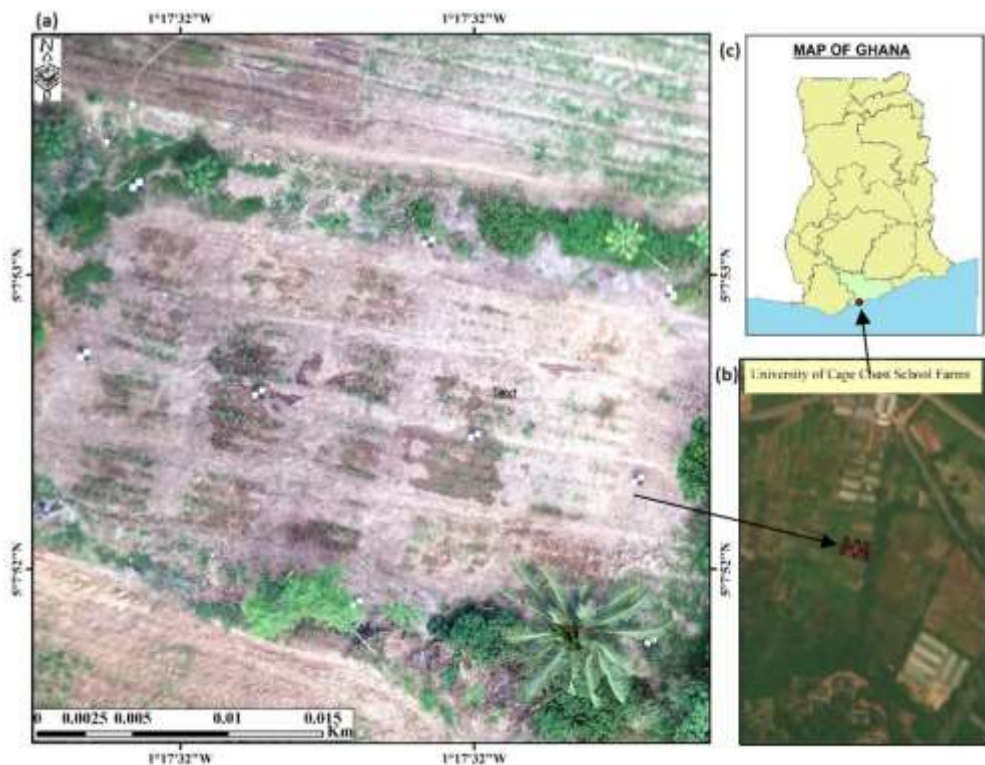


Figure 1: Location of the study site (a) experimental area, (b) the University of Cape Coast research farms, (c) the Central region in Ghana.

##### Climate Conditions

The site usually experiences two rainfall seasons: a major season from March to July and a minor season from September to November. A long dry season follows, lasting from December to February. Temperatures remain relatively

uniform throughout the year, with a mean annual minimum of 25°C and a mean annual maximum of 29°C. Diurnal temperature variations are most pronounced in February and March, while August is the coolest month and March the hottest (Nkrumah et al., 2014). Relative humidity is generally high, ranging from 80 % to 90 % during the night and early morning, dropping to about 70 % in the afternoon. Humidity levels are higher during the rainy season compared to the dry season (Nkrumah et al., 2014).

However, due to climate change, there have been some variations observed in the patterns of the seasons.

The weather conditions for the two seasons show slight variations in temperature but significant differences in precipitation. In Season One, the minimum temperature is 22°C, while in Season Two, it is slightly higher at 23°C. The maximum temperature remains constant at 34°C in both seasons. However, there is a substantial difference in total precipitation, with Season One receiving 220mm of rainfall, whereas Season Two experiences a significantly higher 1133 mm.

### **General Description of Soils and Relief**

At the beginning of the experiment, a soil analysis was conducted to determine the physio-chemical properties of the soil. Soil samples were taken over the whole study area at a mean depth of 20 cm using auger and other standard tools. They were bulked together for soil analysis after air-drying it in the laboratory. Its results are presented in Table 1.

**Table 1: Soil physio-chemical properties at the experiment site**

Soil Property	Value
Sand (%)	79.65
Silt (%)	8.59
Clay (%)	11.76
Organic Carbon (%)	1.073
Organic Matter (%)	1.849
pH	5.17
Total N (%)	0.120
Exch. $\text{Ca}^{2+}$ (cmol $\text{kg}^{-1}$ )	6.30
Exch. $\text{Mg}^{2+}$ (cmol $\text{kg}^{-1}$ )	3.10
Exch. $\text{K}^{+}$ (cmol $\text{kg}^{-1}$ )	0.495
Available P (Mg $\text{kg}^{-1}$ )	55.05
Exch. $\text{Na}^{+}$ (cmol $\text{kg}^{-1}$ )	0.101
ECEC (cmol $\text{kg}^{-1}$ )	2.722

Exch. = Exchangeable

The soils at the study site originate from Sekondian rocks, mainly consisting of shales, sandstones and conglomerates from the Devonian period. The area is located on sloping to gently undulating terrain and includes the Edina, Atabadzi, Benya, and Udu compound association. These soils are highly weathered, base-depleted, and acidic. They are primarily composed of low-activity kaolinite clays and sesquioxide's (Asamoah, 1973).

The elevation above sea level varies from 15.2 to 30.5 meters. The highest points, reaching approximately 30 meters, are two hills located in the southern

part of the farm sites. Most of the poorly drained valley bottoms and flat plains have not been cultivated due to the waterlogged condition of the soil.

## **Materials**

### **Planting materials**

The *Abontem* maize variety seeds produced by the Crops Research Institute of the Council for Scientific and Industrial Research (CSIR -CRI) were used as planting material. The *Abontem*, is an early-maturity maize variety (Abdul Rahman et al., 2022; Ofori et al., 2019).

### **Tractor and Implements**

The tractor used for the tillage is a CASE III brand, model JX75T which is configured as a 4-wheel drive (4WD). It has a 4-cylinder engine with a displacement of 3908 cubic centimetres, 55 kW (75 hp) power and a rated speed of 1400 revolutions per minute. Its wheelbase measures 2160 mm (4WD), while ground clearance reaches up to 500 mm at the front axle and 490 mm at the rear. The implements used for tillage in this study included a disc plough and a disk harrow, each with distinct specifications. The disc plough featured three discs, a weight of 550 kg, a working width of 990 mm, and a working depth of 250 mm. The disk harrow, on the other hand, had 16 harrows, weighed 800 kg, and offered a broader working width of 1800 mm and a working depth of 200 mm, with the discs set at a 36-degree angle.

### **Equipment for Field data collection**

The equipment used in the study included a Penetrometer: Eijkelkamp Penetrologger (Eijkelkamp Agrisearch Equipment, Giesbeek, the Netherlands), a specialized device for measuring soil penetration resistance,

which is a key indicator of soil compaction. It is a digital cone penetrometer that records the force required to push a standardized cone into the soil at a constant speed, typically down to a specific depth. This was done prior to the application of the treatments to the various plots and eventually, the average penetration resistance for the field were found to be 1.12 MPa and 1.046 MPa for seasons one and two respectfully.

A vernier calliper was utilised to measure stem diameter, while a Ceptometer (ACCUPAR LP-80, METER Group, Inc., USA) was employed to measure the Leaf Area Index. Additionally, a 5 m measurement tape was used to measure plant height, and a precise balance was used to weigh yield components.

### **Unmanned Aerial Vehicle technology**

**Drone:** UAV flights were carried out using a DJI Phantom 4 Pro (DJI, Shenzhen, China) equipped with a DJI FC6310S RGB camera of 5472 x 3648 resolution, 8.8 mm focal length, and 2.41 x 2.41  $\mu\text{m}$  pixel size.

**RTK:** An EMLID Reach RTK was used to take the geo-coordinates of the Ground Control Points (GCPs) at a centimetre-level precision. It aimed at enhancing the accuracy of recorded coordinates during flight missions. This involved the use of two GPS units, with one fixed for estimating the error of each geographic coordinate recorded called base station, and another in motion to capture the coordinates of control points, called rover. These control points have been subsequently employed for model calibration and precision measurement.

**Ground Control Points:** 10 GCPs were installed on the field. Each GCP had a square dimension of 60 cm and was painted black and white.

ArcGis: The ArcMap 10.5 software (Esri Inc., Redlands, California, USA) was used for further analysis, —specifically, Raster Calculator and Zonal Statistics.

Metashape: AgiSoft PhotoScan Professional (Version 2.2.1) was used to carry the images procession from pictures retrieved by the UAV to output the Digital Surface Model and Orthomosaic photo of the surveyed area.

## **Methods**

### **Experimental design**

The experimental was laid out in a Randomised Complete Block Design (RCBD) with four treatments (i.e. ploughing only, ploughing followed by harrowing, harrowing only, and No-tillage). There were five replicate blocks making a total of twenty plots as shown in Figure 4 below. Each plot measured 3 m x 4 m size and had a planting distance of 75 cm x 40 cm and a plant population of 40 plants. The alleys created within and between blocks measured one (1) and two (2) m respectively

A brief description of the tillage treatments considered are as follows:

No-tillage (NT): The soil remains undisturbed, with no mechanical intervention.

Disc ploughing (P) only: A tractor-mounted disc plough was employed to invert and bury crop residues and weeds.

Disc Harrowing (H) only: A tractor-mounted disc harrow was utilised to prepare the soil at 20 cm depth.

Disc ploughing followed by harrowing (Ploughing and harrowing - PH): A tractor-mounted disc plough was used at first pass, and the following day a disc harrow was used to cut and turn the soil.

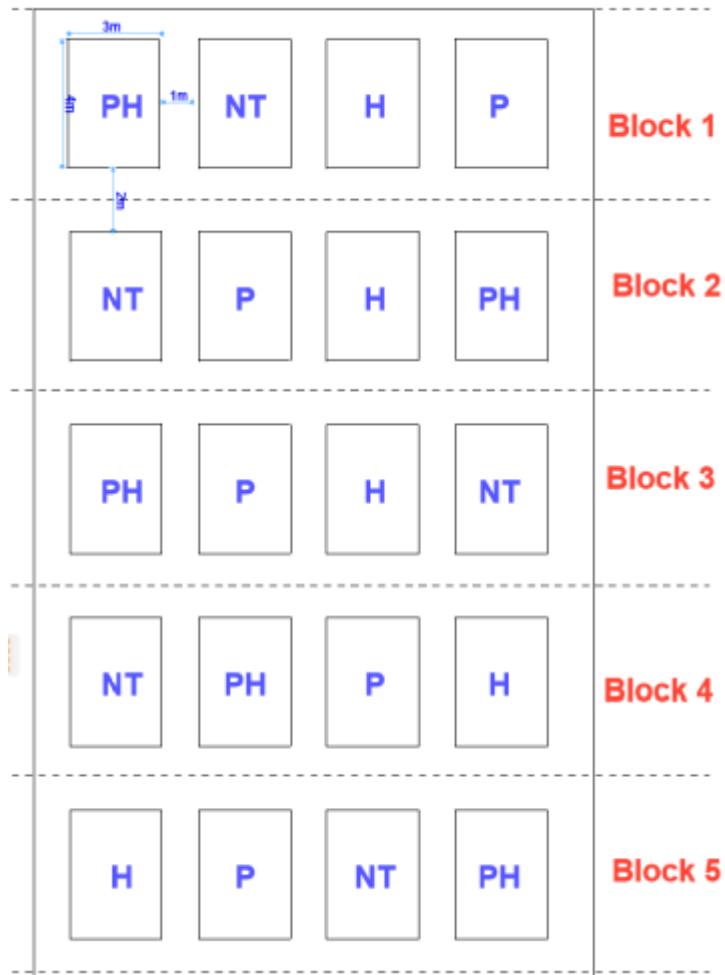


Figure 2: Experiment layout

### Cultural practices

Weed control was performed using a combination of chemical and mechanical methods. At the beginning of each growing season, Paraquat herbicide was applied before tillage to effectively suppress weed growth and prepare the field. Subsequently, manual weed control using hand hoes on weekly basis were carried out from time to time to ensure the field remained clear for UAV image capturing. It was ensured that on no-till soils, very minimum soil disturbance was done with the hoe while weeding.

The plant density was managed after germination by thinning out excess plants to retain only the healthiest individuals. This practice minimised



competition for nutrients, water, and light, promoting uniform growth across the field.

To protect the crop from pest attacks, spraying was conducted every two weeks to manage armyworm infestations, ensuring the maize plants remained healthy throughout the growing period.

### **Manual Field data collection**

#### **Plant height determination (cm), stem diameter (cm), and number of leaves**

Six plants were tagged in the middle in each plot for the data collection. The manual data collection was taken once a week for the two seasons. The plant height was determined by taking the height of the plant from the soil level to the highest leaf on the plant using a 5 m tape and the stem diameter was also taken by a vernier calliper and recorded. Fully deployed leaves were manually counted and recorded per plant.

#### **Leaf Area Index (LAI) measurement**

In each plot, an area of 1.8 m<sup>2</sup> which comprised of the six selected plants was used to determine the LAI representative of the plot. An Accupar Ceptometer (ACCUPAR LP-80, METER Group, Inc., USA) was used to record the LAI. Each measurement was repeated three times in each plot.

#### **Above ground dry biomass determination**

The determination of the above-ground dry biomass of maize was conducted after harvesting. All six tagged plant materials, excluding the roots and cobs, was weighed per plot. A sample of the biomass was taken to the laboratory and dried in an oven at 70°C for 24 hours to expel the moisture

content. Once the sample was dried, the percentage of dry matter was calculated using the formula:

$$\% \text{ Dry Matter} = \frac{\text{Dry weight}}{\text{Fresh weight}} \times 100 \quad (1)$$

Where:

Dry Weight: weight of the sample after oven drying

Fresh Weight: weight recorded in the field.

### **The Maize root system architecture determination**

The root architecture of maize is a crucial determinant of its ability to acquire water and nutrients, thereby influencing crop productivity.

To assess the root architecture, the maize plants were carefully excavated at physiological maturity stage. In the first instance, the soil surrounding the root system of each plant was gently loosened using water to minimize root damage. The entire root system was then carefully extracted from the soil, ensuring that the roots remained intact. Each plant was uprooted carefully and excess soil was removed by gently shaking the root system. The roots were thoroughly washed afterwards with water to remove any remaining soil particles. It was ensured that this was done with special care to avoid breaking fine roots during the process.

Once cleaned, the root systems were prepared for imaging. The roots were spread out on a transparent tray filled with water to minimize overlapping and ensure a flat orientation for imaging. A high-resolution professional camera NIKON D5600 (NIKON Corporation, Japan) with a 55 mm focal length and 300 dpi resolution was used to capture images of the root systems. The resolution and settings were adjusted to ensure that fine root structures were clearly visible.

The images were pre-processed to enhance contrast and remove background noise using ImageJ software. This step included converting images to grayscale, adjusting brightness and contrast, and applying filters. The roots system was then segmented from the background using Otsu thresholding techniques (Otsu, 1979). Segmented images were then converted into binary format, where roots appeared as white pixels against a black background. The root architectural traits were quantified using WinRHIZO. The analysis focused on measuring key parameters, including Total Root Length, Root Surface Area, Root Volume, Root Diameter Distribution and Root Branching Pattern.

The data obtained from the root analysis software were further processed to assess the root architecture's relationship with the treatments.

#### **UAV data collection**

The design and execution of flight plans went through several stages as illustrated in the figure 3. Before creating the flight plans, a comprehensive terrain reconnaissance was done. This step aimed at evaluating the surface conditions that would be covered during the drone flights, identify natural obstacles to be avoided during flight, locating and positioning the GCPs and determining the drone's starting point. The Pix4D mobile application was utilized due to its capability to adapt the flight plan to the specific terrain, thereby maintaining a consistent spatial resolution throughout the flight.

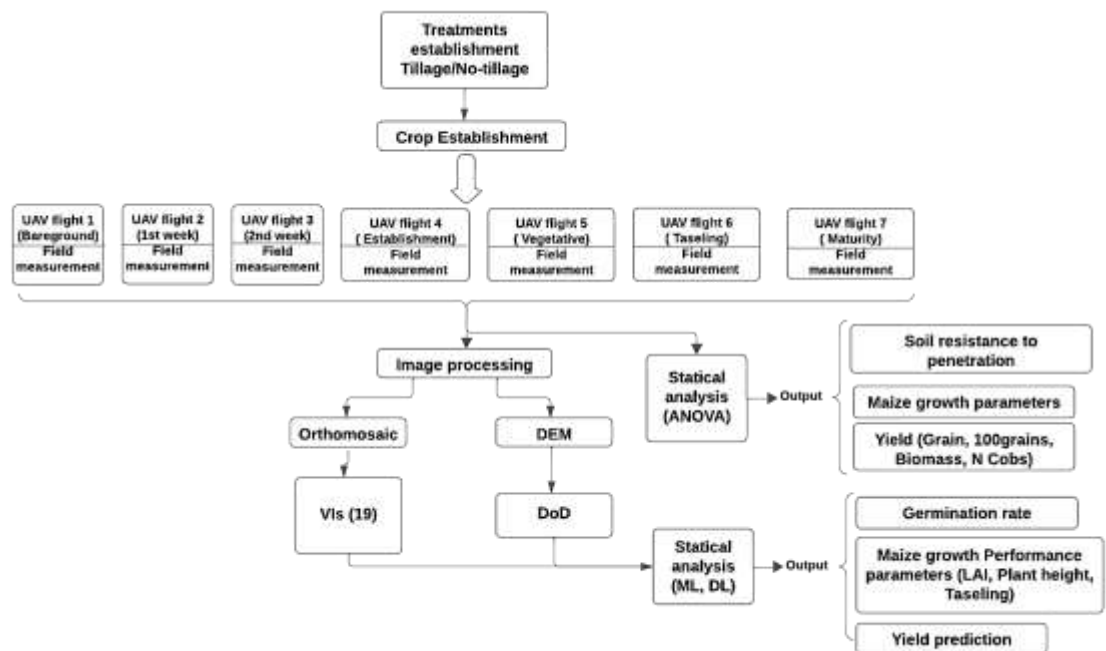


Figure 3: Project flowchart with UAV and manual data collection and processing

### UAV flight accuracy

Table 2: UAV survey accuracy across growth stages

Flight dates	Stage	GSD	DSM (cm/pix)	X error (cm)	Y error (cm)	Z error (cm)	Total error (cm)	Image (pix)
Season One								
24/11/2023	Bare ground	0.847	1.69	2.16	2.94	1.73	4.04	0.63
25/12/2023	Establishment	0.569	1.14	1.91	1.98	1.74	3.25	0.33
29/01/2024	Vegetative	0.495	1.00	1.31	2.27	2.58	3.68	0.61
05/02/2024	Tasseling	0.410	1.14	1.03	0.93	1.45	2.00	3.51
12/02/2024	Maturity	0.568	1.14	1.61	2.11	2.20	3.45	0.40
Season Two								
22/04/2024	Bare ground	0.603	1.20	3.65	2.29	2.38	4.31	4.92
13/05/2024	Establishment	0.557	1.11	2.09	1.40	1.44	2.52	2.90
03/06/2024	Vegetative	0.563	1.13	1.93	1.57	1.03	2.69	0.38
11/06/2024	Tasseling	0.583	1.17	1.24	1.34	1.00	2.08	0.44
18/07/2024	Maturity	0.546	1.09	1.84	1.61	1.43	2.44	2.83

### **Estimation of plant height**

First, the UAV images are imported into the Agisoft Metashape software, and image alignment is performed to identify overlapping areas and establish a sparse point cloud, which represents the scene's structure. This is followed by building a dense point cloud, where the software uses photogrammetry algorithms to reconstruct the 3D surface in high detail. Ground control points (GCPs) are then added at this stage for georeferencing and improving the model's accuracy. Next, the dense point cloud is processed to generate a 3D mesh, which captures the terrain's shape and features. Using the mesh, the DSM is created by interpolating the surface elevations, resulting in a geospatially accurate representation of the terrain that includes all the features such as vegetation, ground and objects present on the field.

Once the DSM has been generated, the next step was to calculate the plant height. In this case, the height of the maize plant was determined by subtracting the Digital Terrain Model (DTM) of the first flight of the season, representing the ground surface, from the DSM of the growth stage involved as described in Figure 4.

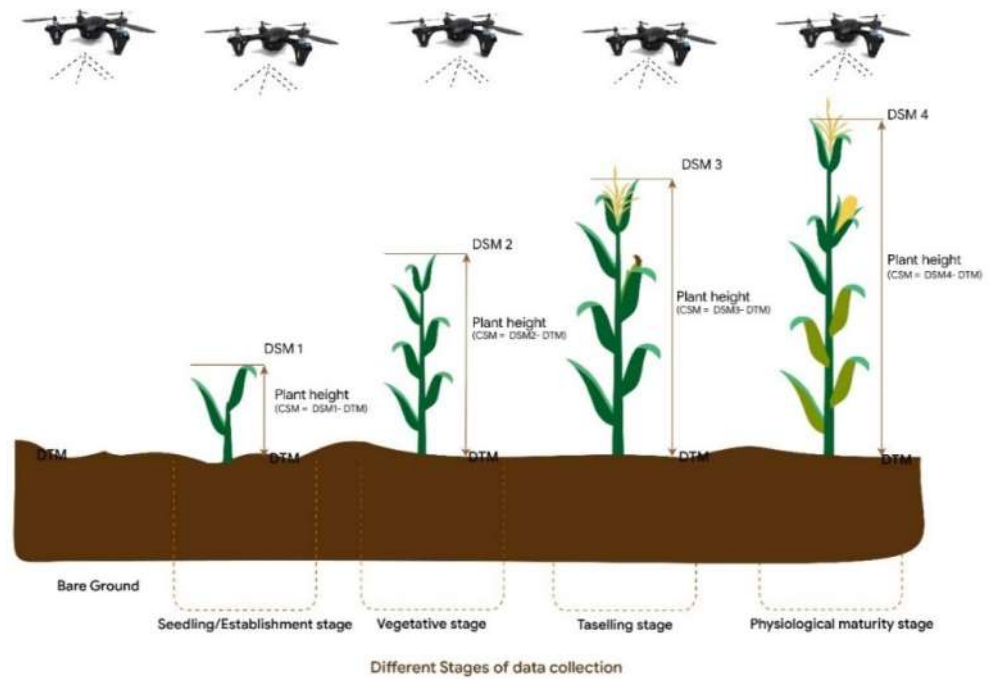


Figure 4: UAV estimation of plant height at different growth stages (source: Akyeaw et al., 2023)

### Assessment of Vis

The vegetation indices were calculated by first acquiring RGB images using a RGB camera. The images were georeferenced and pre-processed for cleaning from any distortions. The individual Red (R), Green (G), and Blue (B) bands were then extracted from the images and segmented using the Excess Green Vegetation index to separate vegetation pixels from the orthomosaic per each plot. Specific formulas of vegetation indices were applied, on a pixel-by-pixel basis. The calculated indices were then visualized and the results were exported for further analysis and integration with additional data. Lóránt et al., (2024), in grouping RGB vegetation indices showed that a set of 16 VIs was structurally unique. These vegetation indices were used in this study as presented in the Table 3.

Table 3: Assessed RGB Vegetation indices

Index	Name	Formula	References
R	Red band	$R$	
G	Green band	$G$	
B	Blue band	$B$	
BGI	Blue-Green Ratio	$\frac{(B - G)}{(B + G)}$	Zarcotejada et al., 2005
ExB	Excess Blue	$1.4 * b - g$	Mao et al., 2003
ExG	Excess Green	$2 * g - r - b$	Woebbecke et al., 1995
GCC	Green Chromatic Coordinate	$\frac{G}{(R + G + B)}$	Richardson et al., 2007
GLI	Green Leaf Index	$\frac{(2 * G - R - B)}{(2 * G + R + B)}$	Louhaichi et al., 2001
GR	Green-Red Ratio	$\frac{G}{R}$	GAMON & SURFUS, 1999
HUE	Overall, Hue Index	$\text{atan}\left(\frac{2 * (B - G - R)}{30.5(G - R)}\right)$	Escadafal et al., 1994
MGRVI	Modified Green Red Vegetation Index	$\frac{(G^2 - R^2)}{(G^2 + R^2)}$	Bendig et al., 2015
MVARI	Modified Visible Atmospherically Resistant Index	$\frac{(G - B)}{(G + R - B)}$	Yang et al., 2008
PRI	Photochemical Reflectance Index	$\frac{R}{G}$	Gamon et al., 1997
RCC	Red Chromatic Coordinate	$\frac{R}{(R + G + B)}$	De Swaef et al., 2021
RGBVI	Red-Green-Blue Vegetation Index	$\frac{(G^2 - R * B)}{(G^2 + R * B)}$	Bendig et al., 2015)
TGI	Triangular Greenness Index	$G - 0.39 * R - 0.61 * B$	Hunt et al., 2013
VEG	Vegetative Index	$\frac{G}{(R^{0.667} * B^{0.333})}$	Hague et al., 2006
vNDVI	Visible Normalized Difference Vegetation Index	$0.5268 * (r^{-0.1294} * g^{0.3389} * b^{-0.3118})$	Costa et al., 2020
WI	Woebbecke Index	$\frac{(G - B)}{(R - B)}$	Woebbecke et al., 1995

### Germination rate assessing using UAV-acquired pictures

The remote assessment of the germination rate was done using the Deep Learning technology, more specifically the single-stage and the two-stage light weight models, namely the Faster R-CNN (Mobilenetv3) and three variants of the YOLOv8 (nano, small, extra-large). The steps used were as follows:

#### UAV images capturing

UAV-acquired images of the maize plots were collected weekly at 3 consecutive times: 2 weeks after sowing, 3 weeks after sowing, and 4 weeks after sowing followed by a manual counting of seedlings on the ground in each instance.

Table 4: Characteristics of the images capturing process and environment

Week	Week 2	Week 3	Week 4
Flight height	20 m	20 m	20 m
GCD	0.59cm/0.23in	0.53cm/0.20in	0.57cm/0.22in
Plant height	7-19 cm	19.2 – 34.8 cm	33.5-61cm
Leaves per plant	3 – 4 leaves	6 - 8 leaves	7-11 leaves
Number of seedlings	239	397	553

#### Object annotation for maize seedlings

Object annotation is a crucial step in training object detection models like YOLOv8 and Faster R-CNN. Both models require labelled datasets to learn to detect objects accurately. This study considered a splitting ratio of 6.5:2:1.5 for training, validation, and test sets, respectively, ensuring a diverse representation of images in each set.

For YOLOv8, annotations were done in the YOLO format, which involved creating text files for each image containing the object class,



bounding box coordinates, and object dimensions of identified objects. Typically, for maize seedlings, annotations were made on maize plants in images, each text file contained lines specifying the class label "maize" and the coordinates of the bounding box around the maize plant.

Similarly, for Faster R-CNN, annotations were done in the PASCAL VOC format, which includes XML files containing object class labels, bounding box coordinates, and image metadata. Each XML file would describe the objects present in the image along with their locations and classes.

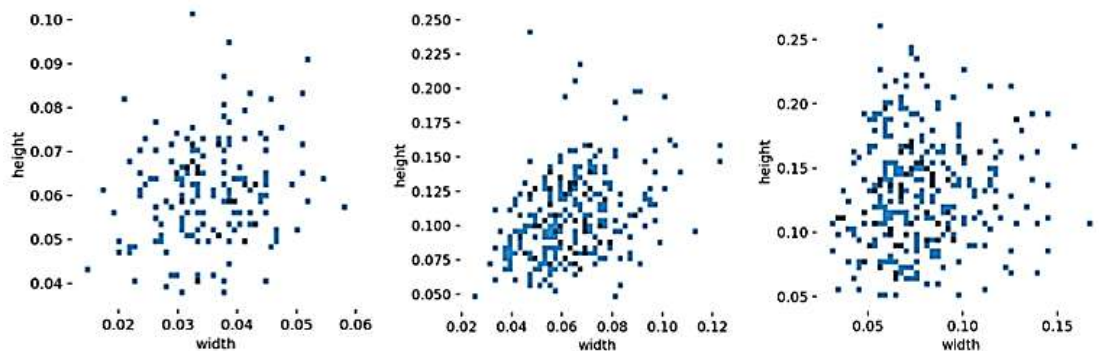


Figure 5: Bounding box sizes per dataset (a - two weeks maize, b – three weeks maize, c - Four weeks maize)

### Model training

The dataset was thus used to train the different models, Faster R-CNN with a Mobilenetv3 backbone, YOLOv8 using three (3) of its variants: YOLOv8 nano, YOLOv8 small and YOLOv8x, making it to be four (4) different model trainings. The framework used for the training the Ultralytics for the YOLOv8 models and PyTorch for the Faster R-CNN model. The parameters used during the training are presented in the Table 5 below.

Table 5: Training parameters of the selected models

Parameter	Value	Parameter	Value
Learning rate(initial)	0.01	Epochs	100
Learning rate (final)	0.01	Pretrained	True
Weight decay	0.0005	Device	Cuda (training), CPU (inference)
Momentum	0.937	Image size	YOLOv8 (640*640), Faster R-CNN (Mobilenetv3) (320*320)
Optimizer	Stochastic Gradient Descent	Batch size	4

YOLO (You Only Look Once) and Faster R-CNN both followed structured training processes with notable differences. For YOLO training, during the forward propagation, input images were passed through the network, generating initial predictions for class probabilities and bounding box parameters. The loss function was then calculated based on the difference between predicted and actual values, comprising classification loss (error in class labels), localization loss (error in bounding box parameters), and confidence loss (error in predicted confidence scores that an object is present in a given bounding box). Gradients of the loss function with respect to model parameters were then computed, indicating each parameter's contribution to the total loss. Model parameters were updated using optimization algorithms, in this case, the Stochastic Gradient Descent (SGD) during the backward

propagation. These steps were repeated for each image batch across multiple epochs until the validation set performance stabilized.

For Faster R-CNN, the training process involved two main steps: region proposal, where the Region Proposal Network (RPN) generated regions with objectless scores, classification, and bounding box regression, where the classifier predicted the class and refined bounding boxes for each proposed region. The loss function in Faster R-CNN is a combination of classification loss, localization loss, and an additional objectless loss which measures the error in the predicted objectless scores from the RPN. The same process of backward propagation, parameter update, and iteration has been followed as in YOLO.

### Model performance evaluation

All the models were evaluated using Precision and Recall metrics, Mean Average Precision and Inference Speed

During the training and validation process, the True Positive (TP) was Correctly identified maize plant at an Intersection Over Union (IOU) value of 0.7, False Positive (FP) as Bare ground soil identified as Plant, False Negative (FN) as a missed maize plant was extracted. These metrics were then used to calculate the Precision, Recall and summary of the classification.

$$\text{Precision}(P) = \frac{TP}{TP+FP} \quad (2)$$

$$\text{Recall}(R) = \frac{TP}{TP+FN} \quad (3)$$

$$AP = \int_0^1 P_i R_i dR_i \quad (4)$$

$$mAP = \frac{1}{n} \sum_{i=0}^n AP_i \quad (5)$$

Where,

TP: True Positive

FP: False Positive

R: Recall

P: Precision

FN: ?

mAP, : Mean Average Precision,

AP: Average Precision

### **Estimation of LAI**

The LAI was estimated by using the plant canopy coverage retrieved from the ExG vegetation index after binary thresholding using ArcGIS (Esri Inc., Redlands, California, USA). The algorithm employed for binary thresholding is the Otsu method, specifically developed to differentiate between the background and foreground in images. It achieved this by creating two distinct classes that minimize the variance within each class (Otsu, 1979). The plant canopy coverage, plant height and growth stage were used as categorical variables to train Support Vector Regressor and three different tree-based machine learning models, the Random Forest Regressor, Decision Tree and Gradient boosting along with Linear models: Ridge Regression, Linear Regression, Lars, Huber Regressor and Polynomial Regression. After training and testing, the RMSE, MAE and  $R^2$  statistics were retrieved for comparison at different growth stages.

## Prediction of Yield

The yield prediction was done by considering the crop growth stages in the aim of assessing how earlier the end-of-season yield can be accurately predicted for that purpose, the processes were split into different combinations of Vegetation indices (19) (

Table 3), the canopy coverage, the plants' height and Growth stage as categorical features.

The first process involved the selection of models and features to be involved. Different models then proposed by the literature, among the most used there were the Neural Networks, Linear Regression, Random Forest, Support Vector Machines and Gradient Boosting Tree (Halder et al., 2023; van Klompenburg et al., 2020). Three models were then selected, the Random Forest Regressor, the Gradient Boosting Tree and the Decision Tree. Due to the quantity of data Deep learning models were judged unsuitable, and Linear Regression due to the feature multi-collinearity of the Vegetation indices where Variance Inflation Factors were all superior to 5 and close to Infinity as they were all calculated based on the same initial bands (RGB). After the selection of models, the next step before the prediction was to select relevant features. To better assess the contribution of all the involved features, the features were grouped by growth stages and the algorithm of Feature Importance was used to select the most important features. Per each model, the model had to run 1023 times taking the features into a subset and the one with a higher  $R^2$  was reported. The process was then replicated 16 times considering the growth stages combination namely: Establishment; Vegetative; Tasselling; Maturity; Establishment, and Vegetative; Establishment and Tasselling; Establishment,

Maturity; Tasselling, Maturity; Vegetative and Tasselling; Vegetative and Maturity; Establishment, Vegetative and Tasselling; Establishment, Vegetative and Maturity; Establishment, Tasselling, and Maturity; Vegetative, Tasselling and Maturity; Establishment, Vegetative, Tasselling, and Maturity. This splitting allowed to assess how growth stages improve each other to improve the accuracy of the yield prediction. The process involved predicting the exact yield and yield interval (classification). For the classification, the interval was chosen using Quartiles (0.25, 0.5, 0.75, 1). Both the yield prediction classification and regression were done at a ratio of 0.8 - 0.2 for respectively the training and testing dataset combining the two growing seasons. The performance was evaluated using  $R^2$  and RMSE for regression tasks and Accuracy and f1-score for classification tasks. The priority has been ranked as follows: Performance ( $R^2$ , RMSE), with/without plant height and then model computing requirement (in order: Decision Tree, Random Forest, Gradient Boosting). The number of trees used for Random Forest and Gradient Boosting was 100 trees (Wald et al., 2013). The Table 6 presents the parameters used with the 3 Machine learning models.

Table 6: Hyperparameters used for the Random Forest, Decision Tree and Gradient Boosting for yield prediction (classification and regression)

Hyperparameters	Random Forest	Decision Tree	Gradient Boosting
Number of estimators	100	-	100
Min samples split	2	2	2
Min samples leaf	1	1	1
Max depth	-	-	3
criterion	Gini	gini	friedman_mse
Learning rate	-	-	0.1
splitter	-	Best	-
Max features	Sqrt	-	-
Min impurity decreases	0	0	0

### **Study methodology limitations**

While the UAV technology has risen the interest in the crop monitoring, its application is not yet sprayed to all the agriculture use cases. For instance, the stem girth assessment using the UAV technology has not yet gotten enough attention in the research community.

Another limitation is the size of the dataset used for Machine learning models. While this study can assess the plant height using a 120 rows size dataset per growth stage (6 plants x 20 plots), the Leaf Area Index and the Yield are limited to plots, resizing the dataset to only 40 rows for the two seasons, further reducing the quality of our analysis

### **Statistical Analyses**

Statistical analysis used in which ANOVA was carried out using the General Linear Model in MINITAB Statistical 21.2 (MINITAB LLC, US) to determine the effects of tillage on different maize performance parameters. The Tukey HSD test was used to determine significant differences among the treatment means at the confidence level of 95%. Linear Regression was used to assess the accuracy of the UAV-based approach in estimating the plant height.

## CHAPTER FOUR

## RESULTS AND DISCUSSION

## Effects of tillage on maize growth parameters

## Effects of tillage on germination rate

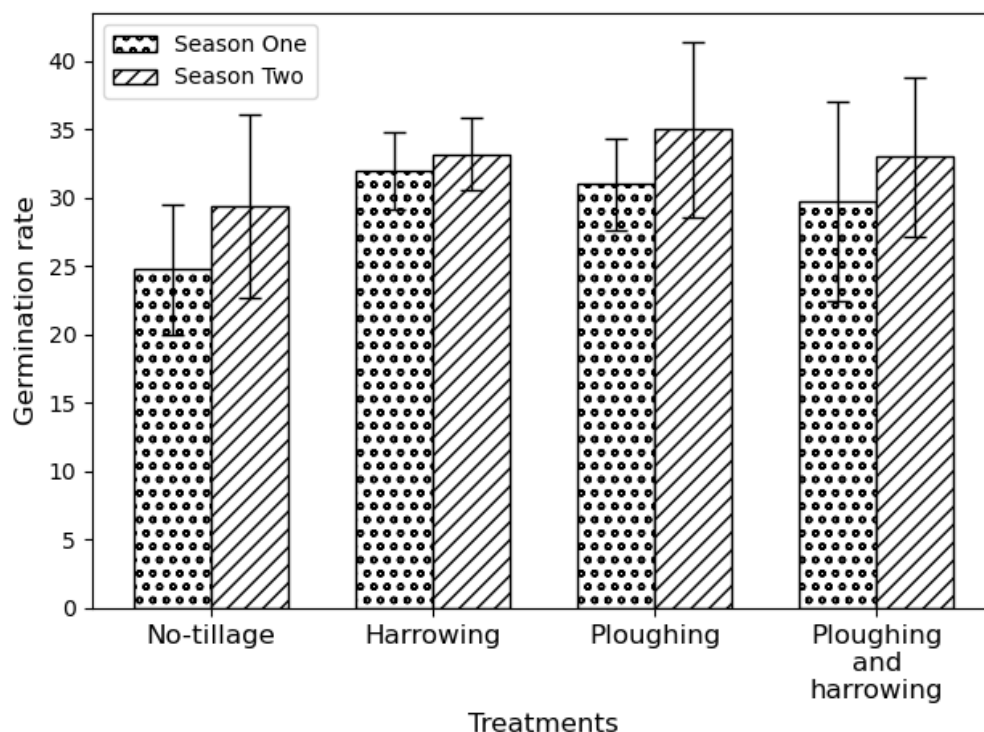


Figure 6: Effects of Tillage on Maize germination rate for the two seasons

Under no-tillage, the germination rate in Season One is around 25, while in Season Two, it increases to approximately 30, showing a slight improvement. Harrowing results in a germination rate of about 30 in Season One and a slightly higher rate of around 32-33 in Season Two. Ploughing leads to a germination rate of approximately 31 in Season One, with an increase to about 35 in Season Two, suggesting a positive impact on maize germination. The combination of ploughing and harrowing shows a germination rate close to 28 in Season One and around 32 in Season Two. In general, all tillage treatments



exhibit higher germination rates in the second season compared to the first, with ploughing alone showing the most notable improvement.

The lowest germination rate was recorded on No-tillage plots in both seasons, while the highest was on Ploughing only during Season Two (Figure 9). The harrowing only tillage showed the lowest variation through the two seasons.

However, there was no significant difference between the treatments with respect to Season Two. Excepted the No-tillage, the tillage treatments performed well during both seasons due to the soil loosening characteristic of harrowing for seedbed preparation (Chisi & Peterson, 2019).

Winkler et al. (2022) and Kabas et al. (2020) observed lower germination performances on no-tillage soils for a number of crops. Generally, soil compaction is associated with no-tillage and this tends to negatively affects germination and plant growth by reducing seed-to-soil contact, increasing penetration resistance, and limiting oxygen availability due to decreased soil porosity (Kahlon et al., 2020; Nawaz et al., 2013) making it harder for seeds to germinate and for seedlings to push through the relatively compacted soil.

### **Effects of Tillage on Plant Height and Stem Diameter**

Figures 10 and 11 show the trend of effects of different tillage systems on maize plant height and stem diameter respectively over some weeks after sowing for the season one. Similarly, Figures 12 and 13 also show the tillage systems effect on maize plant height and stem diameter respectively in season two over the same period as the first season. The growth rate was high at the establishment and early vegetative stages of the maize, especially at 4 - 5 weeks for the stem diameter and plant height. With the No-tillage having the

least performance, the results showed that such conservation tillage systems significantly affected the growth of the plants for both seasons.

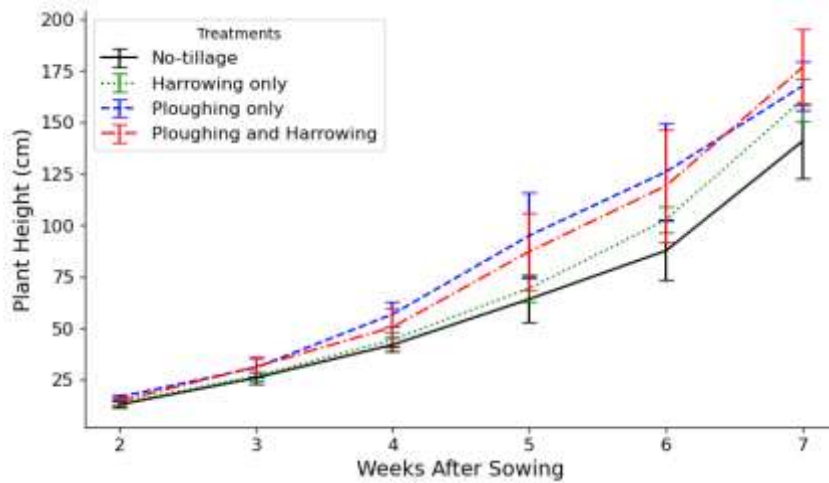


Figure 7: Effects of different tillage systems on maize plant height for Season One

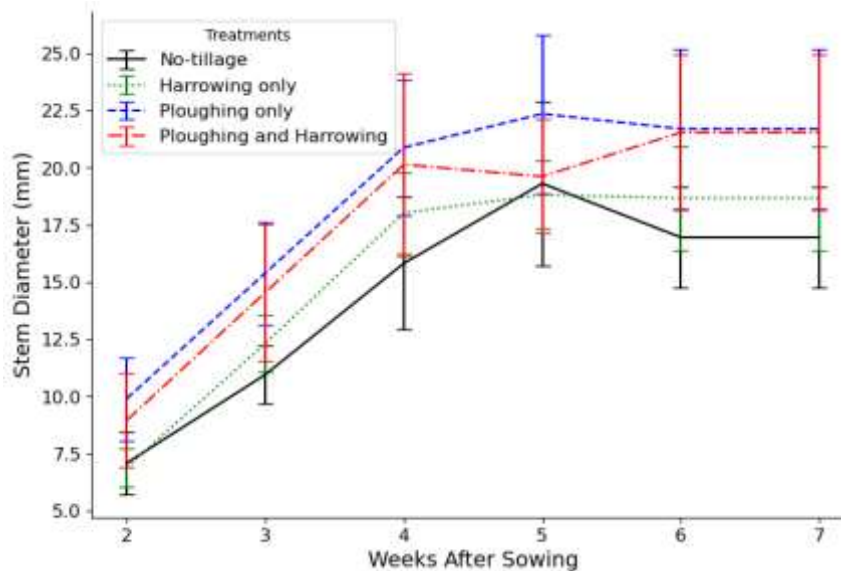


Figure 8: Effects of different tillage systems on maize stem diameter growth rate for Season One

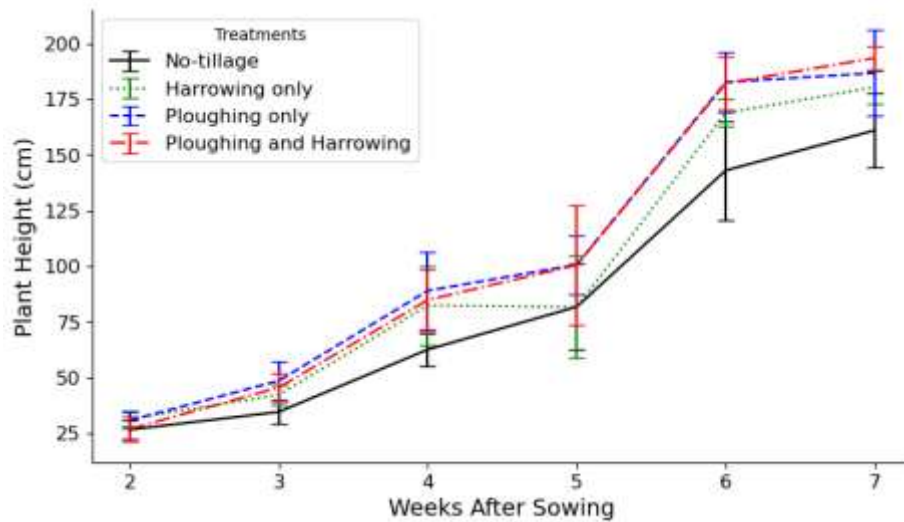


Figure 9: Effects of tillage systems on maize plant height growth rate for Season Two

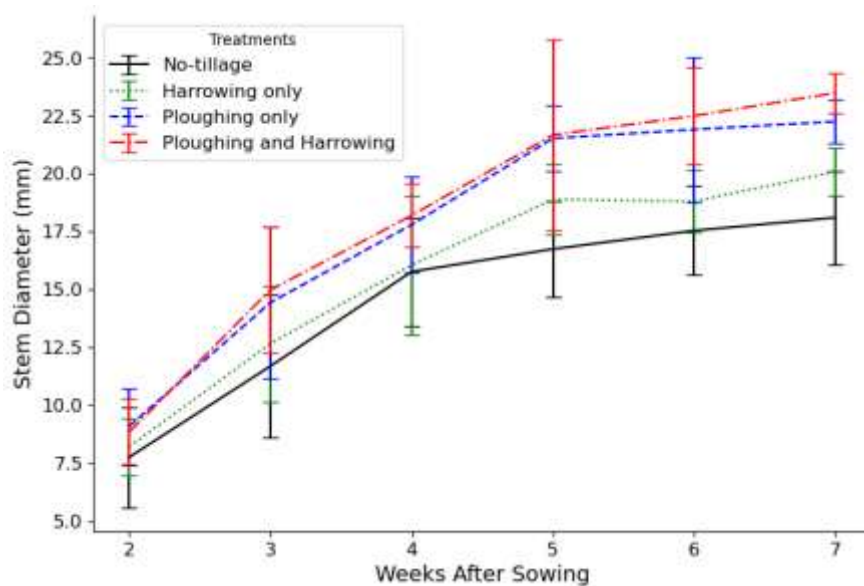


Figure 10: Effects of tillage on maize stem diameter growth rate for Season Two

The four figures (Figure 7, Figure 8, Figure 9 and Figure 10) suggest an almost uniform growth rate among treatments at the first four weeks of the growing stage during both seasons for the Plant height and Stem diameter. This suggest to not be related to the involved treatments as environmental factors such as sunlight.

Crops grow faster because they require full sunlight during both the vegetative and generative stages. This need for sunlight during growth leads to an increase in crop height, allowing the plants to better capture sunlight and maintain continuous photosynthesis. The increase in stem diameter aligns with the rate of height growth as the plant matures (Jamidi et al., 2018).

In Season One, tillage had a significant effect on plant height ( $p = 0.025$ ), indicating that different tillage methods influenced plant growth. Ploughing and Harrowing resulted in the tallest plants, while No-tillage produced the shortest. Ploughing only and Harrowing only had similar plant heights and were grouped together, whereas No-tillage was in a separate group, confirming its lower effectiveness in promoting plant height.

In Season Two, the effect of tillage on plant height was even stronger ( $p = 0.005$ ), reinforcing that tillage enhances plant growth. Ploughing and Harrowing again produced the tallest plants, while ploughing only and Harrowing only had similar results and were grouped together. No-tillage remained in a separate group, producing the shortest plants.

For stem girth in Season One, tillage also had a significant effect ( $p = 0.017$ ), meaning that soil preparation influenced stem thickness. Ploughing only and Ploughing and Harrowing resulted in the thickest stems and were grouped together. Harrowing only had moderate stem thickness and was sometimes grouped with them, while No-tillage had the thinnest stems and was in a separate group.

In Season Two, a very strong effect was observed ( $p < 0.001$ ), further highlighting the importance of tillage for stem development. Ploughing and Harrowing had the thickest stems, while Ploughing only showed similar

results and was grouped together with it. Harrowing only showed moderate stem thickness and was in a different group from Ploughing and Harrowing. No-tillage had the smallest stem girth and was in a separate group, confirming its lower effectiveness. The seasonal effect can improve the growth of crops under conservation tillage specifically in Season Two here and long-term use (Blanco-Canqui & Ruis, 2018; Phillips, 1984).

### Effects of tillage on number of leaves and leaf Area Index (LAI)

Every week during the growth period, the number of leaves and leaf area index were recorded. Figure 11 and 15 respectively show the trend over time of the effect of different tillage systems on maize number of leaves developed in seasons one and two. Likewise, Figures 15 and 16 respectively show the maize leaf area index (LAI) as affected by the different tillage systems in seasons one and two.

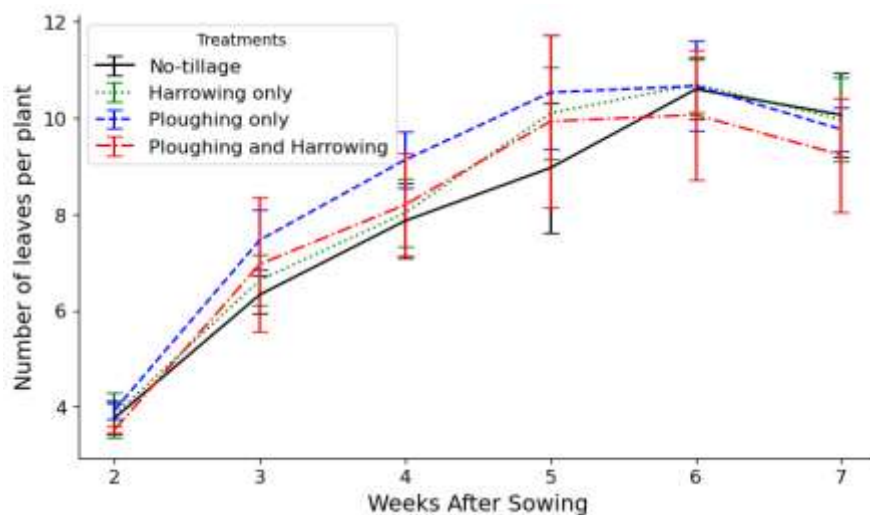


Figure 11: Effects of tillage on Number of leaves growth rate for Season One

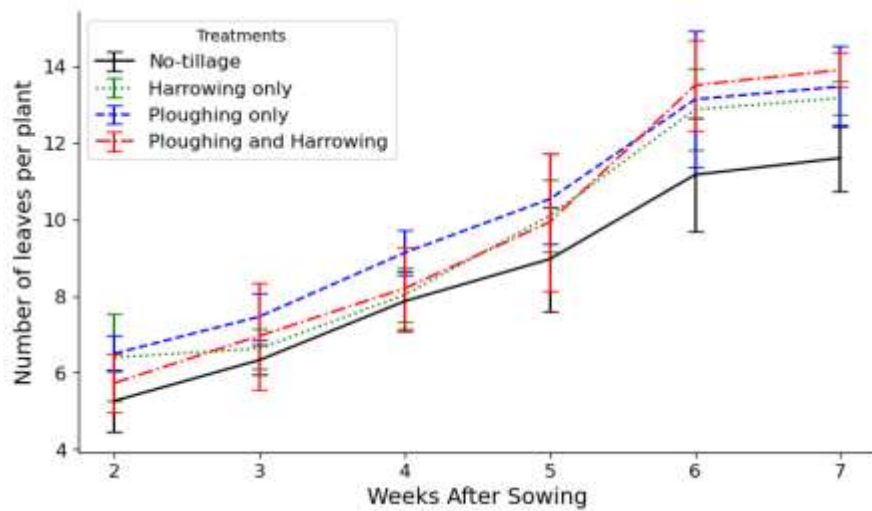


Figure 12: Effects of tillage on Number of leaves growth rate for Season Two

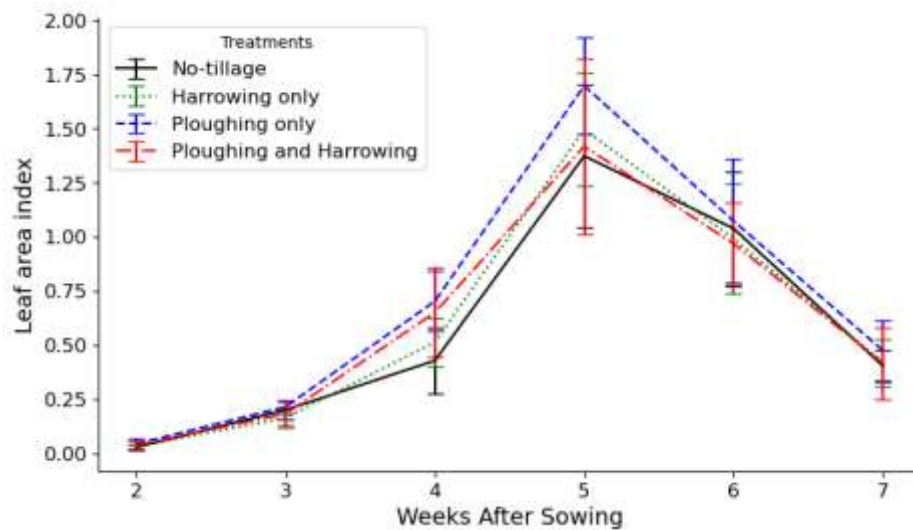


Figure 13: Effects of tillage on Leaf Area Index (LAI) growth rate for Season One

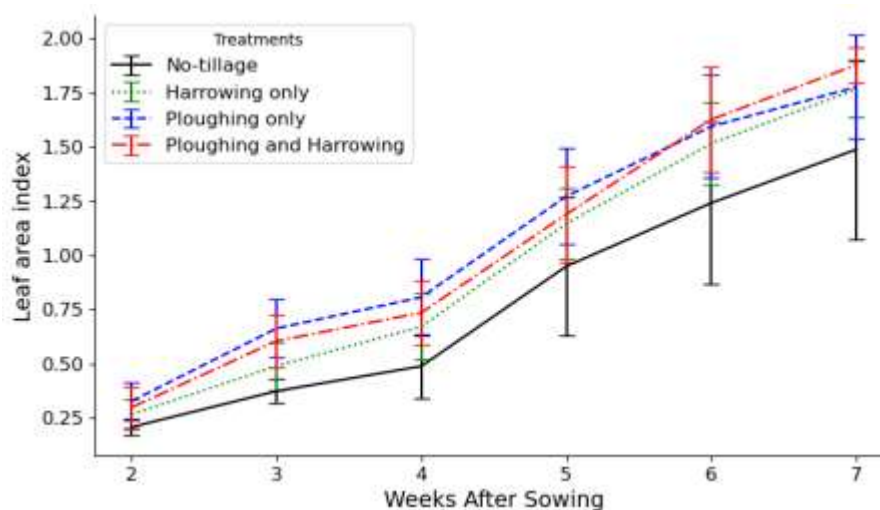


Figure 14: Effects of tillage on Leaf Area Index (LAI) growth rate for Season Two

For the Season One for both number of leaves and LAI parameters, the peak was recorded at the 4<sup>th</sup> week during the vegetative growth stage for Ploughing only and Ploughing and harrowing as highlighted in the four figures (Figure 11, Figure 12, Figure 13 and Figure 14). The No-tillage has shown its peak a week later, same for the Harrowing only. After the peak, the number of leaves and LAI drastically decreased as the plants entered the Tasselling and maturity growth stages. It was observed that Season Two made the treatments almost grow at the same growth rate and pattern, with the no-tillage performing less. The rapid increase of Leaf area index and number of leaves during the establishment and vegetative stage was likely promoted by temperature and photoperiod (Qiao et al., 2019), since these two parameters are strongly dependent on the season. The seasonality made that result to be complementary to the study of Imani et al. (2022) that supported the tillage tends to have a significant effect on chlorophyll pigment and thus the leaf area index.



That explains the prolonged increase of leaf area index during Season Two. At the tasselling and grain-filling stage, the number of leaves and LAI started to decrease due to the senescence process making the leaves quite old, turning yellow and dying off as observed by Woo et al. (2018).

### Effects of Tillage on Days to 50% Flowering

From the end of the vegetative stage, the plants were monitored daily to get the number of days to 50 percent flowering from the day of sowing. Figure 15 presents the days to 50 percent flowering for both seasons. While the no-tillage took more days than the other tillage treatments during the Season One, the days were reduced during the Season Two but the difference was not significant for both seasons ( $p > 0.05$ ).

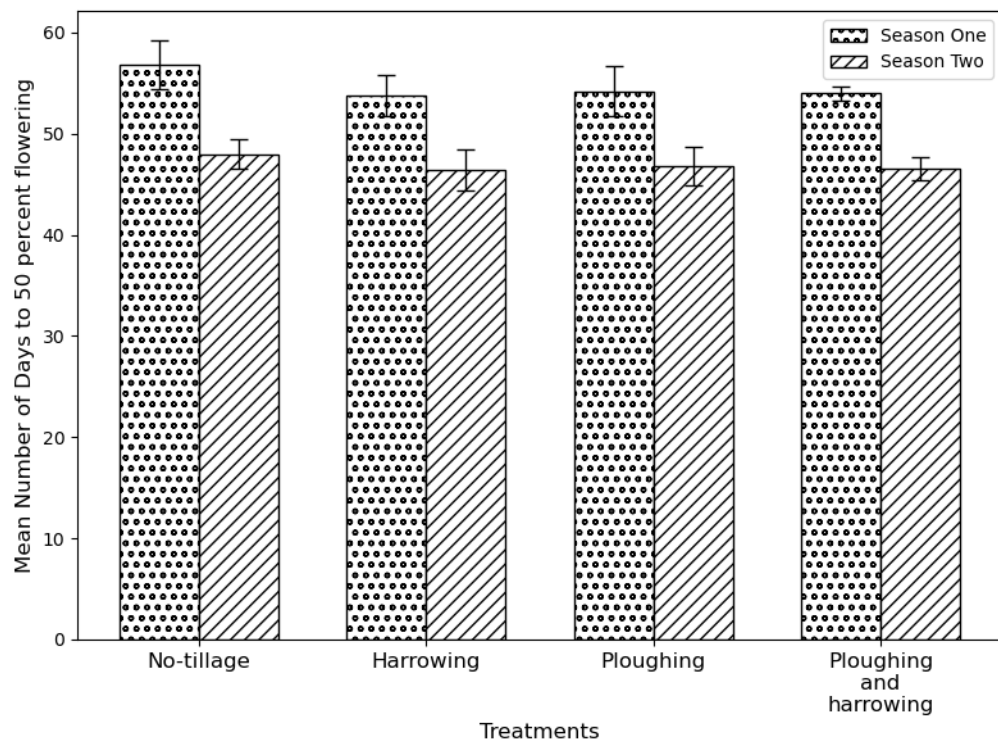


Figure 15: Effects of tillage on the Number of days to 50 percent flowering for both seasons one and two



Among the factors that affected the growth rate of maize are the fertility level of the soil and the climate conditions during the growing stage. However, since in this study, no fertilizer was applied, the fertility conditions involved can be linked to nutrient availability to plants as affected by the soil's physical properties influenced by the tillage method. Literature has shown that long-term tillage has an impact on the absolute growth rate of maize and thus its number of days to flowering (Nayak et al., 2022).

### Effect of Tillage on Root System Architecture of maize

The maize plants were excavated at the physiological maturity stage for the analysis of the root architecture. Table 7 presents the distribution of root features across the four treatments.

Table 7: Effects of tillage on maize Root System Architecture

Root features	No-tillage	Harrowing	Ploughing	Ploughing and Harrowing	P-Value	Tuckey HSD	CV (%)
Maximum Number of Roots	22.50	22.86	23.00	21.71	0.96	1.29	20.00
Number of Root Tips	142.13	159.00	147.67	135.43	0.52	12.24	20.08
Total Root Length (cm)	447.28	503.99	526.50	472.80	0.51	79.22	20.66
Maximum Width (cm)	19.73	21.59	16.95	16.84	0.17	0.12	24.20
Width-to-Depth Ratio	0.67	0.70	0.54	0.54	0.06	0.00	22.83
Lower Root Area (cm <sup>2</sup> )	93.79	117.89	116.73	93.80	0.25	22.95	28.44
Average Diameter (cm)	0.79	0.98	0.86	0.75	0.03	0.11	18.84
Perimeter (cm)	545.74	540.41	585.96	541.34	0.88	45.55	19.88
Root volume (cm <sup>3</sup> )	569.91	1077.19	783.59	508.2	0.02	275.39	54.04
Surface Area (cm <sup>2</sup> )	1120.62	1617.69	1438.31	1144.97	0.03	317.69	28.70
Average Root Orientation deg ??	53.43	51.89	53.00	52.96	0.70	1.54	4.58
Shallow Angle Frequency	0.23	0.24	0.23	0.24	0.82	0.01	11.62
Steep Angle Frequency	0.49	0.46	0.48	0.48	0.64	0.03	9.86

1 mm-Diameter Root Length (cm)	351.28	361.64	398.27	367.60	0.80	46.99	22.82
2 mm-Diameter Root Length (cm)	46.80	62.51	61.48	53.18	0.07	14.68	23.41
3 mm-Diameter Root Length (cm)	28.35	37.40	36.91	34.81	0.012	8.56	18.30
4 mm-Diameter Root Length (cm)	20.85	42.45	29.84	17.21	0.025	12.63	63.90

From Table 7, among all the features gathered, only the 3 mm-diameter Root Length and 4 mm-diameter Root Length were significantly different among the treatments ( $p < 0.05$ ). Although there was no significant difference in total root length, the no-tillage and harrowing were relatively lower than the ploughing, and the ploughing and harrowing treatments. This observation could be due to possible soil compaction on no-tillage and harrowing plots as observed by Sun et al. (2023) and (Duruoha et al., 2007). The same trend is followed by the Average Diameter of the roots and the surface area where the means were found to be significantly different at the diameter range of 3 mm and 4 mm. The reduction in root diameter can be explained by possible soil compaction that could lead to morphological modifications in roots (Lipiec et al., 2003; Pandey et al., 2021).

Effects of Tillage on maize yield components. Table 8 and 9 present the effects of different tillage types on the yield components for seasons one and two respectively.

Table 8: Effects of tillage on the yield components for Season One

Treatments	Dry Biomass (t/ha)	Grain yield (t/ha)	Number of Ears per plant	Ear length (cm)	100 grains weight (g)
No-tillage	3.501b	3.122b	1.23a	15.56a	25.312c
Harrowing only	4.668ab	3.740ab	1.16a	18.96a	27.324b
Ploughing only	6.027ab	4.881a	1.46a	18.22a	26.672b
Ploughing and Harrowing	7.209a	4.619ab	1.26a	19.44a	31.204a
P-value	0.017	0.018	0.161	0.061	0.00
Tuckey HSD (0.05)	0.978	0.625	0.15	1.66	0.362
CV (%)	27.29	22.79	17.65	13.78	1.95
Standard deviation	1.460	0.932	0.27	2.48	0.540

Table 9: Effects of tillage on the yield components for Season Two

Treatments	Dry Biomass (t/ha)	Grain yield (t/ha)	Number of Ears per plant	Ear length (cm)	100 grains weight (g)
No-tillage	7.456b	4.230a	1.13a	20.96a	27.274b
Harrowing only	9.100ab	4.710a	1.10a	20.92a	26.822b
Ploughing only	9.37ab	5.241a	1.33a	21.86a	27.842b
Ploughing and Harrowing	10.933a	5.670a	1.16a	21.76a	32.720a
P-value	0.045	0.246	0.271	0.764	0.00
Tuckey HSD (0.05)	1.024	0.720	0.11	1.04	0.994
CV (%)	16.588	21.67	14.71	7.28	5.173
Standard deviation	1.528	1.075	0.173	1.556	1.482

For both seasons, the No-tillage followed by the Harrowing treatments have yielded less, but at the Season Two all the treatments yielded more in dry biomass and grain yield. The ploughing and harrowing outperformed the other treatments for both seasons in term of dry biomass and 100 grains weight. The treatments had a strong effect on the dry biomass as means were significantly different for both seasons at a P-values of 0.017 and 0.045. The trend corroborated with Al - Kaisi et al. (2015) and Büchi et al. (2017), as well as

Huynh et al. (2019) who reported that conventional tillage practices produced more biomass than no-tillage.

The other yield components that were measured are the grain yield retrieved by shelling the cobs, the ear length, the number of cobs per plant and the weight of 100 grains for each plot.

The results showed the significant influence of tillage methods on maize grain yield across both seasons. In Season One, the Ploughing only treatment achieved the highest grain yield (4.881 t/ha), followed closely by the Ploughing and Harrowing treatment (4.619 t/ha). In contrast, the No-tillage treatment resulted in the lowest grain yield (3.122 t/ha), indicating that minimal soil disturbance limits crop productivity. The observed differences in grain yield among the treatments were statistically significant ( $P = 0.008$ ) as tillage methods influenced the grain yield (Guan et al., 2014).

During Season Two, the Ploughing and Harrowing treatment outperformed all others with the highest grain yield of 5.670 t/ha, while the No-tillage treatment again showed the lowest yield (4.230 t/ha). However, unlike Season One, the grain yield differences among treatments were less pronounced, with no statistically significant effect ( $P = 0.237$ ). Across both seasons, the trend suggests that Ploughing and Harrowing consistently supports higher grain yields compared to reduced or no-tillage methods as supported by Dakhil et al. (2022) and Drobitko et al. (2024). Although, the No-tillage was learnt to result in no soil disturbance, its crop yield increased over time. Mondal & Chakraborty, (2022) noted that no-tillage favourably changed soil structure and porosity that could positively influence the yield of crops.

The impact and effectiveness of tillage methods evolve over time and are largely influenced by soil-specific characteristics. The mechanisms and outcomes of no-tillage practices on yield are highly dependent on factors such as soil type, soil compaction, and other local environmental conditions (VandenBygaart & Liang, 2024). The tillage imposed in Season Two generally impacted the yield for all treatments with the least observed in the harrowing. The improvement can be because the moisture content, higher during in the Season Two than in Season one, is an important factor impacting the yield of maize (Niu et al., 2023).

Further, on a fine-loamy or loamy, mixed, mesic soils, the negative mechanisms associated with No-Tillage required three years to diminish, resulting in a notable improvement in maize yield by the fourth year, indicating its potential for long-term benefits as reported by Lampurlanés et al. (2001). Conversely, a study conducted on sandy soil (Haplic Chernozem) revealed that significant yield differences due to No-Tillage became evident only after the fifth year. Earlier work by Linden et al. (2000) showed with No-tillage, significant positive changes persist in crop performance over 13 years, highlighting the long-term impact of No-Tillage on such soil types. Another study proved that No-tillage generally needs a longer time to significantly influence the yield of maize in sandy soil (Duiker et al., 2006). While this study has not used any fertilizer, the overall yield was between 4 t/ha and 5 t/ha and thus fall into the potential yield for the *Abontem* variety and this corroborated with studies by Essilfie et al. (2024) and MacCarthy et al. (2018). For grain weight, the Ploughing and Harrowing treatments recorded the highest values compared to other treatments.

While tillage methods significantly influenced dry biomass and grain yield, their effect on the number of ears per plant and ear length was limited, suggesting that the latter parameters were dependent more on other factors such as genotype. A genetic study by Khatun et al. (2022) conducted on four traits of the maize ear suggested that heterozygous genotypes play very important role for phenotypic performance of ear length.

### Relationship between growth parameters and yield components

The correlation matrix reveals important relationships between maize growth parameters and yield components under different tillage treatments.

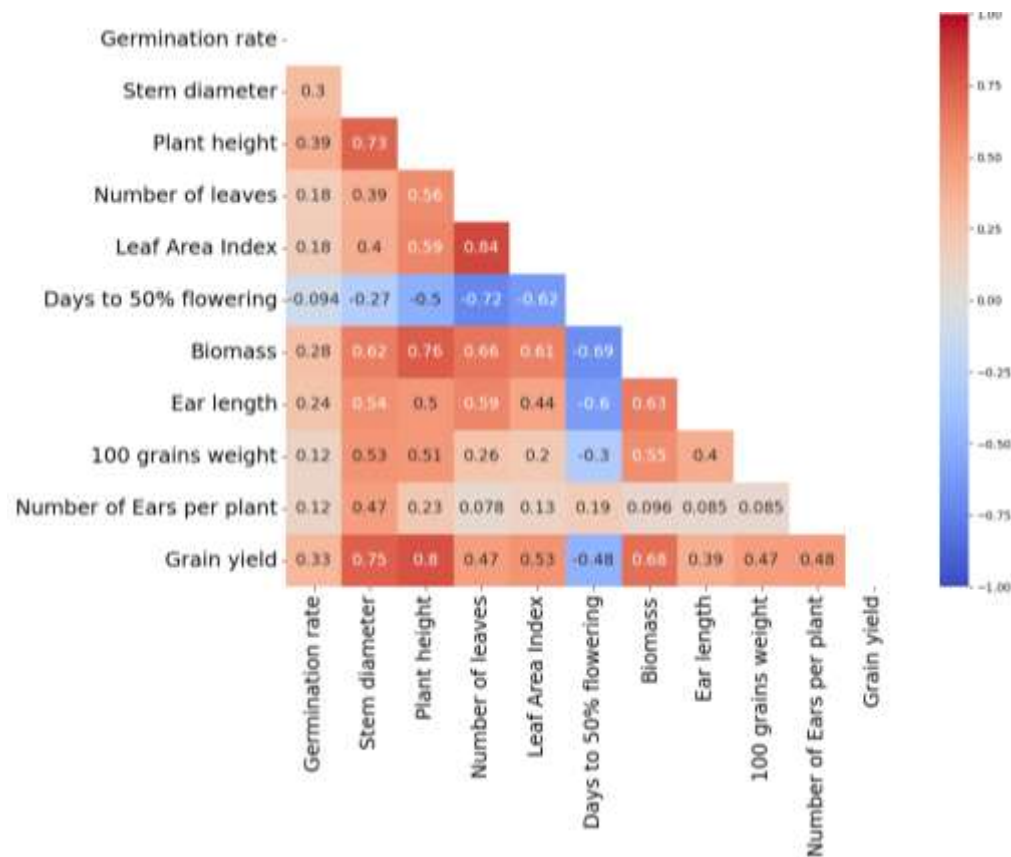


Figure 16: Correlation matrix between growth parameters and yield components of maize

Plant height shows a strong positive correlation (0.80) with grain yield, indicating that taller plants tend to produce higher yields (Shettigar et al.,

2024). Similarly, stem diameter ( $R=0.75$ ) and biomass ( $R=0.68$ ) also have significant positive correlations with grain yield, suggesting that more vigorous plant growth contributes to better productivity. The leaf area index ( $R=0.53$ ) also supports higher grain yield, highlighting the importance of sufficient leaf surface for photosynthesis. On the other hand, days to 50% flowering has a negative correlation ( $R=-0.48$ ) with grain yield, meaning that later flowering reduces productivity, reinforcing the idea that early-flowering varieties may be more advantageous (Alkhazaali et al., 2017). The relationships among growth parameters further emphasize this trend, as stem diameter and plant height (0.73) are strongly correlated, showing that taller plants often have thicker stems, which may enhance structural support and nutrient transport (Hengqi & Ragni, 2024). Similarly, the number of leaves and the leaf area index (0.84) are closely linked, reinforcing the idea that an increased number of leaves contributes to greater photosynthetic potential. Among the yield components, 100-grain weight correlates positively with ear length (0.55), indicating that larger ears may lead to heavier grains, while the number of ears per plant also shows a moderate correlation (0.48) with grain yield. These findings suggest that tillage treatments that promote plant height, stem girth, and biomass accumulation are likely to improve maize yield.

### **UAV Estimation of growth parameters.**

#### **Estimation of Germination rate**

#### **Seedling Detection performance**

This research aimed not just to classify an UAV-acquired image as containing maize seedlings, but also to be able to locate those maize seedlings inside the plots. The Precision and Recall of UAV models were used to detect

the presence of maize seedlings, seedlings count and to localize them at three (3) different early-stage growth times. This was applied for plant recognition (classification), plant counting (germination rate) and localization (refilling or UAV spraying). All these cases required different levels of Precision and Recall thresholds. Thus, the Precision and Recall curve demonstrates the trade-off between those two metrics. The bigger the area under the curve (AUC) of the Precision-Recall curve, the better the model trades off between “False alerts” and “Misses” (Sofaer et al., 2019). From Figure 17, a poor performance from the YOLOv8x (YOLOv8 – extra-large) model was observed although it had been claimed to be the most precise among the YOLOv8 models (nano -YOLOv8n, small - YOLOv8s, and extra-large - YOLOv8x) (Jocher et al., 2023). From the same Figure 19, all the models had the lowest detection of the maize seedlings during the first week, which could be likely due to the size of the maize seedlings (Figure 5) and its visibility at the flight height at which the UAV was capturing the images (Wang & Liu, 2024). The low Recall values were mainly linked to the False Negative thus suggesting that the Faster R-CNN using MobilenetV3 as backbone along with the three YOLOv8 models (nano -YOLOv8n, small - YOLOv8s, and extra-large -YOLOv8x) were missing some maize seedlings taking them as part of the bare ground soil.



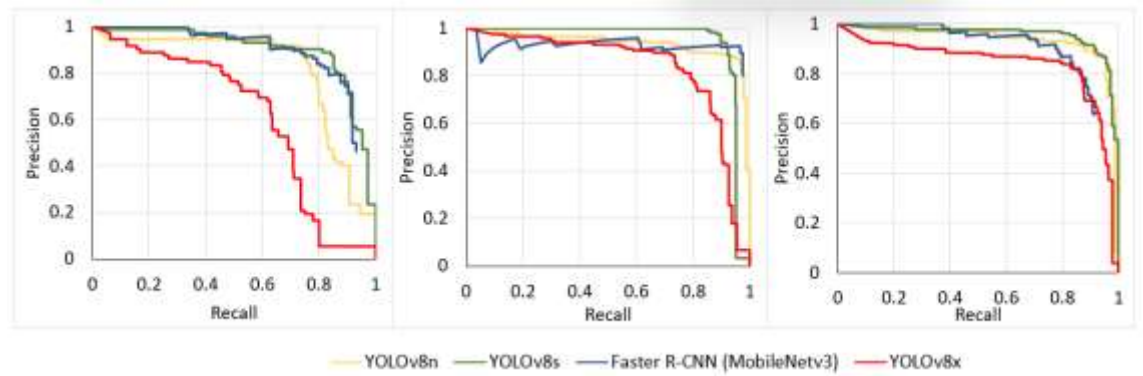


Figure 17: Precision-Recall curves during the validation of the models on three weeks of the early growth stage of maize seedlings (Two weeks aged - left, Three weeks aged - middle, Four weeks aged - right)

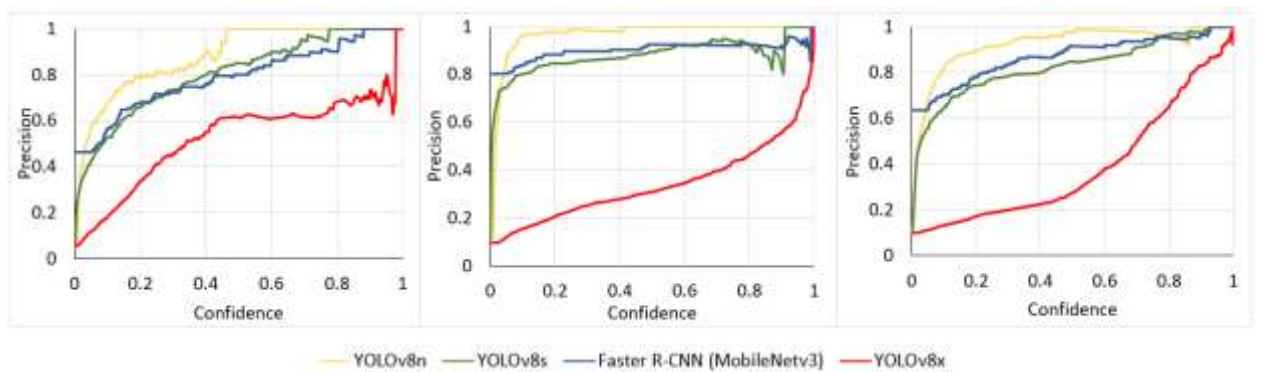


Figure 18: Precision - Confidence curves during the validation of the models on the three weeks of the early growth stage of maize seedlings (Two weeks aged - left, Three weeks aged - middle, Four weeks aged - right)

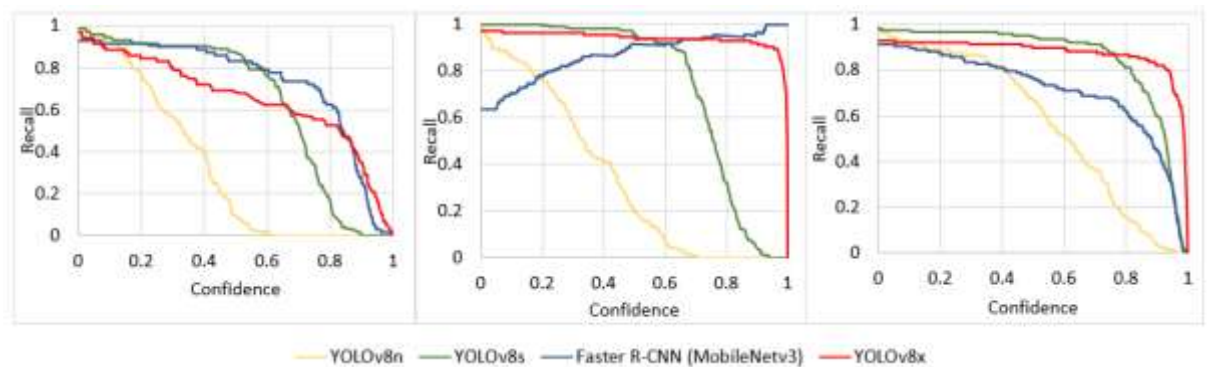


Figure 19: Recall - Confidence curves during the validation of the models on the three weeks of the early growth stage of maize seedlings (Two weeks aged - left, Three weeks aged - middle, Four weeks aged - right)

The reliability of the YOLOv8n, the nano variant was very low at Recall but high at Precision and their respective values grow with the age of the plants (Figure 18 and Figure 19) as opposed to the YOLOv8x, the extra-large variant. This suggests a very high sensitivity to the confidence threshold judged by the direction of their precision and recall curves.

Table 10: Models evaluation summary across the 3 weeks of the early-stage growth of maize seedlings

Growth stage	Models	Precision	Recall	mAP50	Map50-95
2 <sup>nd</sup> Week	YOLOv8n-nano	0.75	0.85	0.81	0.27
	YOLOv8s-small	0.83	0.88	0.89	0.32
	Faster R-CNN (MobileNetv3)	0.50	0.94	0.88	0.28
	YOLOv8x – Extra large	0.65	0.85	0.61	0.18
3 <sup>rd</sup> Week	YOLOv8n-nano	0.92	0.90	0.93	0.46
	YOLOv8s-small	0.87	0.97	0.94	0.48
	Faster R-CNN (MobileNetv3)	0.58	0.98	0.94	0.48
	YOLOv8x – Extra large	0.63	0.90	0.83	0.38
4 <sup>th</sup> Week	YOLOv8n-nano	0.92	0.86	0.93	0.46
	YOLOv8s-small	0.93	0.89	0.95	0.43
	Faster R-CNN (MobileNetv3)	0.76	0.96	0.95	0.48
	YOLOv8x – Extra large	0.83	0.82	0.84	0.38

## Comparison of the sources of confusion and uncertainty across the models

### Effect of plant size and spacing on model performance

As a plant grows, its size increases and affects its original spacing in-between neighbourhoods, making the plant population to be denser and leaves touching each other. At this stage, even the manual counting of plants becomes challenging as segmentation becomes difficult.

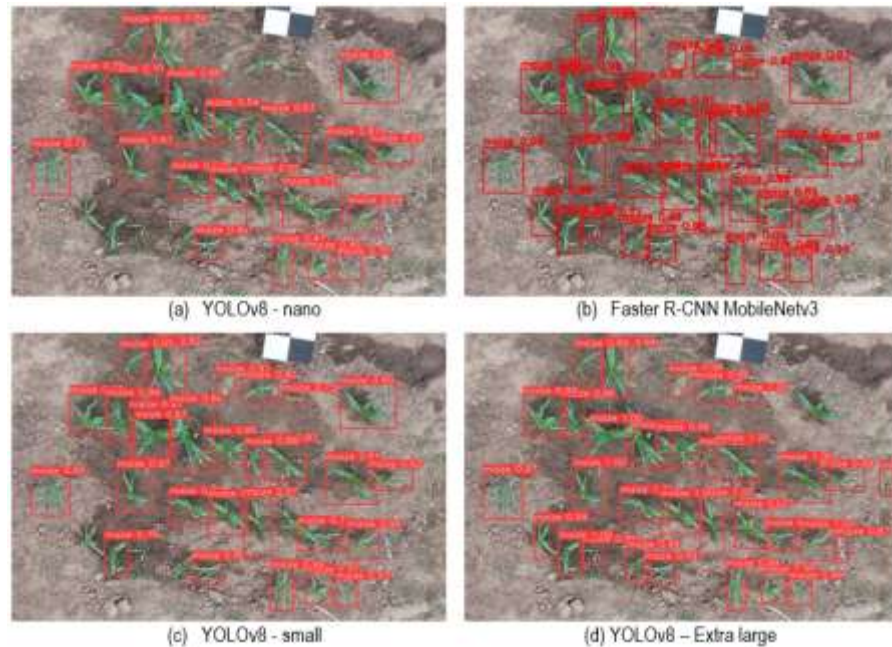


Figure 20: Highlights of model confusion in dense maize seedlings population

The Faster R-CNN (MobilenetV3) outperformed other models in weed discrimination (Figure 20b). This may be due to its feature extraction method (S. Ren et al., 2016). In crowded and dense scenes, images often contain numerous adjacent objects with highly similar appearances. This makes it difficult to avoid overlap between anchor boxes of neighbouring objects, complicating the accurate determination of positive and negative samples using Intersection over Union (IoU) (Xu et al., 2022). This problem may have started with the dataset annotation at the initial stages of the training process. While bounding boxes offer an easy way of annotating objects in the image,

polygon annotation is more precise, and in this figure, at this growth stage of the maize it is more suitable than using a bounding box as it is less subject to plant overlap.

### Effect of weed on model performance

Weeds often grow alongside crops and can be mistaken for crop plants. This can lead to inaccurate detection and classification of plants. Weeds effect on the model performance was found to be more pronounced in the YOLOv8x model, where the model failed at separating the two species of weeds as seen in Figure 21. The YOLOv8x model is the largest trained model of the YOLOv8 models and it expects to get good-resolution images where small objects can be seen. The COCO dataset on which the YOLOv8 model has been trained doesn't contain enough plant data, apart from some fruits, and is not balanced according to object size in the dataset, making the transfer learning not ineffective when it came to training in agriculture field due to the dataset discrepancy (Xu et al., 2023) as the new task was very different from the one the YOLOv8 models and Faster R-CNN model were trained on. One of the challenges in Deep learning applications in agriculture is the lack of enough labeled datasets for the training process (Arsenovic et al., 2019).

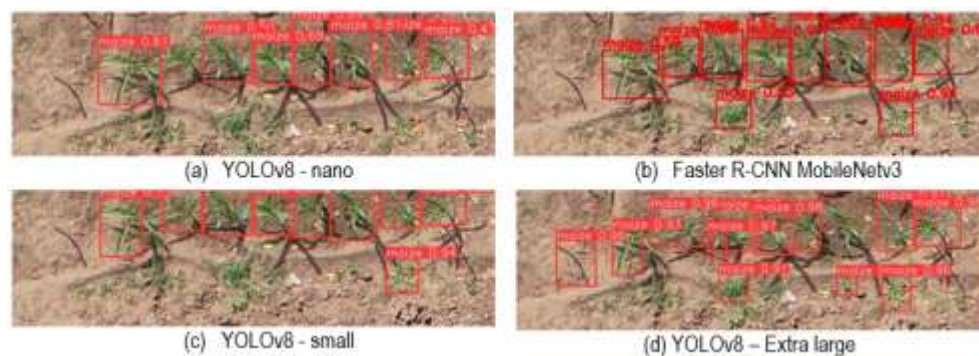


Figure 21: Illustration of inaccuracies caused by the weeds

Although the Faster R-CNN (Mobilenetv3) used a classification backbone, Mobilenetv3 is known to be effective in the classification task, and the resemblance between weeds and plants at their early stage is still confusing the model. Zhao et al. (2023b) have gotten the same conclusion even though their research used a dataset three times bigger than the one used in this study at a flight height of 5m.

### **Comparison of measured and UAV estimated plant growth parameters**

#### **Measured and UAV estimated plant height**

Once per growth stage, the plant heights were measured using the Digital Surface Model acquired by the UAV technology and manual measurements. The performance of the UAV technology was statically assessed with the coefficient of determination ( $R^2$ ), Root Mean Squared Error (RMSE) and Mean Absolute Error (MAE) by way of comparing the UAV-acquired plant heights and the manual measurements. The Linear relationship between the estimated value acquired by the UAV technology and the manual measurements on the field is showed in the Figure 22 and Figure 23 for Season one and Season two respectively.



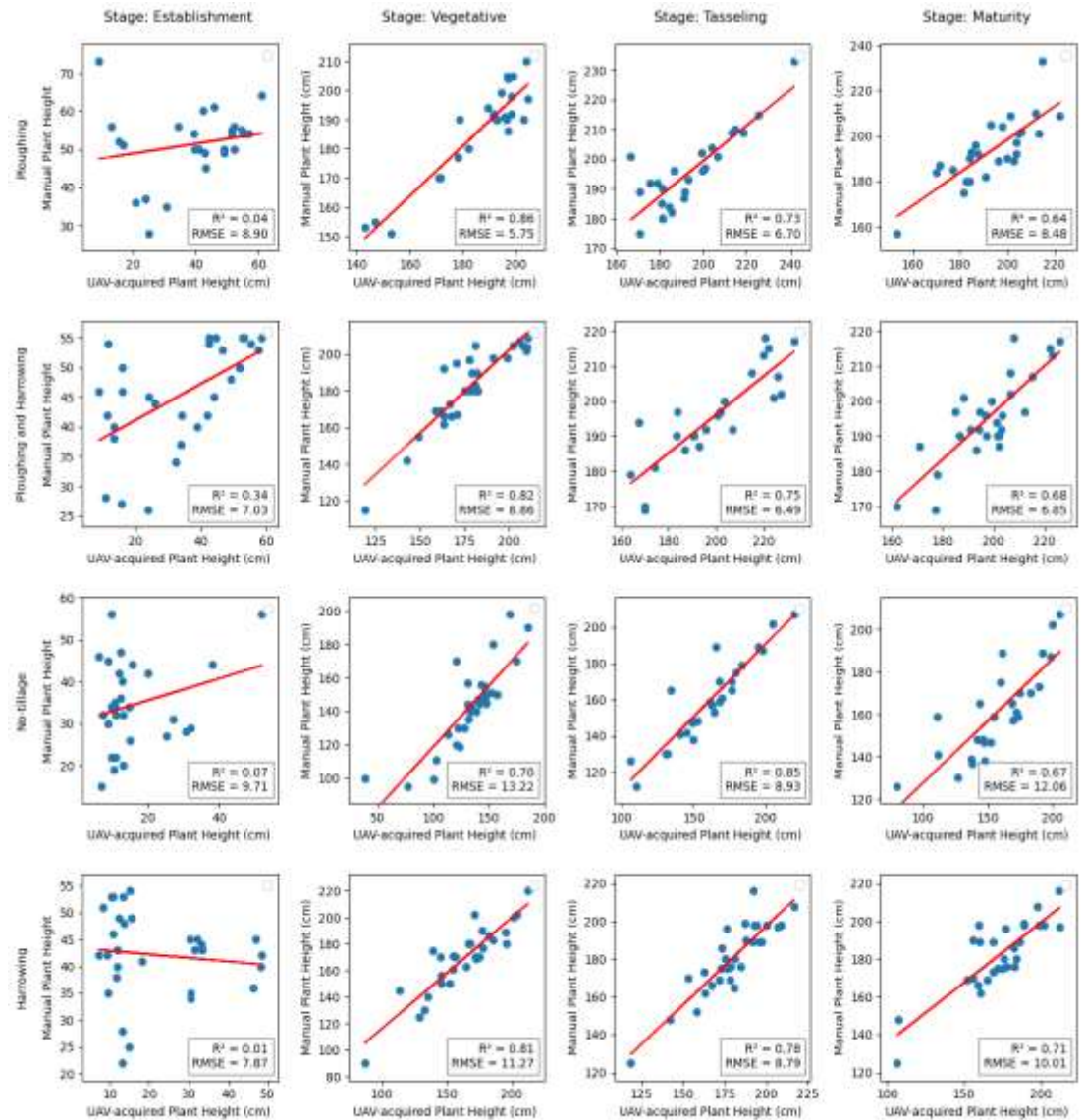


Figure 22: Linear relation between manually measured and UAV technology estimated plant heights across plant growth stages of different tillage treatments in Season one.

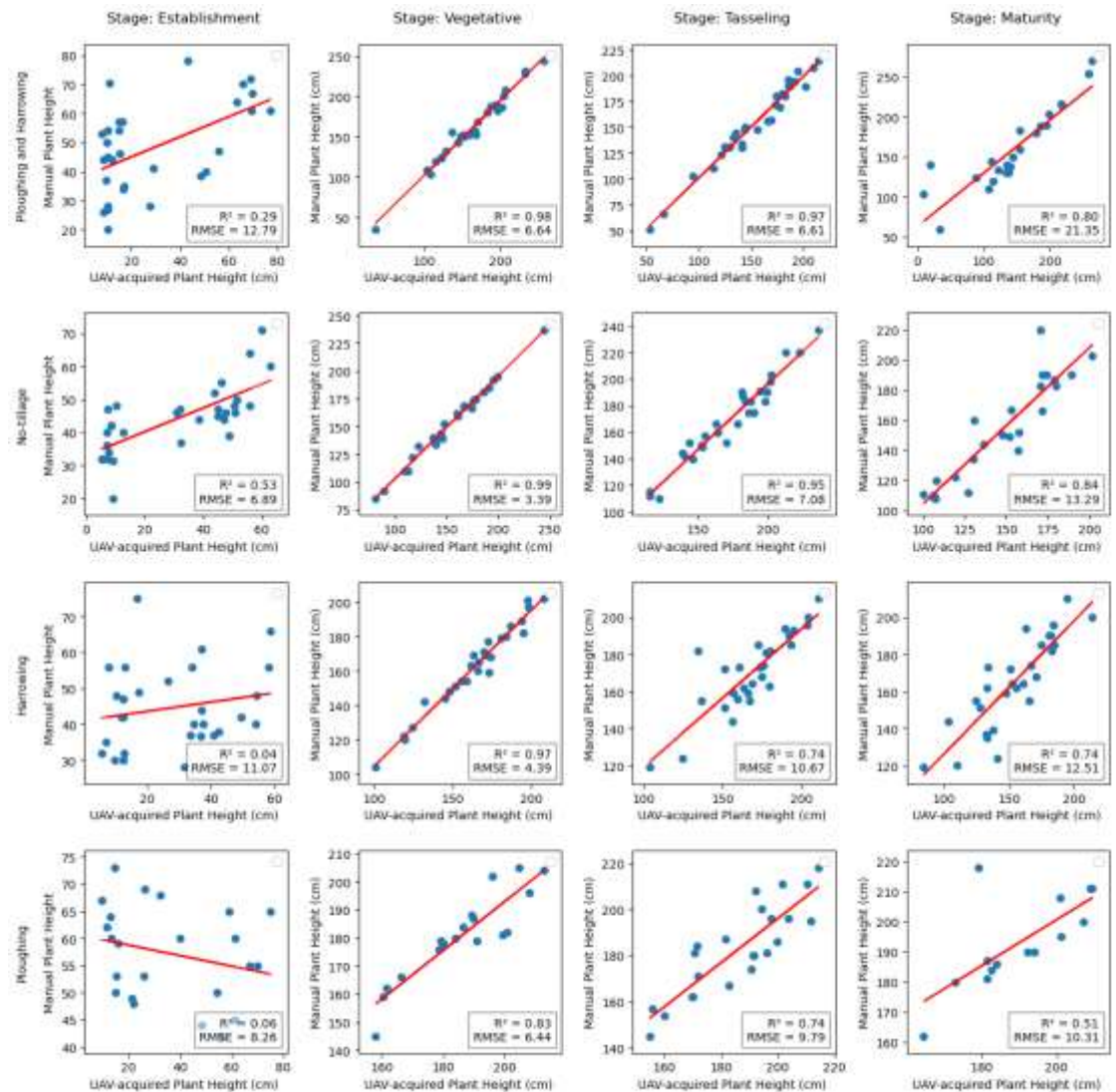


Figure 23: Linear relation between manually measured and UAV technology estimated plant heights across plant growth stages of different tillage treatments in Season Two.

At the vegetative and tasseling stages of the maize, an  $RMSE < 7\text{cm}$  and an  $R^2$  of 0.98, 0.99, 0.97 and 0.97 respectively for the Ploughing and Harrowing and No-tillage at the vegetative stage, Ploughing and Harrowing and Harrowing only at the Tasseling and Vegetative stage were obtained for all the treatments during Season Two (Figure 23), and were judged acceptable as compared to the results reported by Shu (2023). During the Season One, the highest  $R^2$  was at 0.86 score in the Ploughing only treatment

The estimation of the plant heights at the maturity stage were probably less accurate than at the tasselling while the plant heights did not greatly change as maize plants stopped growing in height at the end of the vegetative stage.

A study by Ji et al. (2022) showed an RMSE of around 7cm, which correlated with another UAV survey by Xie et al. (2021). The performance of the regression model at the vegetative and tasselling stage might be due to the LAI of the plots as they had the highest of the experiments (Figure 13 and Figure 14), among the factors there is the sowing space that increases the LAI (Akyeaw et al., 2023). Another study by Oehme et al. (2022) found the accuracy of plant height acquired by UAV technology to be dependent on the LAI and plant growth stages. Observations on the establishment stage in Figure 22 and Figure 23 have highlighted the poor performance of the UAV technology in estimating the plant height when the plants are less than 50 cm height. This can explain the reason behind the negative  $R^2$  as plants are small seen at the 20m flight height at the Establishment stage demonstrated by Akyeaw et al. (2023).

### **Estimation of the Leaf Area Index (LAI)**

The estimation of the Leaf Area Index using the UAV technology were made using different Machine Learning models. The dataset has been divided into growth stages for the estimation at different growth stage, and at the end, an overall estimation has been made using the four growth stages collected data. The models' performances are shown in the table below (Table 11). The RMSE,  $R^2$  and MAE have been computed for each model at the selected growth stage to assess its performance.



Table 11: Linear and Machine Learning models performance in estimating the Leaf Area Index (LAI)

Growth stages	ML Models used	R <sup>2</sup>	RMSE	MAE
Establishment	Ridge Regression	0.54	0.04	0.03
	Linear Regression	0.55	0.04	0.03
	Lars	0.55	0.04	0.03
Vegetative	Linear Regression	0.54	0.20	0.17
	Huber Regressor	0.57	0.19	0.16
	Lars	0.54	0.20	0.17
Tasselling	Linear Regression	0.78	0.16	0.10
	Huber Regressor	0.80	0.15	0.09
	Random Forest	0.76	0.17	0.12
Maturity	Random Forest	0.92	0.17	0.13
	Polynomial Regression (Degree 2)	0.93	0.16	0.12
	Gradient Boosting	0.94	0.14	0.11
	Polynomial Regression (degree=2)	0.94	0.16	0.12
All growth stages involved	Support Vector Regressor (SVR)	0.93	0.17	0.13
	Random Forest	0.89	0.23	0.15

At the early growth stage of the maize, the UAV technology has not been able to assess the LAI at a reasonable  $R^2$  ( $<0.55$ ) using canopy coverage retrieved from the Excess Green vegetation index and Plant height retrieved from Digital Surface Models. At the Establishment stage, the canopy coverage was more involved as the plants at that stage can be segmented easily with less complexity linked to the leaves arrangement thus Linear models were found to be more suitable. The same trend was observed during the vegetative stage too. At the tasselling stage, the performance of the UAV estimation of the vegetative index increased ( $R^2=0.57$ ) and the RMSE (0.19) value found to be better compared to the mean LAI (1.25) at the tasselling stage for both seasons (Table 11). At the maturity stage, the UAV technology has shown great performance ( $R^2=0.94$ ) in assessing the LAI using Polynomial Regression and

Gradient Boosting. This can be due to the proven performance of Tree-based machine learning models in estimating the Leaf Area Index by discriminating the soil bare ground considering only the canopy coverage and multi-spectral UAV (Liu et al., 2023). When involving all the stages at the same time, the estimation of LAI by the UAV models has shown to be better than considering single stages-based processing. The reason behind this could be from the dataset volume, as the models learn better using well-balanced and large dataset (Bottou, 2015; Dong & Rekatsinas, 2019).

### **UAV estimation of the number of tasseled plants**

The YOLOv8 Deep learning model was used to estimate the number of tasselled maize plants inside each plot at the first week of the tasselling stage for both seasons. Different variants of the model were applied and variant S (YOLOv8s – small) had the best performance and was applied for the experiment. The Figure 24 presents its performance on tassel detection and counting.

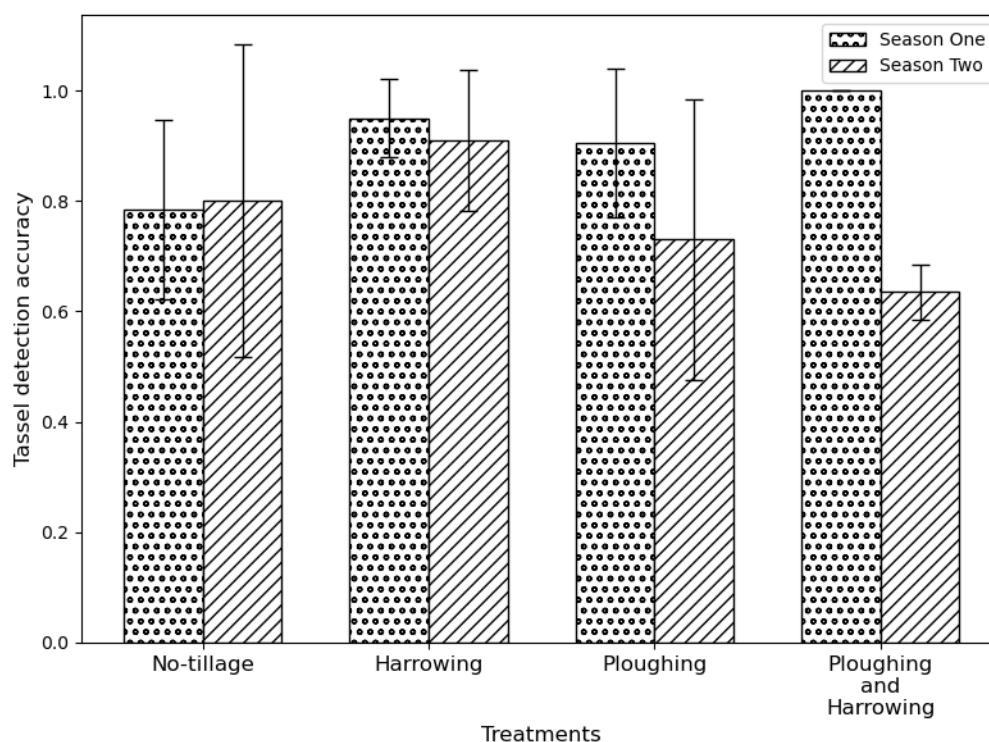


Figure 24: Maize tassel detection using YOLOv8

The counting of the tasselled maize plants was very accurate in the Ploughing and Harrowing stage, and the YOLO model has shown a good performance during Season One. Different factors could be attributed to that observation and the difference in environmental parameters can lead some tassels to be covered by plant leaves when they are not fully deployed and the wind condition which made some of them to bend as shown in the Figure 25. This is further reinforced by the dynamic growth patterns of tassels throughout the developmental stages, as well as the notable differences in tassel characteristics at each stage (Du et al., 2024). This is further emphasised by the finding where in Figure 15 the ANOVA analysis of days to 50 percent flowering had significant differences among treatments. The above reason most likely made the detection of tassels to be challenging as it has been found by a study by Karami et al. (2021).



Figure 25: Sources of inaccuracy in Tassel detection during the Season Two

### Yield Prediction

The features used for the yield prediction are the vegetation indices (VIs) (

Table 3), the Plant's height (Figure 22) and the Canopy coverage at different growth stages.

Table 12: Machine Learning yield prediction performance for yield prediction

Stages	E	V	T	M	E, V	E,T	E,M	E,V,T	E,V,M	E,T,M	T,M	V,T	V, M	V,T,M	E,V,T,M
$R^2$	0.792	0.864	-0.17	0.139	0.907	-0.02	0.088	0.634	0.873	0.088	0.088	0.900	0.873	0.881	0.578
DT RMSE	0.356	0.287	0.844	0.724	0.238	0.789	0.746	0.472	0.278	0.745	0.746	0.246	0.278	0.269	0.507
MAE	0.291	0.239	0.653	0.489	0.179	0.647	0.605	0.321	0.202	0.669	0.605	0.209	0.202	0.167	0.310
$R^2$	0.462	0.791	-0.42	-0.28	0.792	0.239	0.032	0.792	0.829	-0.049	-0.34	0.809	0.754	0.807	0.792
RF RMSE	0.573	0.357	0.932	0.882	0.356	0.681	0.768	0.356	0.323	0.799	0.905	0.341	0.388	0.343	0.356
MAE	0.445	0.342	0.846	0.791	0.302	0.599	0.598	0.319	0.258	0.675	0.737	0.314	0.327	0.311	0.319
$R^2$	0.283	0.889	-0.337	0.341	0.860	0.129	0.310	0.865	0.840	0.001	0.001	0.865	0.737	0.865	0.902
GB RMSE	0.661	0.260	0.903	0.633	0.292	0.728	0.648	0.287	0.312	0.780	0.780	0.287	0.400	0.287	0.244
MAE	0.521	0.236	0.850	0.440	0.253	0.553	0.551	0.250	0.287	0.596	0.596	0.250	0.354	0.250	0.194

E: Establishment, V: Vegetative, T: Tasselling, M: Maturity. DT:

Decision Tree, RF: Random Forest, GB: Gradient Boosting Regressor;  $R^2$ :

Coefficient of determination, RMSE: Root Mean Square Error, MAE: Mean

Absolute Error

Concerning the Decision Tree (DT) and Random Forest (RF) model, the best performances were observed at combined Establishment (E) and Vegetative (V) stages, achieving  $R^2$  of 0.907, RMSE of 0.238, MAE of 0.179 and  $R^2$  of 0.792, RMSE of 0.356, and MAE of 0.302, respectively. In contrast, at the combined Tasselling (T) stages, the worst performance was observed, with an  $R^2$  of -0.17 and -0.42, respectively, indicating poor predictive ability (Table 12).

Additionally, using the Gradient Boosting Regressor (GB) model, the best performance was attained at the combined Establishment, Vegetative, Tasselling, and Maturity stages, it yielded  $R^2$  of 0.902, RMSE of 0.244, and MAE of 0.194, while at the T stage it indicated the worst performance ( $R^2 = -0.337$ , RMSE = 0.903, MAE = 0.850) (Table 12). Overall, the general trend is that across all models that combining data from multiple growth stages, particularly at the Establishment and Vegetative stages, significantly enhanced predictive performance, as evidenced by higher  $R^2$  values and lower RMSE and MAE. However, at the Tasselling stage, the performance was consistently poor across all models, suggesting it is not a reliable stand-alone predictor of the yield of maize. It could be inferred that among the models, the Gradient Boosting Regressor tends to outperform the others, especially when using combined stages, demonstrating the highest  $R^2$  and lowest errors in many cases. This result acknowledges the importance of getting the appropriate growth stages and models for yield prediction in maize production.

The main objective of this study was to predict the end-of-season yield of maize, moreover, it wished to at least offer a certain level of confidence in

the outcome of the prediction in term of yield classification. If the UAV technology cannot predict the exact quantity of grain yield, can it, at least, inform the farmer if the yield will be Good ( $>4.75\text{t/ha}$ , Medium ( $3.5$  to  $4.75\text{t/ha}$ ) or bad ( $<3.5\text{t/ha}$ ) at the end of the season? The answer to this question was implemented through classification variant of the tree-based ML models. Further, considering the four main growth stages, how earlier can the farmer get an accurate expected yield?

Considering the prediction at the Establishment, Vegetative, Tasselling or Maturity taken individually or grouped, the results in Table 12, showed a gain of improvement. Studies have shown that crop growth is a dynamic process, and yield is influenced by cumulative effects across various stages emphasizing the importance of integrating data from multiple phenological stages to capture the complex interactions between environmental factors and crop development (Cao et al., 2021; Pei et al., 2025). Gradient Boosting was found to be more suitable for yield prediction as compared to Random Forest, for instance, Yasaswy et al. (2022) found it 0.987 accurate when used with historical data, same correlated by Singh & Bhavadharini (2023) who compared it to Random Forest, Decision Tree and Multiple Linear Model. This may be the reason the Gradient Boosting required all the growth stages features to yield better accuracy after the Vegetative stage.

In time-related features, the incorporation of the near-future data has been proven to improve the predictive accuracy of the model (Zeng et al., 2024), more specifically the integration of different growth stages can improve the model predictive accuracy of the maize yield (Y. Ren et al., 2023). For

instance, the Vegetative stage improves the prediction linked to Establishment and Vegetative, the maturity stage improving the first two stages.

Despite the improvements brought by the Tasselling and Maturity stages to the overall model performance, the difference in accuracy between the single-stage and multiple-stage approaches remains narrow, with an  $R^2$  variation of only 0.04 to 0.01. Although the Decision Tree achieved an  $R^2$  score of 0.79 at the establishment growth stage, it heavily relied on plant height as a predictive feature. This introduced bias, as the UAV's performance in estimating plant height at this stage was notably low. Given these findings, the optimal stage for yield prediction is the Vegetative stage, as supported by Sunoj et al. (2023), using the Gradient Boosting Regressor.

Table 13: Machine Learning yield prediction performance (classification)

	Stage													E,V,		E,T,		V,T,		E,V,T	
	s	E	V	T	M	E,V	E,T	E,M	E,V,T	M	M	T,M	V,T	V,M	M	,M					
DT	Acc.	0.875	1.000	0.750	0.875	0.875	0.875	0.750	0.875	0.875	0.875	0.875	0.875	0.875	0.875	0.875					
	Prec.	0.938	1.000	0.917	0.938	0.938	0.781	0.838	0.938	0.938	0.775	0.938	0.938	0.938	0.938	0.938					
	Rec.	0.875	1.000	0.750	0.875	0.875	0.875	0.750	0.875	0.875	0.875	0.875	0.875	0.875	0.875	0.875					
	F1	0.887	1.000	0.771	0.887	0.887	0.821	0.715	0.887	0.887	0.819	0.887	0.887	0.887	0.887	0.887					
RF	Acc.	0.875	0.875	0.750	0.750	0.875	0.750	0.875	0.875	0.875	0.875	0.875	0.875	0.875	0.875	0.875					
	Prec.	0.775	0.938	0.844	0.844	0.938	0.844	0.938	0.938	0.938	0.938	0.938	0.938	0.938	0.938	0.938					
	Rec.	0.875	0.875	0.750	0.750	0.875	0.750	0.875	0.875	0.875	0.875	0.875	0.875	0.875	0.875	0.875					
	F1	0.819	0.887	0.738	0.738	0.887	0.738	0.887	0.887	0.887	0.887	0.887	0.887	0.887	0.887	0.887					
GB	Acc.	0.875	0.875	0.750	0.875	1.000	0.875	0.875	1.000	0.875	0.875	0.750	1.000	0.875	1.000	1.000					
	Prec.	0.781	0.938	0.813	0.938	1.000	0.938	0.938	1.000	0.938	0.938	0.850	1.000	0.938	1.000	1.000					
	Rec.	0.875	0.875	0.750	0.875	1.000	0.875	0.875	1.000	0.875	0.875	0.750	1.000	0.875	1.000	1.000					
	F1	0.821	0.887	0.758	0.887	1.000	0.883	0.887	1.000	0.887	0.887	0.740	1.000	0.887	1.000	1.000					

E: Establishment, V: Vegetative, T: Tasselling, M: Maturity. DT:

Decision Tree, RF: Random Forest, GB: Gradient Boosting Regressor; Acc.:

Accuracy, Prec.: Precision

With regard to the performance of the regression task, the classification task aimed at giving a categorical insight about the expected yield. The categories were LOW: <3.5t/ha, MEDIUM: 3.5 to 4.75t/ha and GOOD: >4.75t/ha.

The Table 13 present the performance of the yield prediction as a classification task of 3 Tree-based machine learning models.

From the Table 13, the results indicate that among the individual stages, the Vegetative (V) stage consistently produced the highest model performance across all metrics, particularly for Gradient Boosting, where a perfect score (Accuracy, Precision, Recall, and F1 = 1.000) was achieved. This suggests that data from the Vegetative stage are the most predictive for end-of-season yield classification. In contrast, the model's performance was generally lower for the Tasselling (T) and Maturity (M) stages when considered independently.

In examining the combinations of growth stages, the inclusion of Vegetative (V) data with other stages (e.g., E, V, T and M or V, T, and M) significantly improved model performance. Again, the Gradient Boosting achieved optimum performance in some combinations (e.g., V, T, M), further emphasizing its robustness and ability to leverage additional information from multiple growth stages.

Comparatively, the Decision Tree model also exhibited strong performance for single stages, particularly the Vegetative stage (Precision and Recall = 1.000), but its performance remained constant with increasing complexity when combined with other growth stages. Although, in the case of the Random Forest, it was observed to be less effective than Gradient Boosting, it maintained consistent results across both individual stages and



their combinations, highlighting the dominance of the Vegetative stage (0.875 across all combinations). All these performances were achieved with Vegetation indices, Plant height and Canopy coverage. Their respective contribution to each prediction outcome is given in the figures 25 to 30.

Feature importance in Decision Trees & Random Forests is determined by the decrease in impurity (e.g., Gini impurity or variance reduction) when a feature is used for splitting. In Gradient Boosting Models, it is based on how often a feature appears in boosting iterations and its impact on error reduction.

Higher importance values indicate strong influence on predictions, while lower values suggest minimal impact. If a single feature dominates, the model relies heavily on it, whereas evenly distributed importance means multiple features contribute similarly.

When it comes to the yield classification, the Vegetative (V) stage consistently yielded the highest model performance, with Decision Tree achieving a perfect score (Accuracy, Precision, Recall, F1 = 1.000), thus aligning with the finding of Marapelli et al. (2024) completed by Kumar et al. (2023) highlighting the yield predictive potential of the vegetative stage and Decision Tree model. Tasselling (T) and Maturity (M) stages performed lower when analysed independently. Including Vegetative data in multi-stage models further improved performance, with Gradient Boosting excelling in certain combinations (e.g., V, T, M). Decision Tree performed well for single stages but showed little improvement with added complexity, while Random Forest maintained consistent results, reinforcing the dominance of the Vegetative stage.

Relying on combinations of stages increases the cost due to additional drone surveys. For instance, using three or four growth stages (e.g., E,V,T,M for regression) requires multiple surveys, which may not significantly improve performance compared to using the Vegetative stage alone. While some combinations, such as V,T,M, achieved perfect scores with Gradient Boosting, the added technical cost may outweigh the marginal benefits in scenarios where resources are limited.

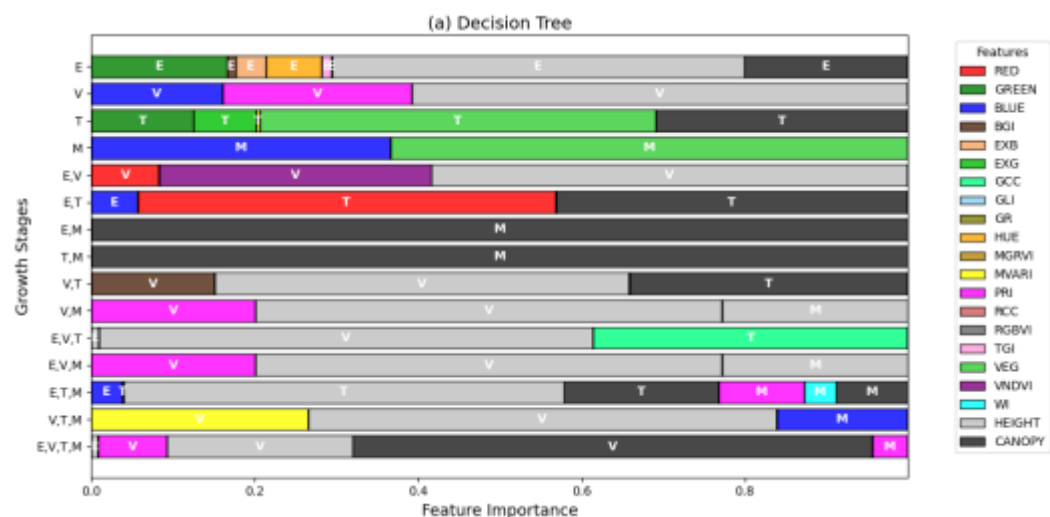


Figure 26: Feature importance scores of yield prediction using Decision Tree (E: Establishment, V: Vegetative, T: Tasselling, M: Maturity growth stages)

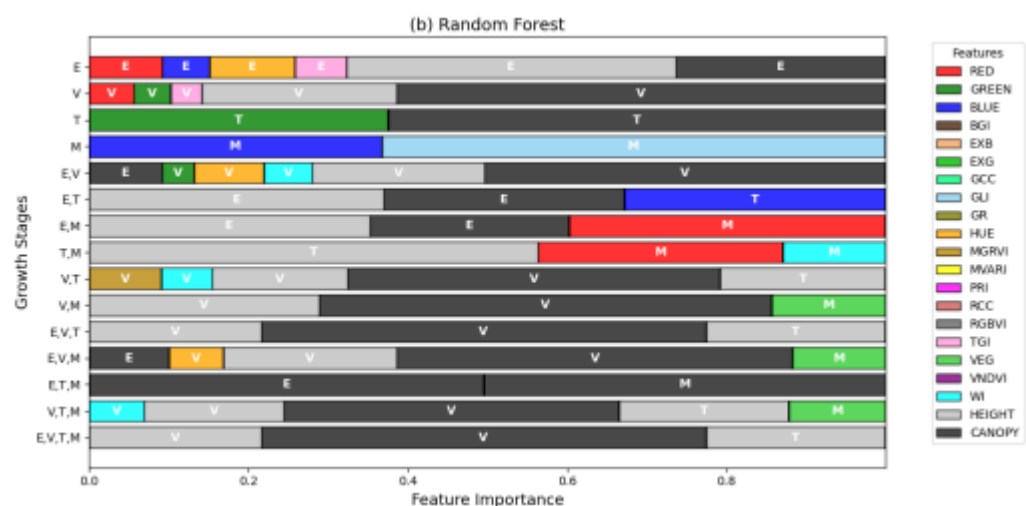


Figure 27: Feature importance scores of yield prediction using Random Forest (E: Establishment, V: Vegetative, T: Tasselling, M: Maturity growth stages)

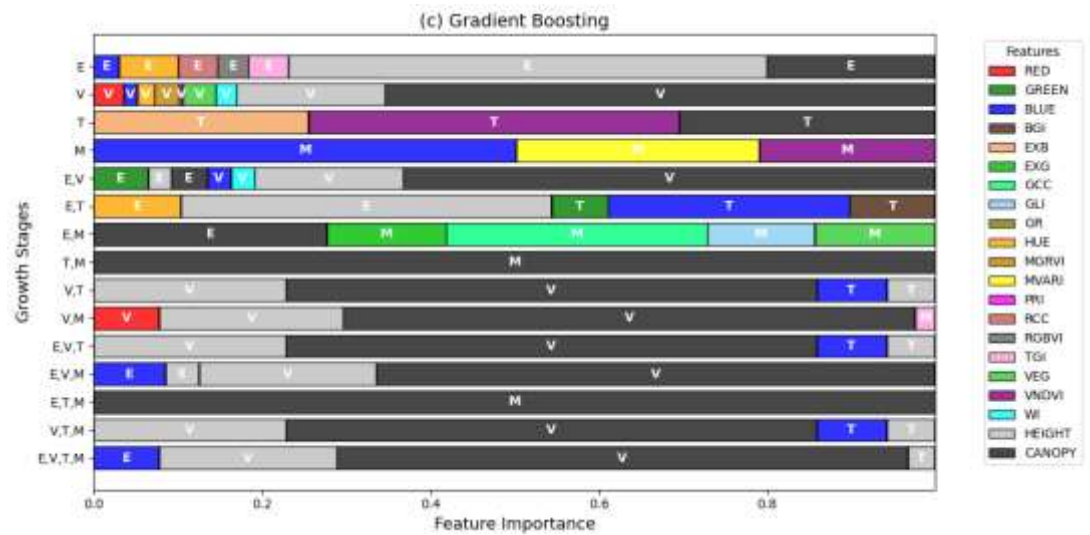


Figure 28: Feature importance scores of yield prediction using Gradient Boosting Machines (E: Establishment, V: Vegetative, T: Tasselling, M: Maturity growth stages)

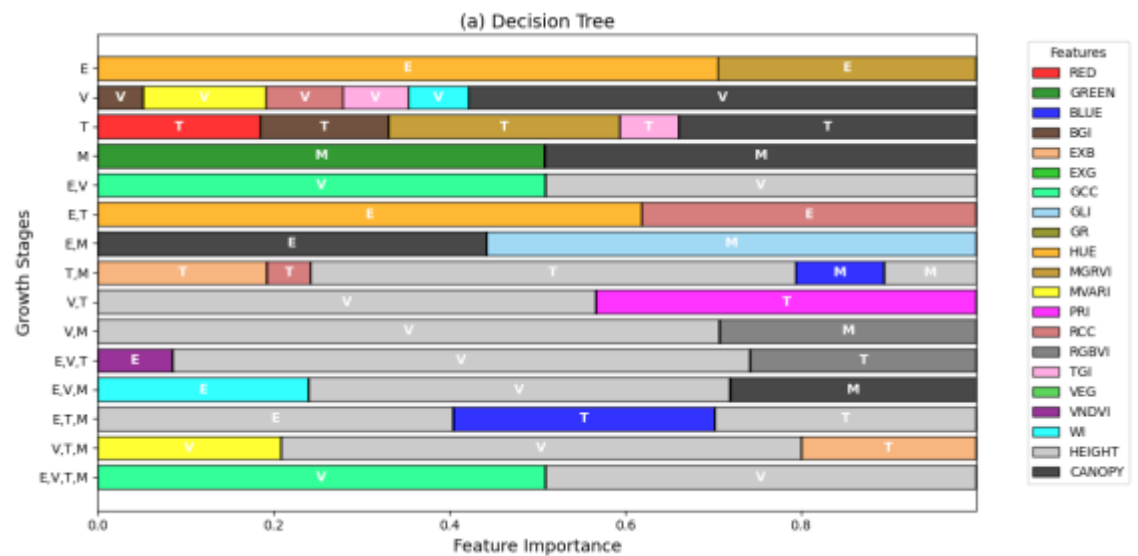


Figure 29: Feature importance scores of yield class prediction using Decision Tree (E: Establishment, V: Vegetative, T: Tasselling, M: Maturity growth stages)

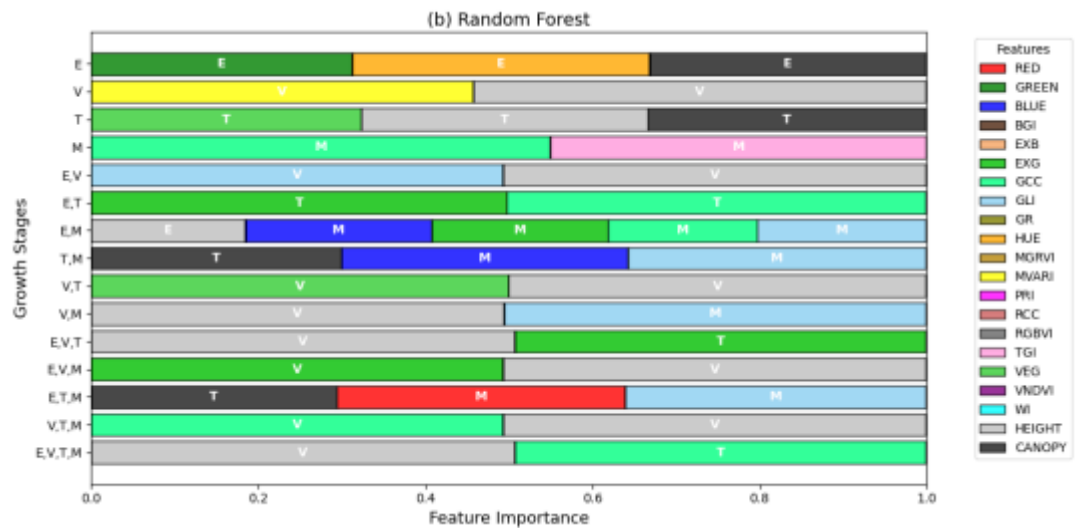


Figure 30: Feature importance scores of yield class prediction using Random Forest (E: Establishment, V: Vegetative, T: Tasselling, M: Maturity growth stages)

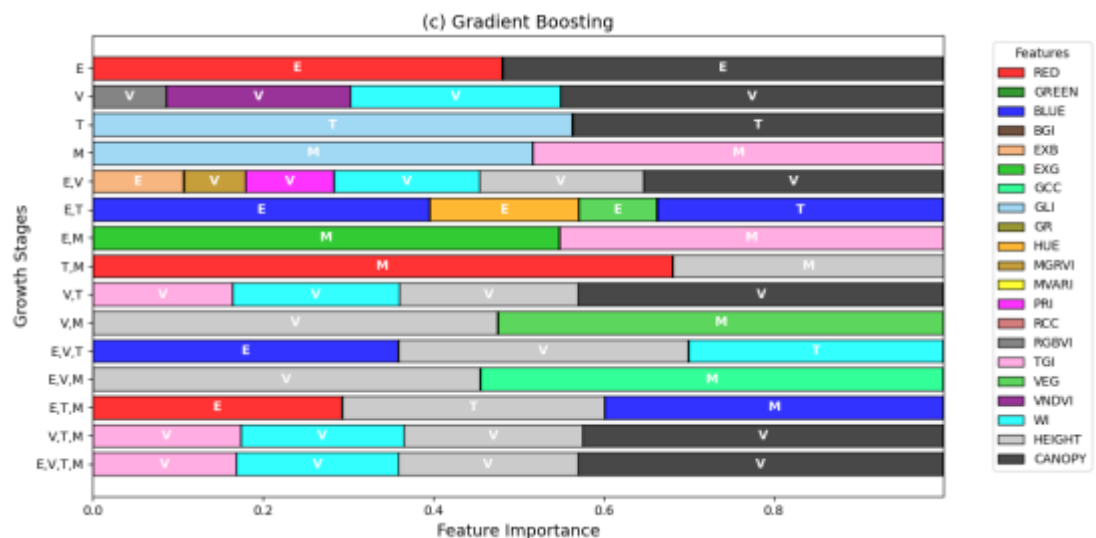


Figure 31: Feature importance scores of yield class prediction using Gradient Boosting Machines (E: Establishment, V: Vegetative, T: Tasselling, M: Maturity growth stages)

Figures 25 to 30 showed the dominance of the Plant height and canopy coverage as predictive features, with contributions ranging 0.2 to 1 in Gradient Boosting and Decision Tree models for both Classification and Regression. However, when selecting the best model, at the vegetative stage where the prediction was the highest, the features used were the Canopy coverage, Plant

height, TGI, RGVBI, RCC, HUE and Blue band, a different trend from the classification where the MGRVI and HUE with respective feature importance of 0.3 and 0.7. The Vegetation indices calculated at the vegetative stage dominated, probably due to their outstanding performance demonstrated with the prediction outcome ( $R^2 = 0.88$  or Accuracy=1) when using a single stage for prediction.

The quality of a prediction model highly depends on the accuracy of the feature data and their respective correlations with the target, here the grain yield. Some spectral indices were highly correlated with each other but had weak or inconsistent relationships with grain yield. The multi-collinearity of features since all the Vegetation Indices were calculated based on the same bands (R, G, B). This phenomenon is known to affect some Machine learning models, such as Linear ones, more specifically when the correlation feature-target is low, as it suggests an easy interchange between vegetation indices and is thus statically problematic (Shrestha, 2020).

Plant height (PH) and canopy coverage are key factors in predicting maize yield using UAV-based measurements. A study found that Plant height alone accounted for over 60% of maize grain yield (MGY) variability in clay loam soils (Machado et al., 2002). Additionally, maize yield responds directly to canopy cover and planting density, which are influenced by leaf orientation and canopy structure (García-Martínez et al., 2020). In several studies, the role of the multispectral vegetation indices, more specifically the NDVI index was acknowledged in the yield prediction, where the feature importance of RGB VIs were actually low ( $<0.1$ ) in Random Forest (Marques Ramos et al., 2020; Sunoj et al., 2021). However, MGRVI was found to correlate better with NDI

and was shown to be effective in yield prediction by Fathipour et al Fathipour et al. (2019) thus justifying its selection for yield classification, alongside HUE and TGI VIs. Moreover, Kumar et al. (2023) demonstrated that incorporating the green band in yield prediction enhances model performance. This supports the selection of the Blue Band and RCC, which exhibit strong correlations with the green band ( $R = 0.96$  and  $R = 0.81$ , respectively).

## CHAPTER FIVE

### CONCLUSION AND RECOMMENDATIONS

#### Conclusion

This study aimed at assessing the influence of tillage on maize performance while using UAV technology. The study found that tillage influenced the growth and yield of maize. It showed that Ploughing and Harrowing had the best grain yield (5.65t/ha) and growth parameters contrary to No-tillage and Harrowing. Despite initial poor performance, No-tillage showed potential for long-term improvement (+1.11t/ha).

The UAV technology was found to be performant in estimating the maize growth parameters. Estimating the germination rate through seedling detection, it was found that the YOLOv8s outperformed other models with an MAP of 0.32, 0.48, and 0.43 for 2, 3, and 3 WAS old maize seedlings respectively, followed by Faster R-CNN (Mobilenetv3). However, depending on the requirement in precision or recall, the Faster R-CNN (MobilenetV3) was found to be more suitable (Recall: 0.94, 0.98, 0.96) where misses are less important than wrong detections in opposition to the YOLOv8-small.

The maize plant height estimation using UAV technology accuracy was found to be highly dependent on the leaf area index with more precision at the Vegetative and Tasselling stages with a RMSE around 10 cm and  $R^2$  of 0.88. For the estimation of the Leaf Area Index, it was found that the UAV technology coupled with Machine Learning failed to estimate the LAI at the establishment and Vegetative Growth stage, however at the Tasselling and Maturity stages respectively its performance increased to an  $R^2$  of 0.80 and

RMSE of 0.15 using Huber Regressor and an  $R^2$  of 0.94 and RMSE 0.14 using Gradient Boosting Machines.

Further, this study highlighted the effectiveness of UAV acquired data in yield prediction. UAV surveys were found suitable to classify the expected yield with an accuracy of 1 and F1-score of 1 using the Decision Tree model with BGI, MVARI, CANOPY, WI, RCC and TGI Vegetation indices. Moreover, when it comes to predicting the exact yield quantity, the accuracy was at 0.88 with an RMSE of 0.281t/ha using blue band, PRI and Plant height as features, this result was found suitable as it involved only one UAV survey and the prediction time was the earliest (Vegetative growth stage) compared to the 0.9  $R^2$  and 0.238t/ha RMSE found using 2 drone surveys (Vegetative and Tasselling stages).

### **Recommendations**

Further research could be done to assess the long-term effect of no-tillage on the growth and yield of maize and propose affordable equipment for planting in No-tillage systems

Also, estimating the stem girth/diameter using the UAV technology could be useful. It is also recommended that future studies consider the cost-benefit analysis of utilizing UAV technology under small farm holding.



## REFERENCES

- Abdelmajeed, A. Y. A., & Juszczak, R. (2024). Challenges and Limitations of Remote Sensing Applications in Northern Peatlands: Present and Future Prospects. *Remote Sensing*, 16(3), 591. <https://doi.org/10.3390/rs16030591>
- Abdul Rahman, N., Larbi, A., Addah, W., Sulleyman, K. W., Adda, J. K., Kizito, F., & Hoeschle-Zeledon, I. (2022). Optimizing Food and Feed in Maize–Livestock Systems in Northern Ghana: The Effect of Maize Leaf Stripping on Grain Yield and Leaf Fodder Quality. *Agriculture*, 12(2), 275. <https://doi.org/10.3390/agriculture12020275>
- Abdullah, A. S. (2014). Minimum tillage and residue management increase soil water content, soil organic matter and canola seed yield and seed oil content in the semiarid areas of Northern Iraq. *Soil and Tillage Research*, 144, 150–155. <https://doi.org/10.1016/j.still.2014.07.017>
- Adu, G., Abdulai, M. s., Alidu, H., Nustugah, S., Buah, S., Kombiok, J., Obeng-Antwi, K., Abudulai, M., & Etwire, P. (2014). *Recommended Production Practices for Maize in Ghana*. <https://doi.org/10.13140/2.1.4376.3527>
- Ahmed, F., Mohanta, J. C., Keshari, A., & Yadav, P. S. (2022). Recent Advances in Unmanned Aerial Vehicles: A Review. *Arabian Journal for Science and Engineering*, 47(7), 7963–7984. <https://doi.org/10.1007/s13369-022-06738-0>
- Akyeaw, B. O., Kumi, F., Adade, R., Ekumah, B., & Osei, G. (2023). UAV-based plant height estimation of maize cultivated using different varieties

- and sowing spacing. *Journal of the Ghana Institution of Engineering (JGhIE)*, 23(4), 42–47. <https://doi.org/10.56049/jghie.v23i4.112>
- Alam, Md. K., Islam, Md. M., Salahin, N., & Hasanuzzaman, M. (2014). Effect of Tillage Practices on Soil Properties and Crop Productivity in Wheat-Mungbean-Rice Cropping System under Subtropical Climatic Conditions. *The Scientific World Journal*, 2014, 1–15. <https://doi.org/10.1155/2014/437283>
- Albahar, M. (2023). A Survey on Deep Learning and Its Impact on Agriculture: Challenges and Opportunities. *Agriculture*, 13(3), 540. <https://doi.org/10.3390/agriculture13030540>
- Alessana, F. S., Marcio, K., Edna, M. B. S., & Tonny, J. A. da S. (2015). Characteristics of maize production irrigation and time-varying doses of nitrogen. *African Journal of Agricultural Research*, 10(8), 821–828. <https://doi.org/10.5897/AJAR2014.9028>
- Ali, A. B., Elshaikh, N. A., Hong, L., Adam, A. B., & Haofang, Y. (2017). Conservation tillage as an approach to enhance crops water use efficiency. *Acta Agriculturae Scandinavica, Section B — Soil & Plant Science*, 67(3), 252–262. <https://doi.org/10.1080/09064710.2016.1255349>
- Al-Kaisi, M. M., Archontoulis, S. V., Kwaw-Mensah, D., & Miguez, F. (2015). Tillage and Crop Rotation Effects on Corn Agronomic Response and Economic Return at Seven Iowa Locations. *Agronomy Journal*, 107(4), 1411–1424. <https://doi.org/10.2134/agronj14.0470>
- Alkhazaali, H. A., Elsahookie, M. M., & Baktash, F. Y. (2017). Flowering Syndrome-Hybrid Performance Relationship in Maize 1-Agromonic

- Traits. *International Journal of Applied Agricultural Sciences*, 3(3), 67–71. <https://doi.org/10.11648/j.ijaas.20170303.12>
- Allam, M., Radicetti, E., Petroselli, V., & Mancinelli, R. (2021). Meta-Analysis Approach to Assess the Effects of Soil Tillage and Fertilization Source under Different Cropping Systems. *Agriculture*, 11(9), 823. <https://doi.org/10.3390/agriculture11090823>
- Alsamin, B., El-Hendawy, S., Refay, Y., Tola, E., Mattar, M. A., & Marey, S. (2022). Integrating Tillage and Mulching Practices as an Avenue to Promote Soil Water Storage, Growth, Production, and Water Productivity of Wheat under Deficit Irrigation in Arid Countries. *Agronomy*, 12(9), 2235. <https://doi.org/10.3390/agronomy12092235>
- Al-Zube, L., Sun, W., Robertson, D., & Cook, D. (2018). The elastic modulus for maize stems. *Plant Methods*, 14(1), 11. <https://doi.org/10.1186/s13007-018-0279-6>
- Amer, K. H. (2010a). Corn crop response under managing different irrigation and salinity levels. *Agricultural Water Management*, 97(10), 1553–1563. <https://doi.org/10.1016/j.agwat.2010.05.010>
- Amer, K. H. (2010b). Corn crop response under managing different irrigation and salinity levels. *Agricultural Water Management*, 97(10), 1553–1563. <https://doi.org/10.1016/j.agwat.2010.05.010>
- Angon, P. B., Anjum, N., Akter, Mst. M., KC, S., Suma, R. P., & Jannat, S. (2023a). An Overview of the Impact of Tillage and Cropping Systems on Soil Health in Agricultural Practices. *Advances in Agriculture*, 2023, 1–14. <https://doi.org/10.1155/2023/8861216>

- Angon, P. B., Anjum, N., Akter, Mst. M., KC, S., Suma, R. P., & Jannat, S. (2023b). An Overview of the Impact of Tillage and Cropping Systems on Soil Health in Agricultural Practices. *Advances in Agriculture*, 2023, 1–14. <https://doi.org/10.1155/2023/8861216>
- Anthony, D., Elbaum, S., Lorenz, A., & Detweiler, C. (2014). On crop height estimation with UAVs. *2014 IEEE/RSJ International Conference on Intelligent Robots and Systems*, 4805–4812. <https://doi.org/10.1109/IROS.2014.6943245>
- Arsenovic, M., Karanovic, M., Sladojevic, S., Anderla, A., & Stefanovic, D. (2019). Solving Current Limitations of Deep Learning Based Approaches for Plant Disease Detection. *Symmetry*, 11(7), 939. <https://doi.org/10.3390/sym11070939>
- Arshad, T., Naqve, M., Mukhtiar, A., Javaid, M. M., Mahmood, A., Nadeem, M. A., & Khan, B. A. (2023). Conservation Tillage for Sustainable Agriculture. In *Climate-Resilient Agriculture, Vol 1* (pp. 313–327). Springer International Publishing. [https://doi.org/10.1007/978-3-031-37424-1\\_15](https://doi.org/10.1007/978-3-031-37424-1_15)
- Asamoah, G. K. (1973). *Soils of the proposed farm sites of the University of Cape Coast* (Issue 88).
- Assouline, S. (2011). *Bulk Density of Soils and Impact on Their Hydraulic Properties* (pp. 95–100). [https://doi.org/10.1007/978-90-481-3585-1\\_22](https://doi.org/10.1007/978-90-481-3585-1_22)
- Bagula, E. M., Majaliwa, J.-G. M., Basamba, T. A., Mondo, J.-G. M., Vanlauwe, B., Gabiri, G., Tumuhairwe, J.-B., Mushagalusa, G. N., Musinguzi, P., Akello, S., Egeru, A., & Tenywa, M. M. (2022). Water Use Efficiency of Maize (*Zea mays* L.) Crop under Selected Soil and

- Water Conservation Practices along the Slope Gradient in Ruzizi Watershed, Eastern D.R. Congo. *Land*, 11(10), 1833. <https://doi.org/10.3390/land11101833>
- Bahadur, T., & Shrestha, J. (2014). Maize Production under No-Tillage System in Nepal. *World Journal of Agricultural Research*, 2(6A), 13–17. <https://doi.org/10.12691/wjar-2-6A-3>
- Bay, H., Ess, A., Tuytelaars, T., & Gool, L. Van. (2008). Speeded-Up Robust Features (SURF). *Comput. Vis. Image Underst.*, 110, 346–359. <https://api.semanticscholar.org/CorpusID:14777911>
- Becker-Reshef, I., Vermote, E., Lindeman, M., & Justice, C. (2010). A generalized regression-based model for forecasting winter wheat yields in Kansas and Ukraine using MODIS data. *Remote Sensing of Environment*, 114(6), 1312–1323. <https://doi.org/10.1016/j.rse.2010.01.010>
- Bendig, J., Yu, K., Aasen, H., Bolten, A., Bennertz, S., Broscheit, J., Gnyp, M. L., & Bareth, G. (2015). Combining UAV-based plant height from crop surface models, visible, and near infrared vegetation indices for biomass monitoring in barley. *International Journal of Applied Earth Observation and Geoinformation*, 39, 79–87. <https://doi.org/10.1016/j.jag.2015.02.012>
- Bhat, S. A., Pandit, B. A., Khan, J. N., Kumar, R., & Jan, R. (2017). Water Requirements and Irrigation Scheduling of Maize Crop using CROPWAT Model. *International Journal of Current Microbiology and Applied Sciences*, 6(11), 1662–1670. <https://doi.org/10.20546/ijcmas.2017.611.199>

- Blanco, H., & Lal, R. (2023). Tillage Systems. In *Soil Conservation and Management* (pp. 127–157). Springer Nature Switzerland.  
[https://doi.org/10.1007/978-3-031-30341-8\\_7](https://doi.org/10.1007/978-3-031-30341-8_7)
- Blanco-Canqui, H., & Ruis, S. J. (2018). No-tillage and soil physical environment. *Geoderma*, 326, 164–200.  
<https://doi.org/10.1016/j.geoderma.2018.03.011>
- Blessie, E. C., Balasubramanian, S., & Kumutha, V. (2024). *Empirical Analysis of Crop Yield Prediction Using Hybrid Model* (pp. 63–85).  
[https://doi.org/10.1007/978-3-031-51195-0\\_4](https://doi.org/10.1007/978-3-031-51195-0_4)
- Bolton, D. K., & Friedl, M. A. (2013). Forecasting crop yield using remotely sensed vegetation indices and crop phenology metrics. *Agricultural and Forest Meteorology*, 173, 74–84.  
<https://doi.org/10.1016/j.agrformet.2013.01.007>
- Bottou, L. (2015). How big data changes statistical machine learning. *2015 IEEE International Conference on Big Data (Big Data)*, 1–1.  
<https://doi.org/10.1109/BigData.2015.7363712>
- Büchi, L., Wendling, M., Amossé, C., Jeangros, B., Sinaj, S., & Charles, R. (2017). Long and short term changes in crop yield and soil properties induced by the reduction of soil tillage in a long term experiment in Switzerland. *Soil and Tillage Research*, 174, 120–129.  
<https://doi.org/10.1016/j.still.2017.07.002>
- Busari, M. A., Kukal, S. S., Kaur, A., Bhatt, R., & Dulazi, A. A. (2015). Conservation tillage impacts on soil, crop and the environment. *International Soil and Water Conservation Research*, 3(2), 119–129.  
<https://doi.org/10.1016/j.iswcr.2015.05.002>

- Cao, J., Zhang, Z., Tao, F., Zhang, L., Luo, Y., Zhang, J., Han, J., & Xie, J. (2021). Integrating Multi-Source Data for Rice Yield Prediction across China using Machine Learning and Deep Learning Approaches. *Agricultural and Forest Meteorology*, 297, 108275. <https://doi.org/10.1016/j.agrformet.2020.108275>
- Cárceles Rodríguez, B., Durán-Zuazo, V. H., Soriano Rodríguez, M., García-Tejero, I. F., Gálvez Ruiz, B., & Cuadros Tavira, S. (2022). Conservation Agriculture as a Sustainable System for Soil Health: A Review. *Soil Systems*, 6(4), 87. <https://doi.org/10.3390/soilsystems6040087>
- Carretta, L., Tarolli, P., Cardinali, A., Nasta, P., Romano, N., & Masin, R. (2021). Evaluation of runoff and soil erosion under conventional tillage and no-till management: A case study in northeast Italy. *CATENA*, 197, 104972. <https://doi.org/10.1016/j.catena.2020.104972>
- Carter, M. R., & McKeyes, E. (2005). CULTIVATION AND TILLAGE. In *Encyclopedia of Soils in the Environment* (pp. 356–361). Elsevier. <https://doi.org/10.1016/B0-12-348530-4/00514-2>
- Chen, S., Zhang, X., Shao, L., Sun, H., Niu, J., & Liu, X. (2020). Effects of straw and manure management on soil and crop performance in North China Plain. *CATENA*, 187, 104359. <https://doi.org/10.1016/j.catena.2019.104359>
- Chen, X., Liu, P., Zhao, B., Zhang, J., Ren, B., Li, Z., & Wang, Z. (2022). Root physiological adaptations that enhance the grain yield and nutrient use efficiency of maize (*Zea mays* L) and their dependency on phosphorus placement depth. *Field Crops Research*, 276, 108378. <https://doi.org/10.1016/j.fcr.2021.108378>

- Chen, Y., Huang, Y., Zhang, Z., Wang, Z., Liu, B., Liu, C., Huang, C., Dong, S., Pu, X., Wan, F., Qiao, X., & Qian, W. (2023). Plant image recognition with deep learning: A review. *Computers and Electronics in Agriculture*, 212, 108072. <https://doi.org/10.1016/j.compag.2023.108072>
- Chisi, M., & Peterson, G. (2019). Breeding and Agronomy. In *Sorghum and Millets* (pp. 23–50). Elsevier. <https://doi.org/10.1016/B978-0-12-811527-5.00002-2>
- Colomina, I., & Molina, P. (2014). Unmanned aerial systems for photogrammetry and remote sensing: A review. *ISPRS Journal of Photogrammetry and Remote Sensing*, 92, 79–97. <https://doi.org/10.1016/j.isprsjprs.2014.02.013>
- Costa, L., Nunes, L., & Ampatzidis, Y. (2020). A new visible band index (vNDVI) for estimating NDVI values on RGB images utilizing genetic algorithms. *Computers and Electronics in Agriculture*, 172, 105334. <https://doi.org/10.1016/j.compag.2020.105334>
- Cutler, H. C., & Cutler, M. C. (1948). Studies on the Structure of the Maize Plant. *Annals of the Missouri Botanical Garden*, 35(4), 301. <https://doi.org/10.2307/2394695>
- Dakhil, N., Aqeel, N., & Sadiq, M. (2022). Yield and Economic Analysis of Maize Production Using Different Combinations of Combined Tillage Machines and Comparison to Conventional Tillage Systems. *University of Thi-Qar Journal of Agricultural Research*, 11(2), 269–279. <https://doi.org/10.54174/utjagr.v11i2.215>
- De Swaef, T., Maes, W. H., Aper, J., Baert, J., Cougnon, M., Reheul, D., Steppe, K., Roldán-Ruiz, I., & Lootens, P. (2021). Applying RGB- and



- Thermal-Based Vegetation Indices from UAVs for High-Throughput Field Phenotyping of Drought Tolerance in Forage Grasses. *Remote Sensing*, 13(1), 147. <https://doi.org/10.3390/rs13010147>
- Deng, J., Dong, W., Socher, R., Li, L.-J., Kai Li, & Li Fei-Fei. (2009). ImageNet: A large-scale hierarchical image database. *2009 IEEE Conference on Computer Vision and Pattern Recognition*, 248–255. <https://doi.org/10.1109/CVPR.2009.5206848>
- Dhillon, R., & Moncur, Q. (2023). Small-Scale Farming: A Review of Challenges and Potential Opportunities Offered by Technological Advancements. *Sustainability*, 15(21), 15478. <https://doi.org/10.3390/su152115478>
- Dong, X. L., & Rekatsinas, T. (2019). Data Integration and Machine Learning. *Proceedings of the 25th ACM SIGKDD International Conference on Knowledge Discovery & Data Mining*, 3193–3194. <https://doi.org/10.1145/3292500.3332296>
- Drobitko, A., Kachanova, T., Markova, N., & Malkina, V. (2024). Modern cultivation technologies in improvement of corn quality. *Ukrainian Black Sea Region Agrarian Science*, 28(1), 19–28. <https://doi.org/10.56407/bs.agrarian/1.2024.19>
- Du, C., Li, L., Xie, J., Effah, Z., Luo, Z., & Wang, L. (2023). Long-Term Conservation Tillage Increases Yield and Water Use Efficiency of Spring Wheat (*Triticum aestivum* L.) by Regulating Substances Related to Stress on the Semi-Arid Loess Plateau of China. *Agronomy*, 13(5), 1301. <https://doi.org/10.3390/agronomy13051301>

- Du, J., Li, J., Fan, J., Gu, S., Guo, X., & Zhao, C. (2024). Detection and Identification of Tassel States at Different Maize Tasselling Stages Using UAV Imagery and Deep Learning. *Plant Phenomics*, 6. <https://doi.org/10.34133/plantphenomics.0188>
- Du Plessis, J. (2003). *Maize production*. Department of Agriculture Pretoria, South Africa.
- Duchene, O., Capowiez, Y., Vian, J.-F., Ducasse, V., Cadiergues, A., Lhuillery, T., & Peigné, J. (2023). Conservation tillage influences soil structure, earthworm communities and wheat root traits in a long-term organic cropping experiment. *Plant and Soil*. <https://doi.org/10.1007/s11104-023-06273-3>
- Duiker, S. W., Haldeman Jr, J. F., & Johnson, D. H. (2006). Tillage maize hybrid interactions. *Agronomy Journal*, 98(3), 436–442.
- Duruoha, C., Piffer, C. R., & Silva, P. A. (2007). Corn Root Length Density And Root Diameter as Affected by Soil Compaction and Soil Water Content. *IRRIGA*, 12(1), 14–26. <https://doi.org/10.15809/irriga.2007v12n1p14-26>
- Duveiller, G., & Defourny, P. (2010). A conceptual framework to define the spatial resolution requirements for agricultural monitoring using remote sensing. *Remote Sensing of Environment*, 114(11), 2637–2650. <https://doi.org/10.1016/j.rse.2010.06.001>
- Edmeades, G. O., Trevisan, W., Prasanna, B. M., & Campos, H. (2017). Tropical Maize (*Zea mays* L.). In *Genetic Improvement of Tropical Crops* (pp. 57–109). Springer International Publishing. [https://doi.org/10.1007/978-3-319-59819-2\\_3](https://doi.org/10.1007/978-3-319-59819-2_3)

- Efremenko, D., & Kokhanovsky, A. (2021). Introduction to Remote Sensing. In *Foundations of Atmospheric Remote Sensing* (pp. 1–35). Springer International Publishing. [https://doi.org/10.1007/978-3-030-66745-0\\_1](https://doi.org/10.1007/978-3-030-66745-0_1)
- El Mekkaoui, A., Moussadek, R., Mrabet, R., Douaik, A., El Haddadi, R., Bouhlal, O., Elomari, M., Ganoudi, M., Zouahri, A., & Chakiri, S. (2023). Effects of Tillage Systems on the Physical Properties of Soils in a Semi-Arid Region of Morocco. *Agriculture*, 13(3), 683. <https://doi.org/10.3390/agriculture13030683>
- Elbasi, E., Zaki, C., Topcu, A. E., Abdelbaki, W., Zreikat, A. I., Cina, E., Shdefat, A., & Saker, L. (2023). Crop Prediction Model Using Machine Learning Algorithms. *Applied Sciences*, 13(16), 9288. <https://doi.org/10.3390/app13169288>
- Erenstein, O., Jaleta, M., Sonder, K., Mottaleb, K., & Prasanna, B. M. (2022). Global maize production, consumption and trade: trends and R&D implications. *Food Security*, 14(5), 1295–1319. <https://doi.org/10.1007/s12571-022-01288-7>
- Escadafal, R., Belghit, A., & Ben-Moussa, A. (1994). Indices spectraux pour la télédétection de la dégradation des milieux naturels en Tunisie aride. In G. Guyot (Ed.), *Actes du 6ème Symposium international sur les mesures physiques et signatures en télédétection* (pp. 253–259).
- Essilfie, M. E., Darkwa, K., & Asamoah, V. (2024). Growth and yield response of maize to integrated nutrient management of chicken manure and inorganic fertilizer in different agroecological zones. *Heliyon*, 10(14), e34830. <https://doi.org/10.1016/j.heliyon.2024.e34830>

- Fang, J., & Su, Y. (2019). Effects of Soils and Irrigation Volume on Maize Yield, Irrigation Water Productivity, and Nitrogen Uptake. *Scientific Reports*, 9(1), 7740. <https://doi.org/10.1038/s41598-019-41447-z>
- Fathipoor, H., Arefi, H., Shah-Hosseini, R., & Moghadam, H. (2019). Corn forage yield prediction using unmanned aerial vehicle images at mid-season growth stage. *Journal of Applied Remote Sensing*, 13(03), 1. <https://doi.org/10.1117/1.JRS.13.034503>
- Finch, H. J. S., Samuel, A. M., & Lane, G. P. F. (2002). Cropping techniques. In *Lockhart and Wiseman's Crop Husbandry Including Grassland* (pp. 183–207). Elsevier. <https://doi.org/10.1533/9781855736504.2.183>
- Franch, B., Vermote, E. F., Becker-Reshef, I., Claverie, M., Huang, J., Zhang, J., Justice, C., & Sobrino, J. A. (2015). Improving the timeliness of winter wheat production forecast in the United States of America, Ukraine and China using MODIS data and NCAR Growing Degree Day information. *Remote Sensing of Environment*, 161, 131–148. <https://doi.org/10.1016/j.rse.2015.02.014>
- Gamon, J. A., Serrano, L., & Surfus, J. S. (1997). The photochemical reflectance index: an optical indicator of photosynthetic radiation use efficiency across species, functional types, and nutrient levels. *Oecologia*, 112(4), 492–501. <https://doi.org/10.1007/s004420050337>
- Gamon, J. A., & Surfus, J. S. (1999). Assessing leaf pigment content and activity with a reflectometer. *New Phytologist*, 143(1), 105–117. <https://doi.org/10.1046/j.1469-8137.1999.00424.x>
- Gao, F. (2021). *Remote Sensing for Agriculture* (pp. 7–24). [https://doi.org/10.1007/978-3-030-66387-2\\_2](https://doi.org/10.1007/978-3-030-66387-2_2)

- García-Martínez, H., Flores-Magdaleno, H., Ascencio-Hernández, R., Khalil-Gardezi, A., Tijerina-Chávez, L., Mancilla-Villa, O. R., & Vázquez-Peña, M. A. (2020). Corn Grain Yield Estimation from Vegetation Indices, Canopy Cover, Plant Density, and a Neural Network Using Multispectral and RGB Images Acquired with Unmanned Aerial Vehicles. *Agriculture*, 10(7), 277. <https://doi.org/10.3390/agriculture10070277>
- Gellatly, K., & Dennis, D. T. (2011). Plant Biotechnology and GMOs. In *Comprehensive Biotechnology* (pp. 9–22). Elsevier. <https://doi.org/10.1016/B978-0-08-088504-9.00272-5>
- Głąb, T., & Kulig, B. (2008). Effect of mulch and tillage system on soil porosity under wheat (*Triticum aestivum*). *Soil and Tillage Research*, 99(2), 169–178. <https://doi.org/10.1016/j.still.2008.02.004>
- Goodfellow, I., Pouget-Abadie, J., Mirza, M., Xu, B., Warde-Farley, D., Ozair, S., Courville, A., & Bengio, Y. (2020). Generative adversarial networks. *Communications of the ACM*, 63(11), 139–144. <https://doi.org/10.1145/3422622>
- Goswami, T., Hasan, M. S., & Ghosal, S. (2022). Site suitability of emerging maize cultivation in a changing agroclimatic setting of eastern India: a fuzzy-MCE integrated analysis. *Environment, Development and Sustainability*, 26(1), 1229–1261. <https://doi.org/10.1007/s10668-022-02756-y>
- Guan, D., Al-Kaisi, M. M., Zhang, Y., Duan, L., Tan, W., Zhang, M., & Li, Z. (2014). Tillage practices affect biomass and grain yield through regulating root growth, root-bleeding sap and nutrients uptake in summer

maize. *Field Crops Research*, 157, 89–97.

<https://doi.org/10.1016/j.fcr.2013.12.015>

Guerrero-Méndez, C., & Abraham-Juárez, M. J. (2023). Factors specifying sex

determination in maize. *Plant Reproduction*.

<https://doi.org/10.1007/s00497-023-00485-4>

Haddaway, N. R., Hedlund, K., Jackson, L. E., Kätterer, T., Lugato, E.,

Thomsen, I. K., Jørgensen, H. B., & Isberg, P.-E. (2017). How does

tillage intensity affect soil organic carbon? A systematic review.

*Environmental Evidence*, 6(1), 30. <https://doi.org/10.1186/s13750-017->

0108-9

Hague, T., Tillett, N. D., & Wheeler, H. (2006). Automated Crop and Weed

Monitoring in Widely Spaced Cereals. *Precision Agriculture*, 7(1), 21–

32. <https://doi.org/10.1007/s11119-005-6787-1>

Halder, M., Datta, A., Siam, M. K. H., Mahmud, S., Sarkar, Md. S., & Rana,

Md. M. (2023). *A Systematic Review on Crop Yield Prediction Using*

*Machine Learning* (pp. 658–667). <https://doi.org/10.1007/978-981-99->

4725-6\_77

Han, L., Yang, G., Dai, H., Yang, H., Xu, B., Li, H., Long, H., Li, Z., Yang,

X., & Zhao, C. (2019). Combining self-organizing maps and biplot

analysis to preselect maize phenotypic components based on UAV high-

throughput phenotyping platform. *Plant Methods*, 15(1), 57.

<https://doi.org/10.1186/s13007-019-0444-6>

Han, X., Thomasson, J. A., Bagnall, G. C., Pugh, N. A., Horne, D. W.,

Rooney, W. L., Jung, J., Chang, A., Malambo, L., Popescu, S. C., Gates,

I. T., & Cope, D. A. (2018). Measurement and Calibration of Plant-

- Height from Fixed-Wing UAV Images. *Sensors*, 18(12), 4092.  
<https://doi.org/10.3390/s18124092>
- Hao, Y., Pei, H., Lyu, Y., Yuan, Z., Rizzo, J.-R., Wang, Y., & Fang, Y. (2022). *Understanding the Impact of Image Quality and Distance of Objects to Object Detection Performance*.
- He, K., Gkioxari, G., Dollár, P., & Girshick, R. (2017). *Mask R-CNN*.
- Hengqi, J., & Ragni, L. (2024). Plant growth: The heavy matter of weight-induced plant stem thickening. *Current Biology*, 34(18), R871–R873.  
<https://doi.org/10.1016/j.cub.2024.08.023>
- Herr, A. W., Adak, A., Carroll, M. E., Elango, D., Kar, S., Li, C., Jones, S. E., Carter, A. H., Murray, S. C., Paterson, A., Sankaran, S., Singh, A., & Singh, A. K. (2023). Unoccupied aerial systems imagery for phenotyping in cotton, maize, soybean, and wheat breeding. *Crop Science*, 63(4), 1722–1749. <https://doi.org/10.1002/csc2.21028>
- Hochholdinger, F. (2004). Genetic Dissection of Root Formation in Maize (*Zea mays*) Reveals Root-type Specific Developmental Programmes. *Annals of Botany*, 93(4), 359–368. <https://doi.org/10.1093/aob/mch056>
- Hochholdinger, F. (2009). The Maize Root System: Morphology, Anatomy, and Genetics. In *Handbook of Maize: Its Biology* (pp. 145–160). Springer New York. [https://doi.org/10.1007/978-0-387-79418-1\\_8](https://doi.org/10.1007/978-0-387-79418-1_8)
- Hochholdinger, F., Marcon, C., Baldauf, J. A., Yu, P., & Frey, F. P. (2018). Proteomics of Maize Root Development. *Frontiers in Plant Science*, 9. <https://doi.org/10.3389/fpls.2018.00143>
- Horning, N. (2019). Remote Sensing. In *Encyclopedia of Ecology* (pp. 404–413). Elsevier. <https://doi.org/10.1016/B978-0-12-409548-9.10607-4>

- Houlsby, N., Giurgiu, A., Jastrzebski, S., Morrone, B., De Laroussilhe, Q., Gesmundo, A., Attariyan, M., & Gelly, S. (2019). Parameter-Efficient Transfer Learning for NLP. In K. Chaudhuri & R. Salakhutdinov (Eds.), *Proceedings of the 36th International Conference on Machine Learning* (Vol. 97, pp. 2790–2799). PMLR. <https://proceedings.mlr.press/v97/houlsby19a.html>
- Hu, Y. (2022). Effect of Conservation Tillage on Soil and Water Quality. *Academic Journal of Science and Technology*, 3(3), 124–126. <https://doi.org/10.54097/ajst.v3i3.2834>
- Hunt, E. R. Jr., Doraiswamy, P. C., McMurtrey, J. E., Daughtry, C. S. T., Perry, E. M., & Akhmedov, B. (2013). A visible band index for remote sensing leaf chlorophyll content at the canopy scale. *Publications from USDA-ARS / UNL Faculty*, 1156. <https://digitalcommons.unl.edu/usdaarsfacpub/1156>
- Huynh, H. T., Hufnagel, J., Wurbs, A., & Bellingrath-Kimura, S. D. (2019). Influences of soil tillage, irrigation and crop rotation on maize biomass yield in a 9-year field study in Müncheberg, Germany. *Field Crops Research*, 241, 107565. <https://doi.org/10.1016/j.fcr.2019.107565>
- Imani, R., Samdeliri, M., & Mirkalaei, A. M. (2022). The Effect of Different Tillage Methods and Nitrogen Chemical Fertilizer on Quantitative and Qualitative Characteristics of Corn. *International Journal of Analytical Chemistry*, 2022, 1–11. <https://doi.org/10.1155/2022/7550079>
- Jabro, J. D. (1992). Estimation of Saturated Hydraulic Conductivity of Soils From Particle Size Distribution and Bulk Density Data. *Transactions of the ASAE*, 35(2), 557–560. <https://doi.org/10.13031/2013.28633>



- Jaidka, M., Bathla, S., & Kaur, R. (2020). Improved Technologies for Higher Maize Production. In *Maize - Production and Use*. IntechOpen. <https://doi.org/10.5772/intechopen.88997>
- Jamidi, Rauf, A., Hanum, C., & Nyak Akop, E. (2018). *High Growth and Diameter of the Stem of Corn Plants (Zea May, S) with a Different Cropping Pattern* (pp. 99–106). <https://doi.org/10.1108/978-1-78756-793-1-00032>
- Ji, Y., Chen, Z., Cheng, Q., Liu, R., Li, M., Yan, X., Li, G., Wang, D., Fu, L., Ma, Y., Jin, X., Zong, X., & Yang, T. (2022). Estimation of plant height and yield based on UAV imagery in faba bean (*Vicia faba* L.). *Plant Methods*, 18(1), 26. <https://doi.org/10.1186/s13007-022-00861-7>
- Jocher, G., Chaurasia, A., & Qiu, J. (2023). *Ultralytics YOLOv8*. <https://github.com/ultralytics/ultralytics>
- Joshi, A., Pradhan, B., Gite, S., & Chakraborty, S. (2023). Remote-Sensing Data and Deep-Learning Techniques in Crop Mapping and Yield Prediction: A Systematic Review. *Remote Sensing*, 15(8), 2014. <https://doi.org/10.3390/rs15082014>
- Kabas, O., Kocaturk, M., Ozkan, C. F., Gumrukcu, E., Canakci, M., & Karayel, D. (2020). Effects of different soil tillage-sowing systems on plant development and emergence traits of second crop soybean. *Bioscience Journal*, 36(6). <https://doi.org/10.14393/BJ-v36n6a2020-49949>
- Kahlon, M. S., Singh, C. B., & Dhingra, M. (2020). Effect of Compaction and Irrigation Regimes on Soil Physical Characteristics, Emergence, Growth

- and Productivity of Summer Moongbean. *LEGUME RESEARCH - AN INTERNATIONAL JOURNAL*, Of. <https://doi.org/10.18805/LR-4362>
- Karami, A., Quijano, K., & Crawford, M. (2021). Advancing Tassel Detection and Counting: Annotation and Algorithms. *Remote Sensing*, 13(15), 2881. <https://doi.org/10.3390/rs13152881>
- Kellogg, E. A. (2015). Description of the Family, Vegetative Morphology and Anatomy. In *Flowering Plants. Monocots* (pp. 3–23). Springer International Publishing. [https://doi.org/10.1007/978-3-319-15332-2\\_1](https://doi.org/10.1007/978-3-319-15332-2_1)
- Khan, S., Shah, A., Nawaz, M., & Khan, M. (2017). Impact of different tillage practices on soil physical properties, nitrate leaching and yield attributes of maize (*Zea mays* L.). In *Journal of Soil Science and Plant Nutrition* (Vol. 17, Issue 1).
- Kharraz, N., & Szabó, I. (2023). Monitoring of plant growth through methods of phenotyping and image analysis. *Columella : Journal of Agricultural and Environmental Sciences*, 10(1), 49–59. <https://doi.org/10.18380/SZIE.COLUM.2023.10.1.49>
- Khatun, M., Monir, M. M., Lou, X., Zhu, J., & Xu, H. (2022). Genome-wide association studies revealed complex genetic architecture and breeding perspective of maize ear traits. *BMC Plant Biology*, 22(1), 537. <https://doi.org/10.1186/s12870-022-03913-1>
- Khurshid, K., Iqbal, M., Arif, M., & Nawaz, A. (2006). *Effect of Tillage and Mulch on Soil Physical Properties and Growth of Maize*. 8.
- Kumar, C., Mubvumba, P., Huang, Y., Dhillon, J., & Reddy, K. (2023). Multi-Stage Corn Yield Prediction Using High-Resolution UAV Multispectral

- Data and Machine Learning Models. *Agronomy*, 13(5), 1277.  
<https://doi.org/10.3390/agronomy13051277>
- Kumar, D., Singh, R. B., & Kaur, R. (2019). *Remote-Sensing Technology* (pp. 27–58). [https://doi.org/10.1007/978-3-319-58039-5\\_3](https://doi.org/10.1007/978-3-319-58039-5_3)
- Lampurlanés, J., Angás, P., & Cantero-Martínez, C. (2001). Root growth, soil water content and yield of barley under different tillage systems on two soils in semiarid conditions. *Field Crops Research*, 69(1), 27–40.  
[https://doi.org/10.1016/S0378-4290\(00\)00130-1](https://doi.org/10.1016/S0378-4290(00)00130-1)
- LeCun, Y., Bengio, Y., & Hinton, G. (2015). Deep learning. *Nature*, 521(7553), 436–444.
- Li, Q., Liu, N., & Wu, C. (2023). Novel insights into maize (*Zea mays*) development and organogenesis for agricultural optimization. *Planta*, 257(5), 94. <https://doi.org/10.1007/s00425-023-04126-y>
- Lin, T.-Y., Maire, M., Belongie, S., Hays, J., Perona, P., Ramanan, D., Dollár, P., & Zitnick, C. L. (2014). *Microsoft COCO: Common Objects in Context* (pp. 740–755). [https://doi.org/10.1007/978-3-319-10602-1\\_48](https://doi.org/10.1007/978-3-319-10602-1_48)
- Lindeberg, T. (2012). Scale Invariant Feature Transform. *Scholarpedia*, 7(5), 10491. <https://doi.org/10.4249/scholarpedia.10491>
- Linden, D. R., Clapp, C. E., & Dowdy, R. H. (2000). Long-term corn grain and stover yields as a function of tillage and residue removal in east central Minnesota. *Soil and Tillage Research*, 56(3–4), 167–174.  
[https://doi.org/10.1016/S0167-1987\(00\)00139-2](https://doi.org/10.1016/S0167-1987(00)00139-2)
- Lipiec, J., Medvedev, V. V., Birkas, M., Dumitru, E., Lyndina, T. E., Rousseva, S., & Fulajtář, E. (2003). Effect of soil compaction on

root growth and crop yield in Central and Eastern Europe. *International Agrophysics*, 17.

Liu, J., Huang, W., Xiao, L., Huo, Y., Xiong, H., Li, X., & Xiao, W. (2023). *Deep Learning Object Detection* (pp. 300–309). [https://doi.org/10.1007/978-3-031-28124-2\\_28](https://doi.org/10.1007/978-3-031-28124-2_28)

Liu, S., Jin, X., Bai, Y., Wu, W., Cui, N., Cheng, M., Liu, Y., Meng, L., Jia, X., Nie, C., & Yin, D. (2023). UAV multispectral images for accurate estimation of the maize LAI considering the effect of soil background. *International Journal of Applied Earth Observation and Geoinformation*, 121, 103383. <https://doi.org/10.1016/j.jag.2023.103383>

Liu, W., Anguelov, D., Erhan, D., Szegedy, C., Reed, S., Fu, C.-Y., & Berg, A. C. (2016). SSD: Single Shot MultiBox Detector. In *Lecture Notes in Computer Science* (pp. 21–37). Springer International Publishing. [https://doi.org/10.1007/978-3-319-46448-0\\_2](https://doi.org/10.1007/978-3-319-46448-0_2)

Liu, Z., Cao, S., Sun, Z., Wang, H., Qu, S., Lei, N., He, J., & Dong, Q. (2021). Tillage effects on soil properties and crop yield after land reclamation. *Scientific Reports*, 11(1), 4611. <https://doi.org/10.1038/s41598-021-84191-z>

Lóránt, B., Veronika, K.-B., & József, B. (2024). Comparison of RGB Indices used for Vegetation Studies based on Structured Similarity Index (SSIM). *Journal of Plant Science and Phytopathology*, 8(1), 007–012. <https://doi.org/10.29328/journal.jpssp.1001124>

Louhaichi, M., Borman, M. M., & Johnson, D. E. (2001). Spatially Located Platform and Aerial Photography for Documentation of Grazing Impacts

- on Wheat. *Geocarto International*, 16(1), 65–70.  
<https://doi.org/10.1080/10106040108542184>
- Lu, Y., & Young, S. (2020). A survey of public datasets for computer vision tasks in precision agriculture. *Computers and Electronics in Agriculture*, 178, 105760. <https://doi.org/10.1016/j.compag.2020.105760>
- Lugato, E., & Jones, A. (2015). Modelling Soil Organic Carbon Changes Under Different Maize Cropping Scenarios for Cellulosic Ethanol in Europe. *BioEnergy Research*, 8(2), 537–545.  
<https://doi.org/10.1007/s12155-014-9529-2>
- MacCarthy, D. S., Adiku, S. G., Freduah, B. S., Kamara, A. Y., Narh, S., & Abdulai, A. L. (2018). Evaluating maize yield variability and gaps in two agroecologies in northern Ghana using a crop simulation model. *South African Journal of Plant and Soil*, 35(2), 137–147.  
<https://doi.org/10.1080/02571862.2017.1354407>
- Machado, S., Bynum, E. D., Archer, T. L., Lascano, R. J., Wilson, L. T., Bordovsky, J., Segarra, E., Bronson, K., Nesmith, D. M., & Xu, W. (2002). Spatial and Temporal Variability of Corn Growth and Grain Yield. *Crop Science*, 42(5), 1564–1576.  
<https://doi.org/10.2135/cropsci2002.1564>
- Mao, W., Wang, Y., & Wang, Y. R. (2003). *Real-time Detection of Between-row Weeds Using Machine Vision*.  
<https://api.semanticscholar.org/CorpusID:112225119>
- Marapelli, B., Anamalamudi, L., Potluri, C. S., Carie, A., & Anamalamudi, S. (2024). *Enhancing Agricultural Decision-Making Through Machine*

*Learning-Based Crop Yield Predictions* (pp. 209–224).

[https://doi.org/10.1007/978-981-99-6755-1\\_16](https://doi.org/10.1007/978-981-99-6755-1_16)

- Marques Ramos, A. P., Prado Osco, L., Elis Garcia Furuya, D., Nunes Gonçalves, W., Cordeiro Santana, D., Pereira Ribeiro Teodoro, L., Antonio da Silva Junior, C., Fernando Capristo-Silva, G., Li, J., Henrique Rojo Baio, F., Marcato Junior, J., Eduardo Teodoro, P., & Pistori, H. (2020). A random forest ranking approach to predict yield in maize with uav-based vegetation spectral indices. *Computers and Electronics in Agriculture*, 178, 105791. <https://doi.org/10.1016/j.compag.2020.105791>
- Mathur, A., & Foody, G. M. (2008). Multiclass and Binary SVM Classification: Implications for Training and Classification Users. *IEEE Geoscience and Remote Sensing Letters*, 5(2), 241–245. <https://doi.org/10.1109/LGRS.2008.915597>
- Meer, F., & Jong, S. (2001). Imaging spectrometry. *Remote Sensing and Digital Image Processing*. Kluwer Academic Publishers.
- Mehra, P., Baker, J., Sojka, R. E., Bolan, N., Desbiolles, J., Kirkham, M. B., Ross, C., & Gupta, R. (2018). A Review of Tillage Practices and Their Potential to Impact the Soil Carbon Dynamics (pp. 185–230). <https://doi.org/10.1016/bs.agron.2018.03.002>
- Mohammed, K., Batung, E., Saaka, S. A., Kansanga, M. M., & Luginaah, I. (2023). Determinants of mechanized technology adoption in smallholder agriculture: Implications for agricultural policy. *Land Use Policy*, 129, 106666. <https://doi.org/10.1016/j.landusepol.2023.106666>
- Mohsan, S. A. H., Othman, N. Q. H., Li, Y., Alsharif, M. H., & Khan, M. A. (2023). Unmanned aerial vehicles (UAVs): practical aspects,

- applications, open challenges, security issues, and future trends. *Intelligent Service Robotics*. <https://doi.org/10.1007/s11370-022-00452-4>
- Mondal, S., & Chakraborty, D. (2022). Global meta-analysis suggests that no-tillage favourably changes soil structure and porosity. *Geoderma*, 405, 115443. <https://doi.org/10.1016/j.geoderma.2021.115443>
- Moriondo, M., Maselli, F., & Bindi, M. (2007). A simple model of regional wheat yield based on NDVI data. *European Journal of Agronomy*, 26(3), 266–274. <https://doi.org/10.1016/j.eja.2006.10.007>
- Müller, L., Lipiec, J., Kornecki, T. S., & Gebhardt, S. (2011). *Trafficability and Workability of Soils* (pp. 912–924). [https://doi.org/10.1007/978-90-481-3585-1\\_176](https://doi.org/10.1007/978-90-481-3585-1_176)
- Murillo, J. M., Moreno, F., Girón, I. F., & Oblitas, M. I. (2004). Conservation tillage: long term effect on soil and crops under rainfed conditions in South-West Spain (Western Andalusia). *Spanish Journal of Agricultural Research*, 2(1), 35–43. <https://doi.org/10.5424/sjar/2004021-58>
- Nafi, E., Webber, H., Danso, I., Naab, J. B., Frei, M., & Gaiser, T. (2021). Can reduced tillage buffer the future climate warming effects on maize yield in different soil types of West Africa? *Soil and Tillage Research*, 205. <https://doi.org/10.1016/J.STILL.2020.104767>
- Nawaz, M. F., Bourrié, G., & Trolard, F. (2013). Soil compaction impact and modelling. A review. *Agronomy for Sustainable Development*, 33(2), 291–309. <https://doi.org/10.1007/s13593-011-0071-8>
- Nayak, H. S., Parihar, C. M., Mandal, B. N., Patra, K., Jat, S. L., Singh, R., Singh, V. K., Jat, M. L., Garnaik, S., Nayak, J., & Abdallah, A. M. (2022). Point placement of late vegetative stage nitrogen splits increase

- the productivity, N-use efficiency and profitability of tropical maize under decade long conservation agriculture. *European Journal of Agronomy*, 133, 126417. <https://doi.org/10.1016/j.eja.2021.126417>
- Negese, W., Mosisa, T., & Mulugeta, G. (2022). *Effects of Lime Application Rate on Acidity of Soil on Maize at Nedjo District, West Wollega Zone, Oromia, Ethiopia*.
- Niu, L., Qin, W., You, Y., Mo, Q., Pan, J., Tian, L., Xu, G., Chen, C., & Li, Z. (2023). Effects of precipitation variability and conservation tillage on soil moisture, yield and quality of silage maize. *Frontiers in Sustainable Food Systems*, 7. <https://doi.org/10.3389/fsufs.2023.1198649>
- Nkrumah, F., Klutse, N. A. B., Adukpo, D. C., Owusu, K., Quagraine, K. A., Owusu, A., & Gutowski, W. (2014). Rainfall Variability over Ghana: Model versus Rain Gauge Observation. *International Journal of Geosciences*, 05(07), 673–683. <https://doi.org/10.4236/ijg.2014.57060>
- Ochieng', I. O., Gitari, H. I., Mochoge, B., Rezaei-Chiyaneh, E., & Gweyi-Onyango, J. P. (2021). Optimizing Maize Yield, Nitrogen Efficacy and Grain Protein Content under Different N Forms and Rates. *Journal of Soil Science and Plant Nutrition*, 21(3), 1867–1880. <https://doi.org/10.1007/s42729-021-00486-0>
- Oehme, L. H., Reineke, A.-J., Weiß, T. M., Würschum, T., He, X., & Müller, J. (2022). Remote Sensing of Maize Plant Height at Different Growth Stages Using UAV-Based Digital Surface Models (DSM). *Agronomy*, 12(4), 958. <https://doi.org/10.3390/agronomy12040958>
- Ofori, H., Amoah, F., Arah, K. I., Aidoo, I. A., & Okley, T. N. (2019). Moisture-dependent physical properties of Opeaburoo and Abontem



- maize varieties during drying. *African Journal of Food Science*, 13(8), 152–162. <https://doi.org/10.5897/AJFS2019.1791>
- OKorie, Benedict, O., & NIRAJ, Y. (2022). Effects of different tillage practices on soil fertility properties: a review. *International Journal of Agriculture and Environmental Research*, 8(1), 176–193.
- Omia, E., Bae, H., Park, E., Kim, M. S., Baek, I., Kabenge, I., & Cho, B.-K. (2023). Remote Sensing in Field Crop Monitoring: A Comprehensive Review of Sensor Systems, Data Analyses and Recent Advances. *Remote Sensing*, 15(2), 354. <https://doi.org/10.3390/rs15020354>
- Osunbitan, J. A., Oyedele, D. J., & Adekalu, K. O. (2005). Tillage effects on bulk density, hydraulic conductivity and strength of a loamy sand soil in southwestern Nigeria. *Soil and Tillage Research*, 82(1), 57–64. <https://doi.org/10.1016/j.still.2004.05.007>
- Otsu, N. (1979). A Threshold Selection Method from Gray-Level Histograms. *IEEE Transactions on Systems, Man, and Cybernetics*, 9(1), 62–66. <https://doi.org/10.1109/TSMC.1979.4310076>
- Pandey, B. K., Huang, G., Bhosale, R., Hartman, S., Sturrock, C. J., Jose, L., Martin, O. C., Karady, M., Voesenek, L. A. C. J., Ljung, K., Lynch, J. P., Brown, K. M., Whalley, W. R., Mooney, S. J., Zhang, D., & Bennett, M. J. (2021). Plant roots sense soil compaction through restricted ethylene diffusion. *Science*, 371(6526), 276–280. <https://doi.org/10.1126/science.abf3013>
- Pei, J., Tan, S., Zou, Y., Liao, C., He, Y., Wang, J., Huang, H., Wang, T., Tian, H., Fang, H., Wang, L., & Huang, J. (2025). The role of phenology in crop yield prediction: Comparison of ground-based phenology and

- remotely sensed phenology. *Agricultural and Forest Meteorology*, 361, 110340. <https://doi.org/10.1016/j.agrformet.2024.110340>
- Pekias, A., Maraslidis, G. S., Tsipouras, M. G., Koumboulis, F. N., & Fragulis, G. F. (2022). An overview of power supply technologies for Unmanned Aerial Vehicles (UAVs) and machine vision applications. *2022 7th South-East Europe Design Automation, Computer Engineering, Computer Networks and Social Media Conference (SEEDA-CECNSM)*, 1–8. <https://doi.org/10.1109/SEEDA-CECNSM57760.2022.9933003>
- Peng, Z., Yang, H., Li, Q., Cao, H., Ma, J., Ma, S., Qiao, Y., Jin, J., Ren, P., Song, Z., & Liu, P. (2023). Tillage Practices Affected Yield and Water Use Efficiency of Maize (*Zea mays* L., Longdan No.8) by Regulating Soil Moisture and Temperature in Semi-Arid Environment. *Water*, 15(18), 3243. <https://doi.org/10.3390/w15183243>
- Phillips, R. E. (1984). Effects of Climate on Performance of No-Tillage. In *No-Tillage Agriculture* (pp. 11–41). Springer US. [https://doi.org/10.1007/978-1-4684-1467-7\\_2](https://doi.org/10.1007/978-1-4684-1467-7_2)
- Pinto, F., Zaman-Allah, M., Reynolds, M., & Schulthess, U. (2023). Satellite imagery for high-throughput phenotyping in breeding plots. *Frontiers in Plant Science*, 14. <https://doi.org/10.3389/fpls.2023.1114670>
- Qiao, K., Zhu, W., Xie, Z., & Li, P. (2019). Estimating the Seasonal Dynamics of the Leaf Area Index Using Piecewise LAI-VI Relationships Based on Phenophases. *Remote Sensing*, 11(6), 689. <https://doi.org/10.3390/rs11060689>
- Ragasa, C., Dankyi, A., Acheampong, P., Wiredu, A. N., Chapoto, A., Asamoah, M., & Tripp, R. (2013). Patterns of adoption of improved rice

- technologies in Ghana. *International Food Policy Research Institute Working Paper*, 35(2), 6–8.
- Rashidi, M., & Keshavarzpour, F. (2007). Effect of Different Tillage Methods on Grain Yield and Yield Components of Maize (*Zea mays* L.). *International Journal Of Agriculture & Biology*, 9. <http://www.fspublishers.org>
- Rashidi, M., & Keshavarzpour, F. (2008). *Effect Of Different Tillage Methods on Soil Physical Properties And Crop Yield Of Melon (Cucumis Melo)*. <https://api.semanticscholar.org/CorpusID:138605003>
- Ren, S., He, K., Girshick, R., & Sun, J. (2016). *Faster R-CNN: Towards Real-Time Object Detection with Region Proposal Networks*.
- Ren, Y., Li, Q., Du, X., Zhang, Y., Wang, H., Shi, G., & Wei, M. (2023). Analysis of Corn Yield Prediction Potential at Various Growth Phases Using a Process-Based Model and Deep Learning. *Plants*, 12(3), 446. <https://doi.org/10.3390/plants12030446>
- Richardson, A. D., Jenkins, J. P., Braswell, B. H., Hollinger, D. Y., Ollinger, S. V., & Smith, M.-L. (2007). Use of digital webcam images to track spring green-up in a deciduous broadleaf forest. *Oecologia*, 152(2), 323–334. <https://doi.org/10.1007/s00442-006-0657-z>
- Roger-Estrade, J., Anger, C., Bertrand, M., & Richard, G. (2010). Tillage and soil ecology: Partners for sustainable agriculture. *Soil and Tillage Research*, 111(1), 33–40. <https://doi.org/10.1016/j.still.2010.08.010>
- Routray, S., Ray, A. K., & Mishra, C. (2017). Analysis of various image feature extraction methods against noisy image: SIFT, SURF and HOG. *2017 Second International Conference on Electrical, Computer and*

- Communication Technologies (ICECCT)*, 1–5.  
<https://doi.org/10.1109/ICECCT.2017.8117846>
- Sakamoto, T., Gitelson, A. A., & Arkebauer, T. J. (2014). Near real-time prediction of U.S. corn yields based on time-series MODIS data. *Remote Sensing of Environment*, 147, 219–231.  
<https://doi.org/10.1016/j.rse.2014.03.008>
- Saldivia-Tejeda, A., Uribe-Guerrero, M. Á., Rojas-Cruz, J. M., Guera, O. G. M., Verhulst, N., & Fonteyne, S. (2024). Conservation agriculture enhances maize yields and profitability in Mexico's semi-arid highlands. *Scientific Reports*, 14(1), 29638. <https://doi.org/10.1038/s41598-024-80928-8>
- Šarauskis, E., Kriauciūnienė, Z., Romaneckas, K., & Buragienė, S. (2018). *Impact of Tillage Methods on Environment, Energy and Economy* (pp. 53–97). [https://doi.org/10.1007/978-3-319-99076-7\\_2](https://doi.org/10.1007/978-3-319-99076-7_2)
- Sasal, M. C., Andriulo, A. E., & Taboada, M. A. (2006). Soil porosity characteristics and water movement under zero tillage in silty soils in Argentinian Pampas. *Soil and Tillage Research*, 87(1), 9–18.  
<https://doi.org/10.1016/j.still.2005.02.025>
- Sauer, C. O. (2008). *The early Spanish main*. Cambridge University Press.
- Schönberger, J. L., & Frahm, J.-M. (2016). Structure-from-Motion Revisited. *2016 IEEE Conference on Computer Vision and Pattern Recognition (CVPR)*, 4104–4113. <https://api.semanticscholar.org/CorpusID:1728538>
- Sheikh, M., Iqra, F., Ambreen, H., Pravin, K. A., Ikra, M., & Chung, Y. S. (2024). Integrating artificial intelligence and high-throughput

- phenotyping for crop improvement. *Journal of Integrative Agriculture*, 23(6), 1787–1802. <https://doi.org/10.1016/j.jia.2023.10.019>
- Shettigar, N., Katragadda, S., Vivek, B. S., Nair, S. K., & Soujanya, P. L. (2024). Association and Diversity Studies for Yield and Its Attributing Traits in Maize (*Zea mays* L.) Hybrids. *Journal of Experimental Agriculture International*, 46(8), 513–517. <https://doi.org/10.9734/jeai/2024/v46i82730>
- Shiferaw, B., Prasanna, B. M., Hellin, J., & Bänziger, M. (2011). Crops that feed the world 6. Past successes and future challenges to the role played by maize in global food security. *Food Security*, 3(3), 307–327. <https://doi.org/10.1007/S12571-011-0140-5/TABLES/3>
- Shorten, C., & Khoshgoftaar, T. M. (2019). A survey on Image Data Augmentation for Deep Learning. *Journal of Big Data*, 6(1), 60. <https://doi.org/10.1186/s40537-019-0197-0>
- Shrestha, N. (2020). Detecting Multicollinearity in Regression Analysis. *American Journal of Applied Mathematics and Statistics*, 8(2), 39–42. <https://doi.org/10.12691/ajams-8-2-1>
- Şimon, A., Moraru, P. I., Ceclan, A., Russu, F., Cheţan, F., Bărdaş, M., Popa, A., Rusu, T., Pop, A. I., & Bogdan, I. (2023). The Impact of Climatic Factors on the Development Stages of Maize Crop in the Transylvanian Plain. *Agronomy*, 13(6), 1612. <https://doi.org/10.3390/agronomy13061612>
- Singh, R., & Bhavadharini, R. M. (2023). An Investigation on Machine Learning Algorithms for Crop Yield Prediction. *2023 International*

- Conference on System, Computation, Automation and Networking (ICSCAN)*, 1–6. <https://doi.org/10.1109/ICSCAN58655.2023.10395193>
- Skaalsveen, K., & Clarke, L. (2021). Impact of no-tillage on water purification and retention functions of soil. *Journal of Soil and Water Conservation*, 76(2), 116–129. <https://doi.org/10.2489/jswc.2021.00012>
- Socolini, A., & Vizzari, M. (2023). *Predictive Modelling of Maize Yield Using Sentinel 2 NDVI* (pp. 327–338). [https://doi.org/10.1007/978-3-031-37114-1\\_22](https://doi.org/10.1007/978-3-031-37114-1_22)
- Sofaer, H. R., Hoeting, J. A., & Jarnevich, C. S. (2019). The area under the precision-recall curve as a performance metric for rare binary events. *Methods in Ecology and Evolution*, 10(4), 565–577. <https://doi.org/10.1111/2041-210X.13140>
- Sokolowski, A. C., Prack McCormick, B., De Grazia, J., Wolski, J. E., Rodríguez, H. A., Rodríguez-Frers, E. P., Gagey, M. C., Debelis, S. P., Paladino, I. R., & Barrios, M. B. (2020). Tillage and no-tillage effects on physical and chemical properties of an Argiaquoll soil under long-term crop rotation in Buenos Aires, Argentina. *International Soil and Water Conservation Research*, 8(2), 185–194. <https://doi.org/10.1016/J.ISWCR.2020.02.002>
- Sparks, E. E. (2023). Maize plants and the brace roots that support them. *New Phytologist*, 237(1), 48–52. <https://doi.org/10.1111/nph.18489>
- Steponavičienė, V., Žiūraitis, G., Rudinskienė, A., Jackevičienė, K., & Bogužas, V. (2024a). Long-Term Effects of Different Tillage Systems and Their Impact on Soil Properties and Crop Yields. *Agronomy*, 14(4), 870. <https://doi.org/10.3390/agronomy14040870>

- Steponavičienė, V., Žiūraitis, G., Rudinskienė, A., Jackevičienė, K., & Bogužas, V. (2024b). Long-Term Effects of Different Tillage Systems and Their Impact on Soil Properties and Crop Yields. *Agronomy*, 14(4), 870. <https://doi.org/10.3390/agronomy14040870>
- Sun, J., Niu, W., Mu, F., Li, R., Du, Y., Ma, L., Zhang, Q., Li, G., Zhu, J., & Siddique, K. H. M. (2024). Optimized tillage can enhance crop tolerance to extreme weather events: Evidence from field experiments and meta-analysis. *Soil and Tillage Research*, 238, 106003. <https://doi.org/10.1016/j.still.2024.106003>
- Sun, Q., Sun, W., Zhao, Z., Jiang, W., Zhang, P., Sun, X., & Xue, Q. (2023). Soil Compaction and Maize Root Distribution under Subsoiling Tillage in a Wheat–Maize Double Cropping System. *Agronomy*, 13(2), 394. <https://doi.org/10.3390/agronomy13020394>
- Sunoj, S., Cho, J., Guinness, J., van Aardt, J., Czymmek, K. J., & Ketterings, Q. M. (2021). Corn Grain Yield Prediction and Mapping from Unmanned Aerial System (UAS) Multispectral Imagery. *Remote Sensing*, 13(19), 3948. <https://doi.org/10.3390/rs13193948>
- Sunoj, S., Yeh, B., Marcaida III, M., Longchamps, L., van Aardt, J., & Ketterings, Q. M. (2023). Maize grain and silage yield prediction of commercial fields using high-resolution UAS imagery. *Biosystems Engineering*, 235, 137–149. <https://doi.org/10.1016/j.biosystemseng.2023.09.010>
- Talaei Khoei, T., Ould Slimane, H., & Kaabouch, N. (2023). Deep learning: systematic review, models, challenges, and research directions. *Neural*

*Computing and Applications*, 35(31), 23103–23124.  
<https://doi.org/10.1007/s00521-023-08957-4>

Tangyuan, N., Bin, H., Nianyuan, J., Shenzhong, T., & Zengjia, L. (2009). Effects of conservation tillage on soil porosity in maize-wheat cropping system. *Plant, Soil and Environment*, 55(8), 327–333.  
<https://doi.org/10.17221/25/2009-PSE>

Taye, G., Poesen, J., Wesemael, B. Van, Vanmaercke, M., Teka, D., Deckers, J., Goosse, T., Maetens, W., Nyssen, J., Hallet, V., & Haregeweyn, N. (2013). Effects of land use, slope gradient, and soil and water conservation structures on runoff and soil loss in semi-arid Northern Ethiopia. *Physical Geography*, 34(3), 236–259.  
<https://doi.org/10.1080/02723646.2013.832098>

Tiab, D., & Donaldson, E. C. (2004). Absolute and Effective Porosity. In *Petrophysics* (pp. 787–797). Elsevier. <https://doi.org/10.1016/B978-075067711-0/50022-0>

Tobiašová, E., Lemanowicz, J., Dębska, B., Kunkelová, M., & Sakáč, J. (2023). The Effect of Reduced and Conventional Tillage Systems on Soil Aggregates and Organic Carbon Parameters of Different Soil Types. *Agriculture*, 13(4), 818. <https://doi.org/10.3390/agriculture13040818>

Treven, J. R., & Cordova-Esparaza, D. M. (2023). *A comprehensive review of YOLO: From YOLOv1 to YOLOv8 and beyond*.  
<https://arxiv.org/pdf/2304.00501.pdf>

Tripathi, K. K., Warriar, R., Govila, O. P., & Ahuja, V. (2011). *Biology of Zea mays* (Maize).  
[http://www.envfor.nic.in/divisions/csurv/geac/Biology\\_of\\_Maize\[1\].pdf](http://www.envfor.nic.in/divisions/csurv/geac/Biology_of_Maize[1].pdf)



- Tripathi, R. P., Sharma, P., & Singh, S. (2005). Tilth index: an approach to optimize tillage in rice–wheat system. *Soil and Tillage Research*, 80(1–2), 125–137. <https://doi.org/10.1016/j.still.2004.03.004>
- Tsouros, D. C., Bibi, S., & Sarigiannidis, P. G. (2019). A Review on UAV-Based Applications for Precision Agriculture. *Information*, 10(11), 349. <https://doi.org/10.3390/info10110349>
- van Klompenburg, T., Kassahun, A., & Catal, C. (2020). Crop yield prediction using machine learning: A systematic literature review. *Computers and Electronics in Agriculture*, 177, 105709. <https://doi.org/10.1016/j.compag.2020.105709>
- VandenBygaart, A. J., & Liang, B. C. (2024). Crop yields under no-till in Canada: implications for soil organic carbon change. *Canadian Journal of Soil Science*, 104(1), 22–27. <https://doi.org/10.1139/cjss-2023-0061>
- Velumani, K., Lopez-Lozano, R., Madec, S., Guo, W., Gillet, J., Comar, A., & Baret, F. (2021). Estimates of Maize Plant Density from UAV RGB Images Using Faster-RCNN Detection Model: Impact of the Spatial Resolution. *Plant Phenomics*, 2021. <https://doi.org/10.34133/2021/9824843>
- Wald, R., Khoshgoftaar, T., Dittman, D. J., & Napolitano, A. (2013). Random Forest with 200 Selected Features: An Optimal Model for Bioinformatics Research. *2013 12th International Conference on Machine Learning and Applications*, 154–160. <https://doi.org/10.1109/ICMLA.2013.34>
- Wang, J., Sun, C., Zhang, Y., Xiao, J., Ma, Y., Jiang, J., Jiang, Z., & Zhang, L. (2024). Straw return rearranges soil pore structure improving soil moisture memory in a maize field experiment under rainfed conditions.

*Agricultural Water Management*, 306, 109164.

<https://doi.org/10.1016/j.agwat.2024.109164>

Wang, L., Tian, Y., Yao, X., Zhu, Y., & Cao, W. (2014). Predicting grain yield and protein content in wheat by fusing multi-sensor and multi-temporal remote-sensing images. *Field Crops Research*, 164, 178–188. <https://doi.org/10.1016/j.fcr.2014.05.001>

Wang, X., & Liu, J. (2024). Vegetable disease detection using an improved YOLOv8 algorithm in the greenhouse plant environment. *Scientific Reports*, 14(1), 4261. <https://doi.org/10.1038/s41598-024-54540-9>

Waqas, M. A., Wang, X., Zafar, S. A., Noor, M. A., Hussain, H. A., Azher Nawaz, M., & Farooq, M. (2021). Thermal Stresses in Maize: Effects and Management Strategies. *Plants*, 10(2), 293. <https://doi.org/10.3390/plants10020293>

Wasaya, A., Yasir, T. A., Ijaz, M., & Ahmad, S. (2019a). Tillage Effects on Agronomic Crop Production. In *Agronomic Crops* (pp. 73–99). Springer Singapore. [https://doi.org/10.1007/978-981-32-9783-8\\_5](https://doi.org/10.1007/978-981-32-9783-8_5)

Wasaya, A., Yasir, T. A., Ijaz, M., & Ahmad, S. (2019b). Tillage Effects on Agronomic Crop Production. In *Agronomic Crops* (pp. 73–99). Springer Singapore. [https://doi.org/10.1007/978-981-32-9783-8\\_5](https://doi.org/10.1007/978-981-32-9783-8_5)

Weatherwax, P. (1916). Morphology of the Flowers of *Zea mays*. *Bulletin of the Torrey Botanical Club*, 43(3), 127. <https://doi.org/10.2307/2479625>

Weiss, M., Jacob, F., & Duveiller, G. (2020). Remote sensing for agricultural applications: A meta-review. *Remote Sensing of Environment*, 236, 111402. <https://doi.org/10.1016/j.rse.2019.111402>

- Wang, S. E., Roh, Y., Song, H., & Lee, J.-G. (2023). Data collection and quality challenges in deep learning: a data-centric AI perspective. *The VLDB Journal*, 32(4), 791–813. <https://doi.org/10.1007/s00778-022-00775-9>
- Wiegand, C. L., Richardson, A. J., Escobar, D. E., & Gerbermann, A. H. (1991). Vegetation indices in crop assessments. *Remote Sensing of Environment*, 35(2–3), 105–119. [https://doi.org/10.1016/0034-4257\(91\)90004-P](https://doi.org/10.1016/0034-4257(91)90004-P)
- Winkler, J., Kopta, T., Ferby, V., Neudert, L., & Vaverková, M. D. (2022). Effect of Tillage Technology Systems for Seed Germination Rate in a Laboratory Tests. *Environments*, 9(2), 13. <https://doi.org/10.3390/environments9020013>
- Woebbecke, D. M., Meyer, G. E., Von Bargen, K., & Mortensen, D. A. (1995). Color Indices for Weed Identification Under Various Soil, Residue, and Lighting Conditions. *Transactions of the ASAE*, 38(1), 259–269. <https://doi.org/10.13031/2013.27838>
- Wong, C. Y., Gilbert, M. E., Pierce, M. A., Parker, T. A., Palkovic, A., Gepts, P., Magney, T. S., & Buckley, T. N. (2023). Hyperspectral Remote Sensing for Phenotyping the Physiological Drought Response of Common and Tepary Bean. *Plant Phenomics*, 5. <https://doi.org/10.34133/plantphenomics.0021>
- Woo, H. R., Masclaux-Daubresse, C., & Lim, P. O. (2018). Plant senescence: how plants know when and how to die. *Journal of Experimental Botany*, 69(4), 715–718. <https://doi.org/10.1093/jxb/ery011>

- Wu, Y., Zhou, G., Song, Y., & Zhou, L. (2024). Thresholds and extent of temperature effects on maize yield differ in different grain-filling stages. *Science of The Total Environment*, 918, 170709. <https://doi.org/10.1016/j.scitotenv.2024.170709>
- Xie, T., Li, J., Yang, C., Jiang, Z., Chen, Y., Guo, L., & Zhang, J. (2021). Crop height estimation based on UAV images: Methods, errors, and strategies. *Computers and Electronics in Agriculture*, 185, 106155. <https://doi.org/10.1016/j.compag.2021.106155>
- Xu, C., Zheng, Y., Zhang, Y., Li, G., & Wang, Y. (2022). A method for detecting objects in dense scenes. *Open Computer Science*, 12(1), 75–82. <https://doi.org/10.1515/comp-2022-0231>
- Xu, X., Zhang, H., Ma, Y., Liu, K., Bao, H., & Qian, X. (2023). TranSDet: Toward Effective Transfer Learning for Small-Object Detection. *Remote Sensing*, 15(14), 3525. <https://doi.org/10.3390/rs15143525>
- Xu, Y., Zhao, B., Zhai, Y., Chen, Q., & Zhou, Y. (2021). Maize Diseases Identification Method Based on Multi-Scale Convolutional Global Pooling Neural Network. *IEEE Access*, 9, 27959–27970. <https://doi.org/10.1109/ACCESS.2021.3058267>
- Xue, Y., Zhou, J., Ran, L., Wu, H., Wei, W., Hu, X., Xia, F., & Wang, J. (2024). Conservation tillage as an economic and ecological farming option for Summer Maize in the oasis region of Northwest China. *Plant and Soil*. <https://doi.org/10.1007/s11104-024-06527-8>
- Yang, Z., Willis, P., & Mueller, R. (2008). Impact of band-ratio enhanced AWIFS image to crop classification accuracy. *Proc. Pecora*, 17(1), 1–11.

- Yasaswy, MYS. K., Manimegalai, T., & Somasundaram, J. (2022). Crop Yield Prediction in Agriculture Using Gradient Boosting Algorithm Compared with Random Forest. *2022 International Conference on Cyber Resilience (ICCR)*, 1–4. <https://doi.org/10.1109/ICCR56254.2022.9995829>
- Youdeowei, A., Ezedinma, F. O. C., & Onazi, O. C. (1986). *Introduction to Tropical Agriculture*. Longman Group Ltd.
- Zarcotejada, P., Berjon, A., Lopezlozano, R., Miller, J., Martin, P., Cachorro, V., Gonzalez, M., & Defrutos, A. (2005). Assessing vineyard condition with hyperspectral indices: Leaf and canopy reflectance simulation in a row-structured discontinuous canopy. *Remote Sensing of Environment*, 99(3), 271–287. <https://doi.org/10.1016/j.rse.2005.09.002>
- Zeng, C., Tian, Y., Zheng, G., & Gao, Y. (2024). *How Much Can Time-related Features Enhance Time Series Forecasting?*
- Zhang, B., Wu, Y., Zhao, B., Chanussot, J., Hong, D., Yao, J., & Gao, L. (2022). Progress and Challenges in Intelligent Remote Sensing Satellite Systems. *IEEE Journal of Selected Topics in Applied Earth Observations and Remote Sensing*, 15, 1814–1822. <https://doi.org/10.1109/JSTARS.2022.3148139>
- Zhang, D., Hao, X., Fan, Z., Hu, X., Ma, J., Guo, Y., & Wu, L. (2022). Optimizing Tillage and Fertilization Patterns to Improve Soil Physical Properties, NUE and Economic Benefits of Wheat-Maize Crop Rotation Systems. *Agriculture 2022*, Vol. 12, Page 1264, 12(8), 1264. <https://doi.org/10.3390/AGRICULTURE12081264>

- Zhao, K., Zhao, L., Zhao, Y., & Deng, H. (2023). Study on Lightweight Model of Maize Seedling Object Detection Based on YOLOv7. *Applied Sciences*, 13(13), 7731. <https://doi.org/10.3390/app13137731>
- Zhao, X., Zhao, J., Zheng, X., Wang, X., Ouyang, C., Shao, X., Norasma, Y. N., Fadzilah, M. A., Roslin, N. A., Zanariah, Z. W. N., Tarmidi, Z., & Candra, F. S. (2019). Unmanned Aerial Vehicle Applications In Agriculture. *IOP Conference Series: Materials Science and Engineering*, 506(1), 012063. <https://doi.org/10.1088/1757-899X/506/1/012063>

## APPENDICES

**Appendix 1: ANOVA table for the effect of tillage on germination rate for the Season One**

Source	DF	Adj SS	Adj MS	F-Value	P-Value
Treatment	3	153.2	51.07	2.2	0.141
Bloc	4	101.3	25.32	1.09	0.404
Error	12	278.3	23.19		
Total	19	532.8			

**Appendix 2: ANOVA table for the effect of tillage on germination rate for the Season Two**

Source	DF	Adj SS	Adj MS	F-Value	P-Value
Treatment	3	82.55	27.52	0.97	0.44
Bloc	4	164.8	41.2	1.45	0.278
Error	12	341.2	28.43		
Total	19	588.55			

**Appendix 3: ANOVA table for the effect of tillage on plant height for the Season One**

Source	DF	Adj SS	Adj MS	F-Value	P-Value
Treatment	3	3463.5	1154.5	4.48	0.025
Bloc	4	541.2	135.3	0.53	0.719
Error	12	3090.8	257.6		
Total	19	7095.4			

**Appendix 4: Tukey HSD means grouping for plant heights of the Season One**

Treatment	N	Mean	Grouping
Ploughing and Harrowing	5	176.7	A
Ploughing only	5	167.7	AB
Harrowing only	5	161	AB
No-tillage	5	140.933	B

### Appendix 5: ANOVA table for the effect of tillage on plant height for the Season Two

Source	DF	Adj SS	Adj MS	F-Value	P-Value
Treatment	3	2945	981.7	7.04	0.005
Bloc	4	1292	322.9	2.32	0.117
Error	12	1673	139.4		
Total	19	5910			

### Appendix 6: Tukey HSD means grouping for plant heights of the Season Two

Treatment	N	Mean	Grouping
Ploughing and Harrowing	5	193.5	A
Ploughing only	5	186.767	A
Harrowing only	5	180.4	AB
No-tillage	5	160.987	B

### Appendix 7: ANOVA table for the effect of tillage on plant stem diameter for the Season One

Source	DF	Adj SS	Adj MS	F-Value	P-Value
Treatment	3	79.88	26.628	5.06	0.017
Bloc	4	71.73	17.933	3.41	0.044
Error	12	63.16	5.264		
Total	19	214.78			

### Appendix 8: Tukey HSD means grouping for plant stem diameter for the Season One

Treatment	N	Mean	Grouping
Ploughing only	5	21.6925	A
Ploughing and Harrowing	5	21.5388	A
Harrowing only	5	18.6647	AB
No-tillage	5	16.9516	B



Appendix 9: ANOVA table for the effect of tillage on plant stem diameter for the Season Two

Source	DF	Adj SS	Adj MS	F-Value	P-Value
Treatment	3	84.89	28.297	18.41	0
Bloc	4	8.514	2.128	1.38	0.297
Error	12	18.442	1.537		
Total	19	111.845			

Appendix 10: Tukey HSD means grouping for plant stem diameter of the Season Two

Treatment	N	Mean	Grouping
Ploughing and Harrowing	5	23.483	A
Ploughing only	5	22.25	AB
Harrowing only	5	20.083	BC
No-tillage	5	18.1	C

Appendix 11: ANOVA table for the effects of tillage on the number of leaves for the Season One

Source	DF	Adj SS	Adj MS	F-Value	P-Value
Treatment	3	2.071	0.6903	0.75	0.545
Bloc	4	1.408	0.3521	0.38	0.818
Error	12	11.103	0.9252		
Total	19	14.582			

Appendix 12: ANOVA table for the effect of tillage on the number of leaves of the Season Two

Source	DF	Adj SS	Adj MS	F-Value	P-Value
Treatment	3	15.056	5.0185	14.12	0
Bloc	4	4.714	1.1785	3.32	0.048
Error	12	4.264	0.3553		
Total	19	24.033			

Appendix 13: Tukey HSD means grouping for plant number of leaves of the Season Two

Treatment	N	Mean	Grouping
Ploughing and Harrowing	5	13.9	A
Ploughing only	5	13.467	A
Harrowing only	5	13.167	A
No-tillage	5	11.6	B

Appendix 14: ANOVA table for the effect of tillage on the Leaf Area Index of the Season One

Source	DF	Adj SS	Adj MS	F-Value	P-Value
Treatment	3	0.03299	0.011	0.16	0.919
Bloc	4	0.20049	0.05012	0.74	0.582
Error	12	0.81133	0.06761		
Total	19	1.04481			

Appendix 15: ANOVA table for the effect of tillage on the Leaf Area Index of the Season Two

Source	DF	Adj SS	Adj MS	F-Value	P-Value
Treatment	3	0.4594	0.15312	4.37	0.027
Bloc	4	0.7534	0.18835	5.37	0.01
Error	12	0.4209	0.03508		
Total	19	1.6337			

Appendix 16: ANOVA table for the effect of tillage on number of days to 50 percent flowering of the Season One

Source	DF	Adj SS	Adj MS	F-Value	P-Value
Treatment	3	29.8	9.933	3.76	0.041
Bloc	4	34.7	8.675	3.28	0.049
Error	12	31.7	2.642		
Total	19	96.2			

Appendix 17: ANOVA table for the effect of tillage on number of days to 50 percent flowering of the Season Two

Source	DF	Adj SS	Adj MS	F-Value	P-Value
Treatment	3	7.75	2.5833	0.75	0.545
Bloc	4	3.7	0.925	0.27	0.893
Error	12	41.5	3.4583		
Total	19	52.95			

Appendix 18: ANOVA table for the effect of tillage on Above ground dry biomass of the Season One

Source	DF	Adj SS	Adj MS	F-Value	P-Value
Treatment	3	38.986	12.995	5.05	0.017
Bloc	4	5.194	1.299	0.51	0.733
Error	12	30.855	2.571		
Total	19	75.035			

Appendix 19: Tukey HSD means grouping for the Above ground dry biomass of the Season One

Treatment	N	Mean	Grouping
Ploughing and Harrowing	5	7.209	A
Ploughing only	5	6.027	AB
Harrowing only	5	4.668	ABC
No-tillage	5	3.501	B

Appendix 20: ANOVA table for the effect of tillage on Above ground dry biomass of the Season Two

Source	DF	Adj SS	Adj MS	F-Value	P-Value
Treatment	3	30.423	10.141	3.64	0.045
Bloc	4	8.197	2.049	0.74	0.585
Error	12	33.425	2.785		
Total	19	72.045			

Appendix 21: Tukey HSD means grouping for the Above ground dry biomass of the Season Two

Treatment	N	Mean	Grouping
Ploughing and Harrowing	5	10.933	A
Ploughing only	5	9.37	AB
Harrowing only	5	9.1	AB
No-tillage	5	7.456	B

Grain yield

Appendix 22: ANOVA table for the effect of tillage on Grain yield of the Season One

Source	DF	Adj SS	Adj MS	F-Value	P-Value
Treatment	3	9.827	3.2757	4.95	0.018
Bloc	4	1.524	0.381	0.58	0.685
Error	12	7.933	0.6611		
Total	19	19.285			

Appendix 23: ANOVA table for the effect of tillage on Grain yield of the Season Two

Source	DF	Adj SS	Adj MS	F-Value	P-Value
Treatment	3	5.892	1.964	1.58	0.246
Bloc	4	5.192	1.298	1.04	0.426
Error	12	14.945	1.245		
Total	19	26.028			

Appendix 24: ANOVA table for the effect of tillage on the weight of 100 grains for the Season One

Source	DF	Adj SS	Adj MS	F-Value	P-Value
Treatment	3	95.79	31.93	95.76	0.00
Bloc	4	1.121	0.2804	0.84	0.525
Error	12	4.001	0.3334		

Total	19	100.913
-------	----	---------

Appendix 25: Tukey HSD means grouping for the weight of 100 maize grains for the Season One

Treatment	N	Mean	Grouping
Ploughing and Harrowing	5	31.204	A
Harrowing only	5	27.324	B
Ploughing only	5	26.672	B
No-tillage	5	25.312	C

Appendix 26: ANOVA table for the effect of tillage on the weight of 100 grains of the Season Two

Source	DF	Adj SS	Adj MS	F-Value	P-Value
Treatment	3	112.26	37.42	19.97	0
Bloc	4	16.52	4.131	2.2	0.13
Error	12	22.48	1.874		
Total	19	151.27			

Appendix 27: Tukey HSD means grouping for the weight of 100 maize grains of the Season Two

Treatment	N	Mean	Grouping
Ploughing and Harrowing	5	32.72	A
Ploughing only	5	27.842	B
No-tillage	5	27.274	B
Harrowing only	5	26.822	B

Appendix 28: ANOVA table for the effect of tillage on the Number of ears per plant for the Season One

Source	DF	Adj SS	Adj MS	F-Value	P-Value
Treatment	3	0.2544	0.08479	2.05	0.161
Bloc	4	0.3635	0.09088	2.2	0.131
Error	12	0.4966	0.04138		
Total	19	1.1145			

Appendix 29: ANOVA table for the effect of tillage on the Number of ears per plant for the Season Two

Source	DF	Adj SS	Adj MS	F-Value	P-Value
Treatment	3	0.1606	0.05354	1.47	0.271
Bloc	4	0.2843	0.07107	1.96	0.165
Error	12	0.4356	0.0363		
Total	19	0.8805			

Appendix 30: ANOVA table for the effect of tillage on ear length of the Season One

Source	DF	Adj SS	Adj MS	F-Value	P-Value
Treatment	3	44.95	14.982	3.23	0.061
Bloc	4	52.75	13.187	2.84	0.072
Error	12	55.7	4.641		
Total	19	153.39			

Appendix 31: ANOVA table for the effect of tillage on ear length of the Season Two

Source	DF	Adj SS	Adj MS	F-Value	P-Value
Treatment	3	3.813	1.271	0.39	0.764
Bloc	4	4.065	1.016	0.31	0.866
Error	12	39.419	3.285		
Total	19	47.297			